POTENTIAL SITES PREDICTION FOR SALT-MAKING PRIOR TO THE 19TH CENTURY USING SPATIAL MODELING: A CASE STUDY IN NAKHON RATCHASIMA PROVINCE

Montri Thanaphattarapornchai

A Thesis Submitted in Partial Fulfillment of the Requirements for the Degree of Master of Science in Geoinformatics

Suranaree University of Technology

Academic Year 2018

การพยากรณ์แหล่งศักยภาพสำหรับการผลิตเกลือสินเธาว์ก่อนคริสต์ศตวรรษ ที่ 19 ด้วยแบบจำลองเชิงพื้นที่: กรณีศึกษาในจังหวัดนครราชสีมา

นายมนตรี ธนภัทรพรชัย

วิทยานิพนธ์นี้เป็นส่วนหนึ่งของการศึกษาตามหลักสูตรปริญญาวิทยาศาสตรมหาบัณฑิต
สาขาวิชาภูมิสารสนเทศ
มหาวิทยาลัยเทคโนโลยีสุรนารี
ปีการศึกษา 2561

POTENTIAL SITES PREDICTION FOR SALT-MAKING PRIOR TO THE 19TH CENTURY USING SPATIAL MODELING: A CASE STUDY IN NAKHON RATCHASIMA PROVINCE

Suranaree University of Technology has approved this thesis submitted in partial fulfillment of the requirements for a Master's Degree.

Thesis Examining Committee

(Assoc. Prof. Dr. Suwit Ongsomwang)

Chairperson

(Asst. Prof. Dr. Sunya Sarapirome)

Member (Thesis Advisor)

(Assoc. Prof. Dr. Songkot Dasananda)

Member

(Asst. Prof. Dr. Pantip Piyatadsananon)

Member

(Assoc. Prof. Flt. Lt. Dr. Kontorn Chamniprasart)

Vice Rector for Academic Affairs

and Internationalization

(Assoc. Prof. Dr. Worawat Meevasana)

Dean of Institute of Science

มนตรี ธนภัทรพรชัย : การพยากรณ์แหล่งศักยภาพสำหรับการผลิตเกลือสินเธาว์ก่อนคริสต์ศตวรรษที่ 19 ด้วยแบบจำลองเชิงพื้นที่: กรณีศึกษาในจังหวัดนครราชสีมา (POTENTIAL SITES PREDICTION FOR SALT-MAKING PRIOR TO THE 19TH CENTURY USING SPATIAL MODELING: A CASE STUDY IN NAKHON RATCHASIMA PROVINCE) อาจารย์ที่ปรึกษา : ผู้ช่วยศาสตราจารย์ ดร.สัญญา สราภิรมย์, 146 หน้า.

เพื่อหลีกเลี่ยงการทำลายแหล่งผลิตเกลือโบราณโดยไม่ได้ตั้งใจ ข้อมูลพื้นที่ที่มีศักยภาพที่จะพบแหล่งผลิตเกลือโบราณจึงเป็นที่ต้องการอย่างมากสำหรับการวางแผนและพัฒนาด้านการใช้ประโยชน์ที่ดินและงานด้านโบราณคดี งานวิจัยนี้จึงมุ่งที่จะทำนายพื้นที่ที่มีศักยภาพพบแหล่งผลิตเกลือโบราณในพื้นที่จังหวัดนครราชสีมา โดยใช้การจำลองเชิงพื้นที่ด้วยอัตราส่วนความถี่ (Frequency ratio) และ การถดถอยลอจิสติก (Logistic regression) ข้อมูลนำเข้าเป็นข้อมูลคุณลักษณะเชิงกายภาพและวัฒนธรรมรวมถึงความสัมพันธ์ของข้อมูลซึ่งสกัดได้จากตัวอย่างของแหล่งผลิตเกลือโบราณที่ค้นพบในพื้นที่ ข้อมูลเหล่านี้ได้แก่ ตำแหน่งพื้นที่ตั้งอยู่บนหน่วยหินมหาสารคามและหน่วยหินที่เกี่ยวข้อง ระยะห่างจากโครงสร้างธรณีวิทยา การตั้งอยู่บนพื้นที่ที่มีความหลากหลายของผลกระทบจากเกลือ ดัชนีความแตกต่างความเค็มแบบนอร์มอลไลซ์ (Normalized Difference Salinity Index) ระยะห่างจากที่ตั้งชุมชนโบราณ และระยะห่างจากแหล่งน้ำ สัมประสิทธิ์ของตัวแปรนำเข้าของแบบจำลองการถดถอยลอจิสติกสามารถอธิบายว่าตัวแปรเหล่านี้มีอิทธิพลต่อการค้นพบแหล่งผลิตเกลือโบราณในพื้นที่อย่างไร พบว่า ปัจจัยที่มีอิทธิพลสูงสุด คือ ระยะห่างจากที่ตั้งชุมชนโบราณ ตามด้วยการตั้งอยู่บนพื้นที่ที่มีความหลากหลายของผลกระทบจากเกลือและ ระยะห่างจากแหล่งน้ำ ผลของการค้นพบเหล่านี้ได้รับการสนับสนุนอย่างหนักแน่นจากดัชนีอัตราส่วนความถี่ ผลลัพธ์สุดท้ายของทั้งสองแบบจำลองได้เป็นแผนที่กริดเซลแสดงศักยภาพการพบแหล่งผลิตเกลือโบราณด้วยดัชนีความน่าจะเป็นแหล่งผลิตเกลือ (Salt-making sites probability index) จากวิธีอัตราส่วนความถี่และค่าความเป็นไปได้จากแบบจำลองการถดถอยลอจิสติกได้ใช้วิธีเส้นโค้งอาร์โอซี (Receiver Operating Characteristic Curve) การทดสอบความถูกต้องของแผนที่ทั้งสอง ซึ่งได้ผลพื้นที่ใต้เส้นโค้ง (Area Under the Curve) เป็น 0.810 และ 0.908 ตามลำดับ ทำให้สามารถบอกได้ว่าแบบจำลองการถดถอยลอจิสติกให้ผลลัพธ์ที่ดีกว่าอย่างแน่นอน ผลการศึกษาบรรลุวัตถุประสงค์ของการวิจัยได้อย่างสมบูรณ์

สาขาวิชาภูมิสารสนเทศ ลายมือชื่อนักศึกษา มนตรี ธนภัทรพรชัย

ปีการศึกษา 2561 ลายมือชื่ออาจารย์ที่ปรึกษา สัญญา สราภิรมย์

MONTRI THANAPHATTARAPORNCHAI : POTENTIAL SITES PREDICTION FOR SALT MAKING PRIOR TO THE 19^{TH} CENTURY USING SPATIAL MODELING : A CASE STUDY IN NAKHON RATCHASIMA PROVINCE. THESIS ADVISOR : ASST. PROF. SUNYA SARAPIROME, Ph.D. 146 PP.

ANCIENT SALT-MAKING SITE/ARCHAEOLOGICAL PREDICTIVE MODEL/FREQUENCY RATIO MODEL/LOGISTIC REGRESSION MODEL

To avoid damaging ancient salt-making sites unintentionally, data on areas having high potential to discover ancient salt-making sites are required for effective land-use and archaeological development and planning. This research aims at predicting ancient salt-making potential areas using spatial modeling of the frequency ratio and logistic regression in Nakhon Ratchasima province. Input data are physical and cultural characteristics and their relationship extracted from samples of existing ancient salt-making sites. These include locating on the Maha Sarakham Formation and its related units, distance to geologic structures, locating on the varying degree of salt-affected areas, Normalized Difference Salinity Index (NDSI), distance to ancient settlements, and distance to water bodies. The coefficients of input variables from the logistic regression model could explain how much they influence the chance to discover the new ancient sites in the study area. The most influential factor was a distance to the ancient settlement, followed by locating on the varying degree of salt-affected areas and distance to water bodies. Frequency ratio indexes strongly supported these findings. Final results from the models were raster-based maps of salt-making site probability index (SMSPI) from Frequency ratio and ancient salt-making site probability from logistic regression. Relative Operating Characteristics (ROC) of maps was performed and resulted in an area under the curve (AUC) of 0.810 and 0.908, respectively. It revealed that logistic regression could conclusively provide a better result. The study results fruitfully serve the objectives of the research.

School of Geoinformatics Student's Signature Montri THANAPHATTARAPORNCHAI

Academic Year 2018 Advisor's Signature ______________

ACKNOWLEDGEMENTS

This research project would not have been possible without the support of many people. I would like to express my sincere gratitude to my thesis advisor, Asst. Prof. Dr. Sunya Sarapirome for the continuous support of my study, for his patience, motivation, enthusiasm, and immense knowledge. His guidance helped me in all the time of the study, research and writing of this thesis.

Besides my advisor, I would like to appreciate my gratitude to the committee members, Assoc. Prof. Dr. Songkot Dasananda, Assoc. Prof. Dr. Suwit Ongsomwang and Asst. Prof. Dr. Pantip Piyatadsananon for their encouragement and insightful comments. I would also like to thank Dr. Siripon Kamontum for valuable suggestions.

I extend my thanks to all the staffs and students of the School of Geoinformatics for their help and support during my study here, especially Mrs. Ratchaneekorn Somakul, Miss Silirak Tanang, Miss. Waruuee Aunphoklang, Mr. Athiwat Phinyoyang, Mr. Khompheak Mom, and Mrs. Pimprapai Piphatnawakul.

Finally, I wish to thank my family for their understanding and encouragement throughout my study.

Montri Thanaphattaraporncha

CONTENTS

Page

ABSTRACT IN THAI I

ABSTRACT IN ENGLISH II

ACKNOWLEDGEMENTS IV

CONTENTS V

LIST OF TABLES VIII

LIST OF FIGURES IX

LIST OF ABBREVIATIONS XI

CHAPTER

I INTRODUCTION 1

1.1 Background and significance of the study 1

1.2 Research objectives 4

1.3 Scope and limitations 4

1.4 Study area 5

1.5 Benefit of the study 6

II LITERATURE REVIEWS 7

2.1 Archaeology of salt production 7

2.2 Ethnoarchaeological studies of salt-making 12

2.2.1 Traditional salt- making methods 12

2.2.2 Local history of the salt trade 16

CONTENTS (Continued)

Page

2.2.3 Landscape and environment of the salt-making sites 17

2.2.4 Inner structure of salt-making mound site 20

2.2.5 Distribution of salt mounds in the region 21

2.3 Defining archaeological site boundaries 22

2.4 Surface expression of salt structure, salt-affected soil, and salt-making sites 24

2.5 Remote sensing techniques for soil salinity and archaeological studies 28

2.5.1 Remote sensing applications for salt-affected soil detection 28

2.5.2 Remote sensing applications for archaeological study 32

2.6 Spatial modeling 33

2.6.1 Concepts and theories 33

2.6.2 Previous studies on saline soil classification using spatial modeling 36

2.6.3 Archaeological predictive modeling application 38

III MATERIALS AND METHODS 40

3.1 Data collection and preparation 42

3.1.1 Related Factor Selection and their data preparation 43

3.1.2 Tools 52

3.1.3 Population / Samplings 53

3.2 Using spatial modeling for ancient salt-making potential area analysis 54

CONTENTS (Continued)

Page

3.2.1 Frequency ratio (FR) method 54

3.2.2 Logistic regression (LR) method 55

3.3 Validation and comparison of the model results 59

IV RESULTS AND DISCUSSIONS 60

4.1 Factor data for modeling 60

4.2 Probability map of ancient salt-making sites from FR 63

4.3 Probability map of ancient salt-making sites from LR 72

4.4 Validation and comparison of model result 78

V CONCLUSION AND RECOMMENDATIONS 85

REFERENCES 88

APPENDICES

APPENDIX A DATA TRANSFORMATION 101

APPENDIX B SPATIAL AUTOCORRELATION (GLOBAL MORAN'S I) REPORT 138

CURRICULUM VITAE 146

LIST OF TABLES

Table **Page**

3.1 Details of the data used in this study. 44

4.1 Frequency ratio of salt-making sites occurrence. 64

4.2 Salt-making probability classes, SMSPI, and coverage area percentage using the FR model. 71

4.3 The skewness of data based on the method used for data transformation of each variable. 73

4.4 A set of coefficients expressing the relationship between the dependent and independent variables, including the Variance Inflation Factor (VIF). 74

4.5 Salt-making probability classes and coverage area percentage using the LR model. 78

LIST OF FIGURES

Figure **Page**

1.1 Map of the study area and vicinity. 6

2.1 Comparison of ancient salt production and modern salt production in Nakhon Ratchasima Province. 9

2.2 Distribution of sites. 11

2.3 General principles of salt production 13

2.4 Traditional salt-making area has four elements of microtopography 15

2.5 Schematic drawing of salt-affected landscape elements at Ban Khok Sung near Bung Kaen Nam Ton, Muang Khon Kaen District 18

2.6 Arrangement of salt mounds and ditch at Ban Khok Sung near Khon Kaen . 20

2.7 Exposed profile of a salt mound at Ban Nong Suang, Kham Sakaesaeng District, Nakhon Ratchasima Province. 21

2.8 Interpretive curvilinear features and solution depression by using Radar images interpretation. 27

3.1 Conceptual flowchart of data processes for mapping the salt-making site probability. 41

3.2 Example of salt-making sites from the visual interpretation and field survey at Ban Bing, Non Sung District, Nakhon Ratchasima Province 50

LIST OF FIGURES (Continued)

Figure **Page**

3.3 Distribution of existing ancient salt-making sites in the study area 53

3.4 Flowchart for the LR method 59

4.1 Factor maps in the form of GIS data layers 61

4.2 The training sites and test sites in the study area 62

4.3 Salt-making occurrence probability map using the FR model........................ 72

4.4 Salt-making occurrence probability map using the LR model. 77

4.5 ROC curves for ancient salt-making site probability map validation. 80

4.6 122 Test sites showing in salt-making occurrence probability maps of FR and LR models. 81

4.7 The distribution of newly discovered salt-making sites over FR probability maps 83

4.8 The distribution of newly discovered salt-making sites over LR probability maps 84

LIST OF ABBREVIATIONS

ASTER	Advanced Spaceborne Thermal Emission and Reflection Radiometer
AUC	Area under the curve
DMR	Department of Mineral Resources
FAD	The Fine Arts Department
FR	Frequency ratio
GIS	Geographic Information System
KTms	The Maha Sarakham Formation
LDD	Land Development Department
LR	Logistic regression
NDSI	Normalized Differential Salinity Index
OLS	Ordinary Least Square analysis
Qa	Quaternary alluvial sediments
Qt	Quaternary terrace deposit
ROC	Receiver Operating Characteristics
RS	Remote sensing
RTSD	Royal Thai Survey Department
SI	Salinity index
SMSPI	Salt-making site probability index
SUT	Suranaree University of Technology

LIST OF ABBREVIATIONS (Continued)

VIF Variance Inflation Factor

CHAPTER I

INTRODUCTION

1.1 Background and significance of the study

The main part of the Khorat Basin is underlain by the Maha Sarakham Formation, containing rock salt, and salt contained upper clastic member in the Plio-Pleistocene formation cause severe problems of saline soils and saline water scattered throughout the region (Wongsomsak, 1986 quoted in Wannakomol, 2005). Salt-affected areas in northeastern Thailand occupy about 28,400 km^2 or about 17% of the northeastern region (Arunin, 1992). Natural water bodies of the region contain saltwater while salt crusts scatter over the terrain. Soil salinity and salinization have affected people since prehistoric time until now. The distributions of ancient settlements and salt-making mound sites in this area are the evidence related to the human adaptability and salt exploitation using available technologies of the age. Nowadays, many of them located in Nakhon Ratchasima Province. From previous studies, archaeologists found that the ancient people in northeastern Thailand used salt-making techniques at least since early history (Nitta, 1997). The local people use salt as a traditional food preservative, exclusively for fermented fish. The salt-making areas are situated on the natural salt domes with soil salinity and surficial salt crust (Rivett and Higham, 2007). These salt-makers could produce salt in the vicinity of their settlements for local consumption and trade their product to inland communities and the Ancient Khmer Empire (ชาร์ลส ไฮแอม และ รัชนี ทศรัตน์, 2542; ชลิต ชัยครรชิต, 2540; ศรีศักร วัลลิโภดม, 2535; Rivett and Higham).

Indeed, salt production activity affected the surrounding landscape, and land use of ancient sites in the northeastern region of Thailand. Generally, dry ponds have some open space; at that point, small trees and halophytes cover some prominent hills. This landscape is a condition that resulted from the salt-making activities. The ancient process of salt production caused the mound accumulating quickly and became the large numbers of ancient salt-making mounds in the clusters close to habitation sites and near to flat stream valleys in several areas of the Northeastern such as salt-making mound sites in Thung Kula Rong Hai area as well as the Mun River Basin (กรมศิลปากร, 2544). These ancient settlements probably linked to the salt-making mound sites since late prehistory and the industrial scale of salt production occurred from early history to the Ayutthaya period (Higham, 1977, 1996; Rivett and Higham, 2007).

As mentioned before, the occurrence of salt-making mound sites strongly correlates to the source of salt, the location of settlements and water bodies and salt-making techniques. Moreover, moats next to ancient moated settlements always appear as annular depression landform locating above the salt domes (Supajanya, Vichapan, and Sri-israporn, 1992). The distribution of these depressions associated with landforms and geological structures of the Maha Sarakham Formation. Hence, moats of ancient settlements and salt-making areas are located in the vicinity of each other.

However, there are a limited number of the studies of the relationship between ancient salt industries and ancient settlements in this region (กรมศิลปากร, 2544; Higham, 1977; Nitta, 1992, 1997; Rivett and Higham, 2007). Archaeologists cannot detect correctly the salt-making sites, where locate sparsely in the vast, and lack the appropriate conservation and management. Most of existing ancient salt-making sites are found in the central and northern areas of Nakhon Ratchasima Province, where having the area of rock salt resources with a total area of 7,734.68 km^2 (กรมทรัพยากรธรณี, 2553). Unfortunately, rock salt and potash have been substantial raw materials for various kinds of industrial uses, new salt mines using solution mining technology have been established and operated in the province. This, more or less, can damage ancient salt-making sites.

For this reason, predicted site locations using spatial modeling are necessary data for management and safeguarding unknown ancient salt-making sites from mining activities and poor land-use development. This research attempts to determine the correlation between land and cultural characteristics to ancient salt-making sites so that their potential areas can be located. For predicting potential areas of ancient salt-making activities, the integration of Geographic Information System (GIS) and remote sensing technology can be used to detect the surface expression and other related variables and input to operate spatial modeling. Ancient salt-making site probability maps from selected spatial models, logistic regression and frequency ratio, could allow discovering the unknown salt-making places and assist in generating a cost-effective plan to explore and improve the capacity of archaeologists to detect sites in the broad area.

1.2 Research objectives

The specific objectives of the study are:

(1) To determine the relationship between physical and cultural characteristics of existing ancient salt-making sites and apply it to discovering potential sites.

(2) To validate and compare the results of predicted ancient salt-making potential areas from two different methods; the logistic regression and frequency ratio.

1.3 Scope and limitations

(1) The Fine Arts Department's GIS data on archaeological sites, i.e., locations of ancient settlement investigated in the field are considered reliable for the study.

(2) Based on dating data of existing ancient salt-making sites in the study area, this study focuses on the ancient salt-making site before the 19^{th} Century.

(3) For the best result of surface expression of variables, ASTER imageries were selected on the date of the dry season from December 2001 to December 2004.

(4) NDSI is the primary satellite index used for salt-affected area detection.

(5) Based on available samples, dependent variable (*y*) for logistic regression analysis is either 1 or 0 for existing or non-existing ancient mining site.

(6) As modeling input, a salt-making mound of a site has to be larger than 4 m^2 and separated from each other at least 2 m. This criterion data is based on field investigation to confirm data of the Fine Arts Department.

1.4 Study area

The study area is located in the portion of Nakhon Ratchasima Province between 101°43´47" to 103°00´45" E longitude and 14°46´23" to 15°48´33" N latitude, covering the area about 9,170 km^2. The area has the underlying Maha Sarakham Formation as the bedrock, which is covered partly by thin younger Quaternary sediments (Figure 1.1). This region is characterized by a semi-arid climate and the presence of many saline soils and salt structures. River courses run through the study area, causing landforms of flood plain along the center and rolling landform on both sides.

Monsoons influence the whole area where is located in the tropical zone. The part is relatively dry with an average annual rainfall of 1,035 mm computed from meteorological data of 30 years (1971–2000), most of which occurs in the rainy season from May to October. The winter season lasts from November to February (Shrestha and Farshad, 2008). Summer season starts in March or April and continues until the beginning of May. Most times of the year, evaporation is higher than rainfall except during August and September when evaporation is slightly lower than rain. A significant part of the native dipterocarp forest has been converted into agricultural land (Sukchan and Yamamoto, 2002).

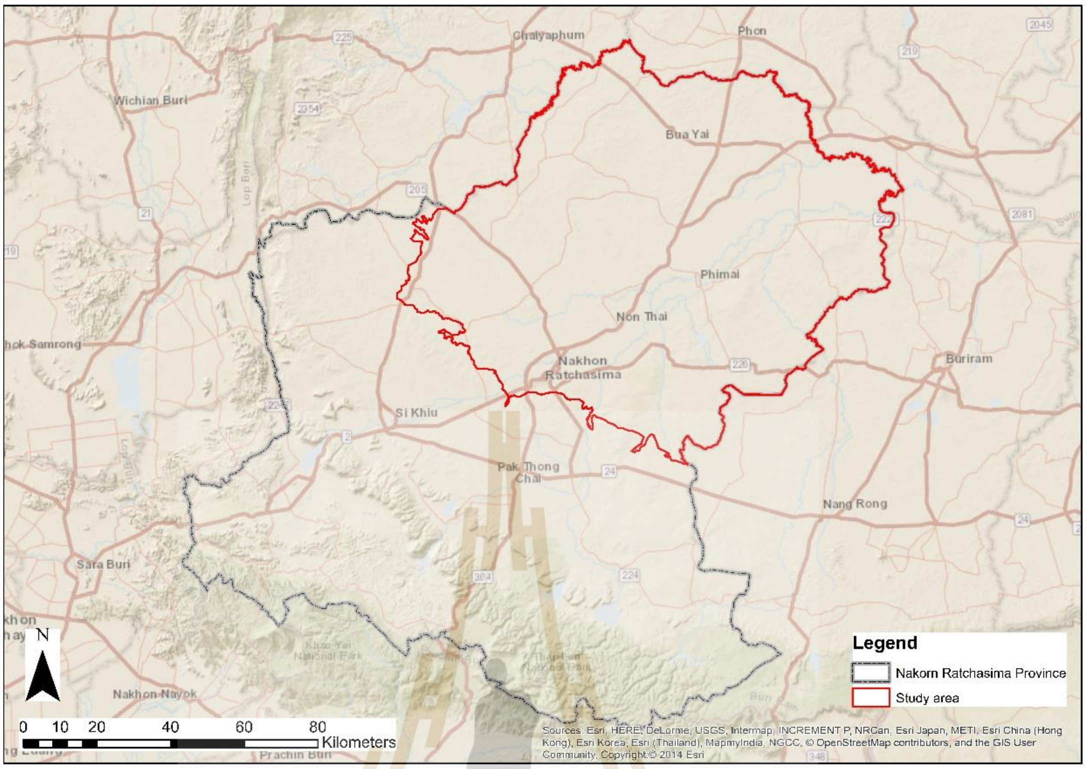

Figure 1.1 Map of the study area and vicinity.

1.5 Benefits of the study

The accomplishment of this research provides benefits as follows:

(1) The relationship between ancient salt-making sites, surface expression, and other related factors.

(2) The probability maps of ancient salt-making sites as results from the logistic regression model and frequency ratio analyses which are efficient for land-use and archaeological planning and development.

(3) The better model between logistic regression and frequency ratio for salt-making site prediction.

CHAPTER II

LITERATURE REVIEWS

2.1 Archaeology of salt production

Salt has historical importance to many civilizations in the past. Also, salt was a crucial component of many complex societies around the world. Then, the archaeology of salt focuses on the history of salt production, salt production methods, and salt distribution.

Antonites (2013) found that a mineral spring in the South African Lowveld, Baleni, had the episodic production during 2,000 years ago closely mirrored that of more recent ethnographic accounts. Archaeological evidence shows that agricultural communities periodically extracted salt at Baleni for nearly 2,000 years. The patterns of carbon deposition and pitting of ceramic vessels would further suggest a comparable process of reducing brine to salt crystals in ceramic containers.

In the East Asia region, Hoi (2011) studied salt production and management of the Erlitou and Erligang cultures from the Yi-Luo River basin along the Yellow River and of Zhongba in the Ganjing River valley in the Yangzi's Three Gorges region. These Bronze Age sites show the transportation routes network between the political centers of these cultures and their external resources. Consequently, local customs and polities had a strong influence on the growth and combination of external resources.

Similar to different parts of the world, in Northeast Thailand, salt was a valuable product. The exploitation of salt was underway by at least the middle of the first millennium BC at Bo Phan Khan in Roi-et Province, where large salt-work mounds clustered around the sizeable moated site of Non Düa (Higham 1977, 1996). Similarly, in the Khorat basins, a large amount of sizeable salt-making mound sites located around the ancient moated settlements (Rivett and Higham, 2007). Moreover, the excavations in salt-making sites focused on visible evidence of the salt-making process with dating, settlement patterns, and the proximity of the nearby ancient settlement (Nitta, 1992, 1997).

Nitta (1992, 1997) excavated Non Tung Phi Phon, the first - sixth centuries AD site, at Ban Ngui Mai, Bua Yai District, Nakhon Ratchasima Province. The ancient salt-making techniques and the structures used in the salt-making process are similar to those used today. Furthermore, Nitta argued that Nong Tung Pie Pone represents a site that underwent salt-making for a short period and that salt-makers run many furnaces at the same time. The procedure of salt-making means that the mound accumulates rapidly and as each mound that the ancient people abandoned, new sites to continue the activities occur near this area. As a result, the continuation of the industry and the expansion of the area. These sites are along the edges of flat stream valleys that are the flooded areas during the rainy season. Then, large numbers of salt-making mounds in clusters close to habitation sites and adjacent stream valleys.

Furthermore, Duke, Carter, and Chang (2010) proposed that Iron Age clay-lined working floors found in the excavation at Ban Non Wat in Nakhon Ratchasima Province associated with small-scale metal and salt production at the site. For this reason, they suggest that a family unit or kin group in the Iron Age may have used it. Then, they argue that the patterns of features may result from a seasonal rotation between activities within family units, generating the ancient resources people needed to live comfortably during the Iron Age (Figure 2.1).

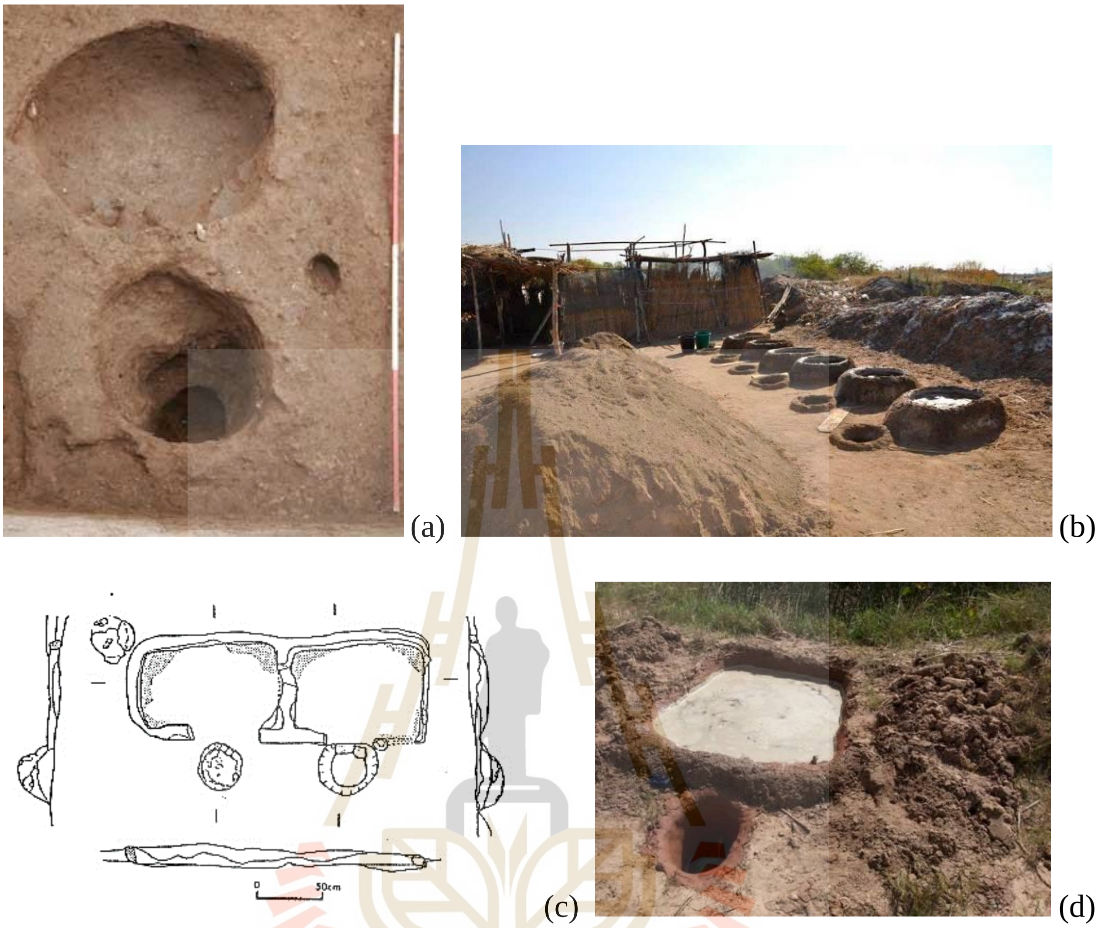

Figure 2.1 Comparison of ancient salt production and modern salt production in Nakhon Ratchasima Province. Using round shape filtering basins. Features from Ban Non Wat (a) Tambol Phon Songkram, Non Sung District and Ban Don Phangat, Tambol Phangat, Khamsakaesang District (b). Using square shape salt processing basins filtering Features form Non Tung Phi Phon, Baan Ngui Mai, Bua Yai District (c) and Ban Marum, Tambol Makha, Non Sung District (d).

From Nitta (1997); Duke et al. (2010); Yankowski (2014).

Rivett and Higham (2007) proposed that the presence of salt dome relates to a cluster of salt-making mound sites lies to the southwest of Phimai City. This dome, centered on the moated site of Ban Bing, has a total of 25 salt-making areas represented by small mounds rising above the alluvial plain. These salt-making mounds show up clearly on the aerial photographs (Figure 2.2). There is a large amount of these sites in close vicinity. In nearly all cases they associated with a prehistoric site, or group of ancient sites and located close to former river channels. There is also pottery dating to the historical periods of Ayutthaya and Sukhothai, which gives some indication to the importance and the interval of the industry. Besides, they argue that these salt mounds situated in a naturally occurring salt dome. Relatively, the recent upward movement has seen the solid rock salts of the Maha Sarakham Formation move closer to the surface. As a result of this movement, in some areas, the salt is closer to the surface, and during the dry season, the evaporation of water brings thick layers of crystallized salt to the surface. As this causes salt domes to occur in specific places, the salt-making sites distribute accordingly, so the clustering and the localized activity of salt production. The traditional basis of the Northeast Thai diet is sticky rice and fermented fish. It is possible that the ancient people caught substantial numbers of fish at these communities situated near the major rivers and preserved them as fermented fish. This local food preservation technique developed, significant quantities of fish were potentially being preserved, leading to a large number of salt-making sites and the transmission of traditional salt-making methods in the area of these salt domes.

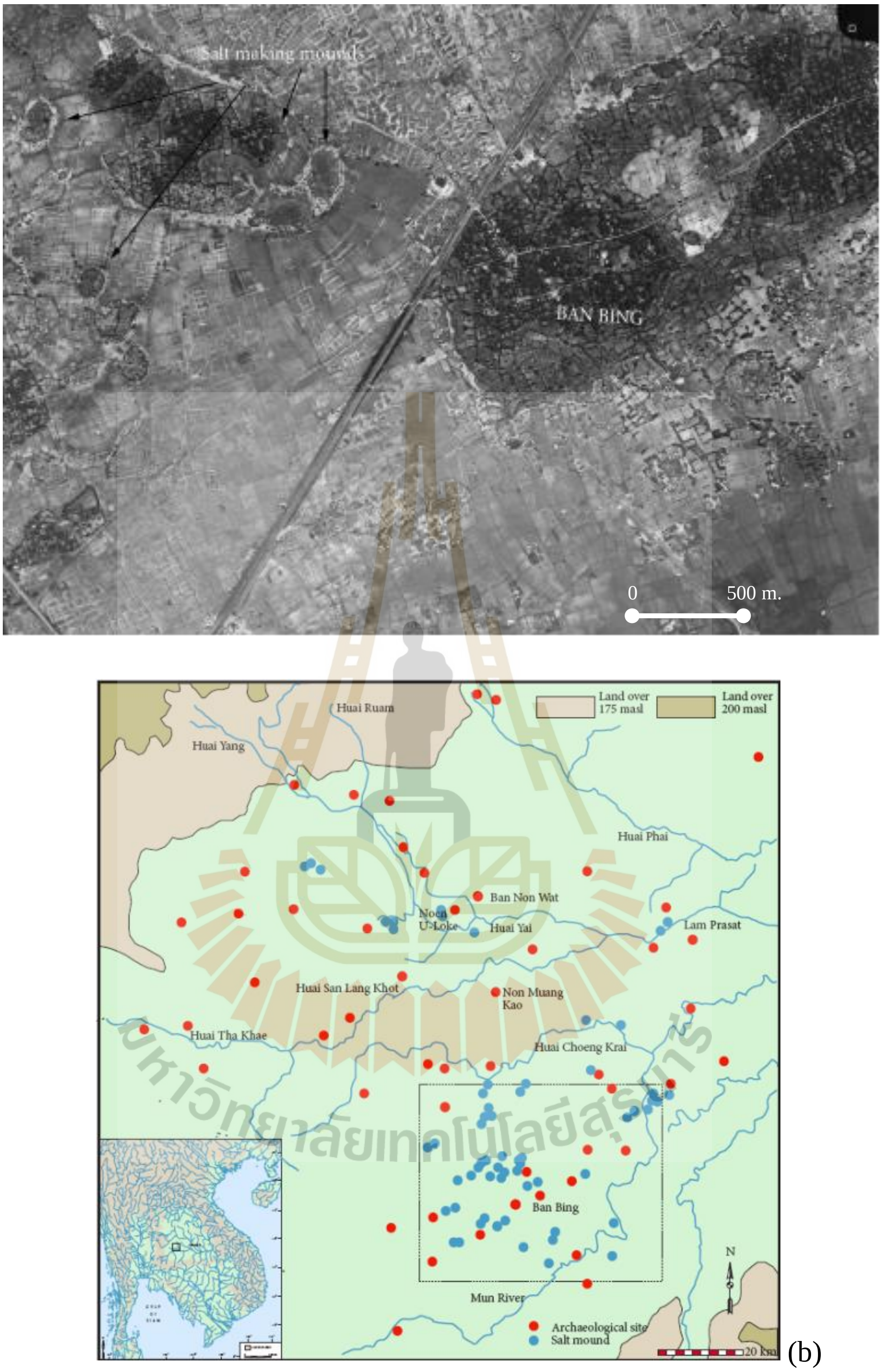

(a)

(b)

Figure 2.2 Distribution of sites. (a) Aerial photograph of salt-making mound sites of Ban Bing and the vicinity area. (b) The distribution of salt-making mounds.

From Rivett and Higham (2007).

Similarly, ศรีศักร วัลลิโภดม (2535) studied the ancient salt-making sites in the Northeast region, and he also reported Nakhon Ratchasima Province is dense with the salt-making areas, where the groups of ancient salt-makers frequently settled nearby to produce salt. Ancient settlement sites typically locate near the early salt-making mound sites and play an essential role as the salt distribution center, salt storage, woodshed, salt container craftsmanship, and salt trader. Today, the archaeologists can investigate some of the salt-making activities from field survey and remote sensing. These activities commonly occur in salt-affected areas where ancient ruins, waste of salt-making and settlements of early salt-makers are preserved in various scales.

2.2 Ethnoarchaeological studies of salt-making

In Northeast Thailand, salt was one of the most valuable products as well as iron. Salt-making was an essential mainstay for the people in the dry season. They have exploited salt since ancient time and transmitted their procedures to the next generation. Nowadays, ethnoarchaeological researches on local salt-making methods and salt resources can gain a better comprehension of the historical significance of this natural resource and commodity in the region (Yankowski and Kerdsap, 2013).

2.2.1 Traditional salt- making methods

There are two necessary steps for salt production from saline soil (Figure 2.3). The first is to immerse the soils in water to dissolve the soluble salts and produce the high concentrated brine. Later, the salt solution is drained and gradually boiled to obtain recrystallized NaCl (Yankowski and Kerdsap, 2013).

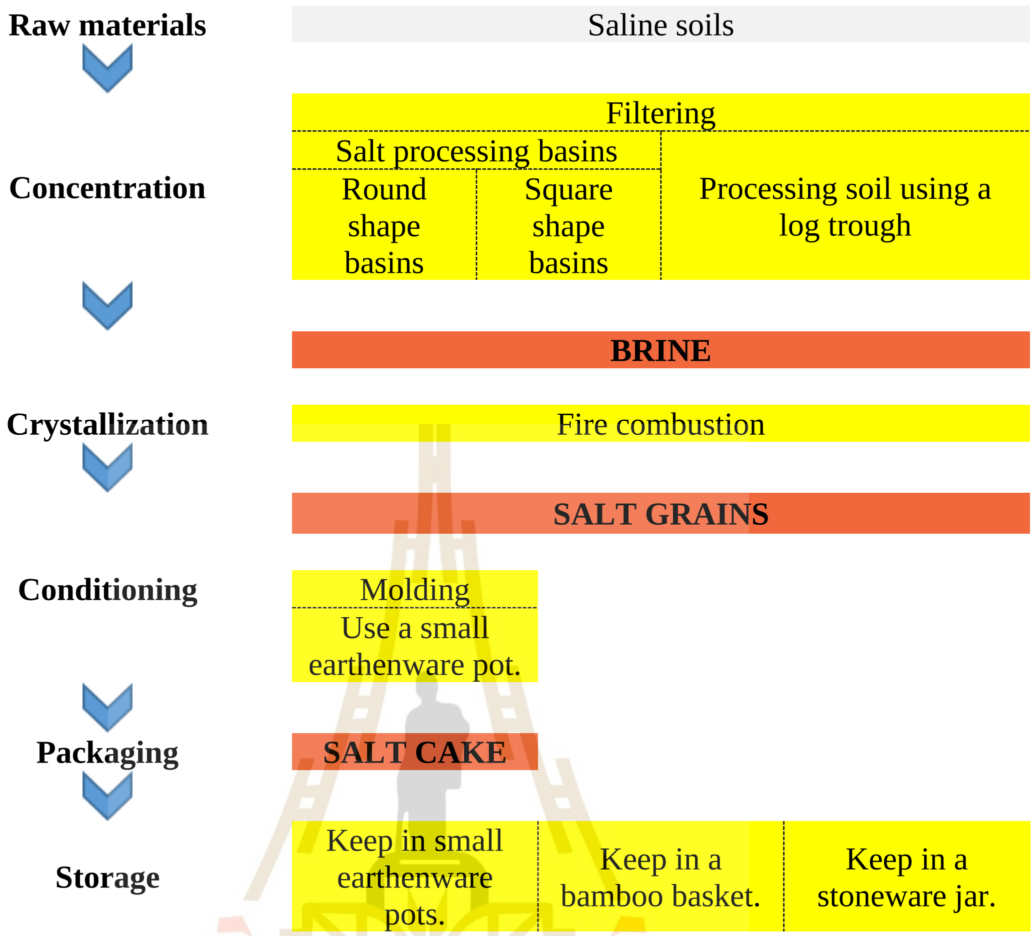

Figure 2.3 General principles of salt production (modified from Gouletquer and Welter, 2015).

Salt resources where has four elements of microtopography (Figure 2.4): salt crust site, wet and potentially saline belt, a naturally inundated depression where artificial ditch are frequently made, and disposed sand mound (Hisao and Wichaidit, 1989). In the salt-affected area near the communities, the local salt-makers collect the saline soils with salt crusts or “Din Ead” or “Din Ki Ka Tha” which formed in sandy spots (Thanaphattarapornchai, 2013). Salt crust site occurs on a slightly elevated portion, or at the foot of the human-made mound. Salt crusts always scrape together with sandy soils and are put into the filtering basin for percolating.

The two most popular and traditional methods for preparing the brine are to use a leaching trough or dig a small square or circular filtering basin for containing the saline sediment and water. For the first method, the salt-makers use various sizes of the log troughs. If they use the trough about 3 m in length and 50 centimetres in diameter, it can accommodate about 250 kilograms of saline sand (Hisao and Wichaidit, 1989). The trough has a few holes on the bottom, and conducting pipes are inserted to them. Before putting sand, people spread rice husks at the bottom of the trough to keep a proper percolation in the leaching process. Wet and potentially saline belt site with clay soil, although it does not produce salt crust, is also essential for keeping the water off to be salty, and its clay texture prevents the dug pond or ditch from being disrupted. People carry water from the marsh and pour it into the trough until the sand is immersed, and keep the salt to be leached. The salty leachate or brine coming out from the holes is led to a receiving basin. The salt solution is boiled on the tin pan at the soil-made furnace. From 100 1itre of the brine, 20 kilograms of salt is produced (Hisao and Wichaidit). The sand in the trough is disposed of nearby. Usually salt-making is continued for an extended period at fixed spots, and subsequently, after a prolonged period of salt-making, the debris of sand makes up the high and large mound. The recently abandoned salt mound is bare. However, older piles, since salt is leached away, are covered with grass and shrub-like “Sakae” (*Combretum quadrangulare Kurz*) on the top, and surrounded by salt-tolerant shrub-like “Nam Daeng” (*Carissa carandas L.*) at the foot.

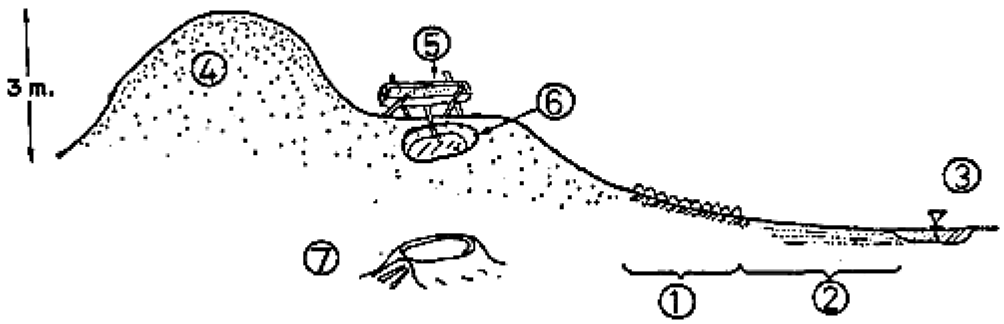

Figure 2.4 Traditional salt-making area has four elements of microtopography; salt crust site (1), wet and potentially saline belt (2), naturally inundated depression where the human-made ditch is frequently made (3), and disposed sand mound (4). Moreover, the salt-making structures are composed of a leaching trough (5), a brine receiving basin (6), and a soil-made furnace (7).

From Hisao and Wichaidit. (1989).

For the second method, the salt-makers dig a small square or circular filtering basin in the ground or along a small mound or embankment. The size of this basin is approximately a meter to a meter and a half in diameter. Some bundled grasses or rice husks are placed in the bottom of the basin overlaid with a burlap bag or rice husks to help in draining the brine. A second deeper hole is dug adjacent to this for draining off the salt solution through a small bamboo feeder tube between the two pits. Traditionally, these are clay lined to make them impermeable. The resulting product from these pits is a clear brine for recrystallization process. Presently, for boiling the salt solution, the local salt-makers use a shallow metal sheeting trough. They place this trough over an outdoor furnace, and they boil the salt solution in multiple batches. Then, they collected and put the salt in baskets to further drain, and stored them in large stoneware jars or bamboo baskets (Thanaphattarapornchai, 2013; Yankowski and Kerdsap, 2013).

Yankowski and Kerdsap (2013) studied the ethnoarchaeological research on local salt-making and salt resources in Tambon Phan Song Khram, Non Sung District, Nakhon Ratchasima Province. They focus on the local technology of salt-making and the use and trade of salt in the vicinity of Ban Non Wat archaeological site where the preliminary archaeological research suggests that some of these salt-making sites date back to the Iron Age, circa 500 BC, or even earlier. They visited fifteen villages to interview the local salt makers. They found that the salt-makers collect the saline soils to dissolve the soluble salts and create the brine. Then, they concentrated the salinity of the water and boiled this brine is drained and boiled to obtain recrystallized NaCl. The salt-makers of nowadays still use their traditional salt-making process. Also, they found that the technologies of salt production were many similarities in the methods across the region and closely related to the archaeological evidence from ancient salt-making sites in this region. The household-scale production structure, clay-lined reservoirs, is similar to clay-lined features in the excavations at Ban Non Wat and other neighboring sites (Duke et al., 2010).

2.2.2 Local history of the salt trade

From early history to the Ayutthaya period, many salt-making villages in the Upper Mun Basin were well known by salt traders from Phimai City, and salt merchants from other cities went there to buy salt. They carried cartloads of salt to be sold or exchange in Phimai City, Nakhon Ratchasima City, and towns in Cambodia. The salt surplus was traded to inland communities and exported to the ancient Khmer empire. Archaeologists and historians believe that there are many salt routes to

Cambodia. There are three primary routes: Phimai City to Angkor, Chanthaburi City to Bodhisattva, and Prachinburi City to Battambang. The path that was popular during the Rattanakosin period started in Nakhon Ratchasima City continued to Prachinburi City and ended in the Cambodian city of Battambang.

In the early Rattanakosin period (18th century – early 20th century), inland salt traders used caravan transport to get from Nakhon Ratchasima City to Bangkok and other major cities. Traders travelled in a group of wagons to ensure utmost security; they usually passed through forests and rural communities. In the past, the administrative center of Non Sung District (Klang City) was located at Ban Non Wat, so Ban Marum situated on a vital salt trade route encompassing Nakhon Ratchasima City. Currently, in addition to the local traders who come from neighbouring communities within a radius of five kilometres from Ban Marum, salt traders from other provinces, such as Prachin Buri Province come to this village to buy salt for making fermented fish (Thanaphattarapornchai, 2013). However, after the salt factory was built in Non Sung District, many people instead chose to work at the factory, and they abandoned their traditional salt-making activities. Today, the majority of salt-makers make salt primarily for personal use and consumption, but some individuals also sell their salt or trade it for rice (Yankowski and Kerdsap, 2013).

2.2.3 Landscape and environment of salt-making sites

In Northeast Thailand, raw materials for salt mining comes from the clastic members of the Maha Sarakham formation, and also from the Plio-Pleistocene formation (Takaya, Hattori and Wichaiyut, 1984 quoted in Hisao and Wichaidit, 1989 pp.8). It affects some areas that show very salty pond waters, and salt crust at sandy patches at the foot of the hill. The clastic members of the Maha Sarakham formation involve veinlets or vein or varied evaporites such as halite, lime, sodium carbonate, and gypsum. These evaporites are released from the weathering saprolite, producing salt crusts at sandy spots, and lime nodules in the soil (Figure 2.5).

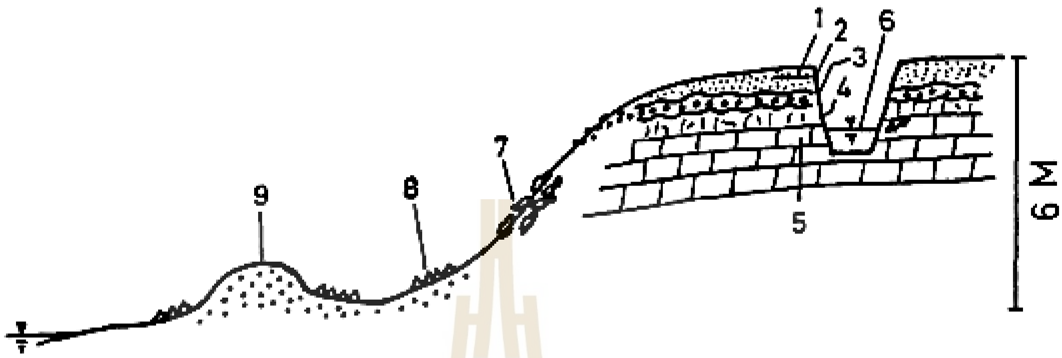

Figure 2.5 Schematic drawing of salt-affected landscape elements at Ban Khok Sung near Bung Kaen Nam Ton, Muang Khon Kaen District; soil profile exposed at pond well (1) - (5), salty water pond (6), lime nodule (7), salt crust (8), and salt mound (9). From Hisao and Wichaidit. (1989).

Consequently, the landscape of the salt-making site and the plan of working area relate to the raw materials, the location of the settlement, and water bodies. Besides, the variation of the size of salt-making mounds relies on type and quality of the salt resource, and continuity of salt production. If salt spots persist and salt production is engaged for an extended period, the salt mounds become quite large.

In Chi basin, the small salt-making mounds sites at Ban Khok Sung near Muang Khon Kaen District, Khon Kaen Province are not exceeding 4 m in height and 15 m in diameter. For salt working area preparation, salt-makers dig the long ditches from a pond to facilitate the water supply. So, they make a diversion dam, then arrange the ditch and mounds in a systematic plan (Hisao and Wichaidit, 1989) (Figure 2.6).

Also, large salt mounds are found at Nong Yai near Muang Khon Kaen District, Ban Si That and vicinity such as Ban Phai, and Mancha Khiri (Hisao and Wichaidit, 1989). Discovery of 70 mounds indicates that the west area of Ban Phai is one of the core areas of salt production in ancient times. While, the salt mounds at Nong Yai that consist of several smaller mounds salt, and the size of the composite mound is 100 m in length, 40 m in width and 7 m in height. There are other two composite mounds which were cut to level. One of these hillocks produces salt at its basement.

Furthermore, their potsherds are similar to those found at the archaeological site of Non Chai. This evidence is dated about 500 years BC It provides the relative dating of salt mounds at Nong Yai. This evidence provides the relative dating of salt mounds at Nong Yai.

However, in Mun basin, Hisao and Wichaidit (1989) claimed that one of the most prominent salt mounds is located at Ban Don Kwang near Tambol Choho, Muang Nakorn Ratchasima District. It has 200 m in length, 70 m in width and 10 m in height. For relative dating, potsherds which are found at the foot of the hill are Khmer or Lopburi ceramic sherds and cord-marked pottery sherds.

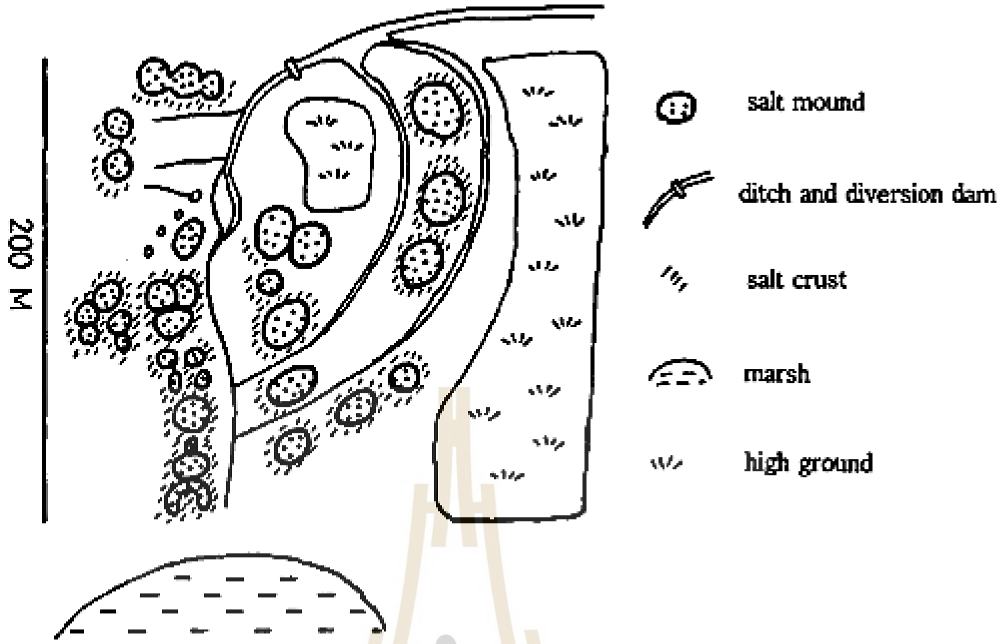

Figure 2.6 Arrangement of salt mounds and ditch at Ban Khok Sung near Khon Kaen. From Hisao and Wichaidit. (1989).

2.2.4 Inner structure of the salt-making mound site

Hisao and Wichaidit (1989) observed the inner structure of these salt mounds at Ban Nong Suang, Kham Sakaesaeng District, Nakhon Ratchasima Province (Figure 2.7). Burned sand appears red, and indicates the furnace. Pottery sherds also show burned traces and are exfoliated on both faces by the prolonged boiling of brine, and characteristic to the potteries used for salt boiling. Salty water which permeated into the pottery wall is crystallized there, thus exfoliates the pottery wall. Salt boiling pottery is the earthenware with cord-marked decoration. They concluded that the formation process of salt mound consists of three stages; disposal of leached sand and furnace bottom ash, boiling, and processing of salt, and again dumping of filtered sand.

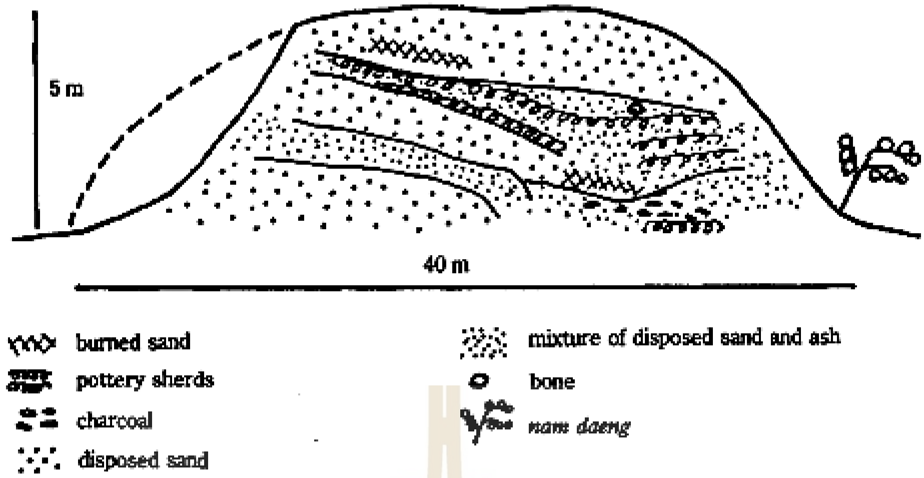

Figure 2.7 Exposed profile of a salt mound at Ban Nong Suang, Kham Sakaesaeng District, Nakhon Ratchasima Province.

From Hisao and Wichaidit. (1989).

2.2.5 Distribution of salt mounds in the region

Hisao and Wichaidit (1989) classified the distribution of salt mounds in the Northeast region as two groups; the isolated salt mound situated outside the villages and the composite mounds that is on the communities and originated as the result of the layering of foreign material carried in through salt-making, iron smelting, and pottery making. This classification is likely to be consistent with the recent archaeological and ethnoarchaeological studies (Rivett and Higham, 2007; Cawte and Bongsasip, 2009; Duke et al., 2010; สมเดช ลีลามโนธรรม, 2556; Yankowski and Kerdsap, 2013; Halliwell, Yankowski and Chang, 2016).

A large number of salt mound clusters scattered over the flood plain of Northeast region, particularly in the sub-basins of the Mun-Chi Basin such as the Upper Part of Lam Nam Mun (Rivett and Higham, 2007), Lam Choengkrai (Hisao and

Wichaidit, 1989), Lam Sa Thaet (Hisao and Wichaidit; สมเดช ลีลามโนธรรม, 2556), Lam Sieo Yai (Higham, 1977, 1996; Hisao and Wichaidit), Huai Aek, the Second Part of Lam Nam Chi, the Third Part of Lam Nam Chi, Huai Luang, and the Upper Part of Lam Pao (Hisao and Wichaidit). However, salt mounds are concentrated in the hilly area that rock salt members are exposed or close to the surface, and because of this, salt crust on the valley slope is remarkable (Takaya et al., 1984 quoted in Hisao and Wichaidit).

2.3 Defining archaeological site boundaries

The classification and designation of the site border should be one of the main results of the site area survey. Accordingly, the establishment of the site's limit is an essential consideration because it should include all the resources that contribute to the significance of a place. The site border has legal and management impacts as it specifies the area that will be subject to regulatory control (Seifert, 1995).

Sutton (2016) proposed that site boundaries determination depends on some factors, including the distance between the two concentrations, the kinds of artefacts found, and the geography of the localities. Moreover, to define a site, there ought to be some detectable evidence of activity, such as the presence of artefacts, features, or ecofacts. A site needs to have a geographic boundary that separates it from other sites because sites are also logical units - constructs that archaeologists apply to collect the record of the past organized.

National Register of Historic Places (1997) listed the following techniques for obtaining an indication to define site limits during archaeological assessment fieldwork such as surface observations, subsurface observations, observations of topography and other natural features, views of impacts and alterations, the background information study.

Nevertheless, the observed distribution of cultural features and artefacts is the primary criterion for establishing the site boundary. Other factors should be taken into consideration. The border should define the limits of the site and include all the factors, both cultural and natural, that contribute to its significance.

Archaeologists can define archaeological site boundaries on three types of boundary limits: natural site boundaries, observed site boundaries, or arbitrary site boundaries, or any combination thereof, according to the following hierarchy. Firstly, the natural barriers are those defined by the scope of a natural landform or physical feature, where it can be practically deduced that geomorphological site formation processes constrain the size of archaeological remains. Moreover, where the natural landform is significantly larger than the archaeological remains observed boundaries, professional judgment will be applied for determining whether a physical border or the marked border is affirmed, and thorough rationale will be determined in the site form. Next, the observed borders are those determined from the horizontal border of archaeological evidence detected on the surface, in exposures, or through subsurface testing during a field study. Mainly, observed boundaries will be drawn to capture the known extent of archaeological remains tightly; they should combine a modest buffer to mitigate spatial and investigative error. Lastly, arbitrary boundaries are the presence of existing disturbance or developments, or where sites extend beyond project area boundaries (British Columbia Association of Professional Archaeologists, 2012).

However, in the case of salt-making mound site boundaries, archaeologists use the landforms or natural site boundaries and the extent of the observed archaeological remains or observed site boundaries to define site limits. Also, when a natural landform forming part of a site boundary is significantly larger than the marked extent of one or more clusters of archaeological materials, they will use professional judgment to delimit or discrete sites located on that landform from a set distance.

2.4 Surface expression of salt structure, salt-affected soil, and salt-making sites

The distinctive topographic features of the earth's surface are the surface expression of specific internal earth processes. Accordingly, they refer to the form and pattern of forms expressed by a surficial material at the land surface. The study of both the quantity and characteristics of the surface expressions is one of the most critical factors to indicate soil and water salinity. The aim of surface expressions analysis from remote sensing data is to locate the potential areas for ancient salt-making by using the intensity and orientation of the topographic features as clues.

In this sense, archaeology, anthropology, geomorphology, geology, and knowledge about salinization can be used to interpret the surface expression of salinity and ancient salt-making mound site. Some of the lineaments and curvilinear are surface expressions of rock fractures that may provide pathways for the upward transport of groundwater from subsurface (Wannakomol, 2005). Also, pits, collapse sinkholes (Monjai, 2007), and the annular depression landform that are the solution phenomena or dissolution of the underlain shallow salt dome structure of the Maha Sarakham Formation (Supajanya et al., 1992).

Also, salt domes usually support the natural marsh areas with surrounded dunes

(นเรศ สัตยารักษ์ และ ทรงภพ พลจันทร์, 2533) and the severe salt-affected soil areas will be located in the lower fluvial terrace with little vegetation (สมนึก ผ่องใส, 2534).

Hisao and Pichai Wichaidit (1989) studied traditional salt production in Northeast Thailand. They had a hypothesis that corrosion of salt beds of the Maha Sarakham formation has been the primary factor in the topography development in Northeast Thailand. They presented the observation on salt-making, which seems to have its origin in the ancient period. Hisao and Wichaidit studied on the possible source of salt. Their observations indicate that contrary to the conventional view to presume thick clastic deposits are covering the Maha Sarakham formation; this formation is exposed precisely on the ground surface. Because of this situation, salt crust is so typical at valley floor where "short-distance interflow" seepages out — also, a sinkhole hypothesis on the topography of this region. Salt dome development and its collapse due to the salt corrosion are presumed to be the cause of sinkhole topography. Each salt dome development causes an anticlinal dome which can be identified as an assemblage of turtle-back shaped polygons in the aerial photographs. In the course of corrosion, anticlinal dome collapses. This phenomenon leads to the initiation of sinkhole topography. At advanced stages of corrosion, large-scale sinkholes are developed. This study presents a first approximation for demarcating anticlinal salt domes and sinkholes based on LANDSAT imageries. The results show mass movement phenomena caused by sinkholes. Laterite pan and gravel beds retard this mass movement process. They concluded that Khorat Plateau is a corrosion basin.

Supajanya et al. (1992) commented strictly about a relationship between the annular depression landform and the existing thick salt layers of the Maha Sarakham

Formation. Indeed, it is not found in the area covered by younger deposits except on a high terrace where thin alluvium might be expected. They also discussed the hypothesis of surface expression of the shallow salt dome that is an annular depression landform.

Sarapirome, Tassanasorn, and Suwanwerakamtorn (1995) studied on the geological structure as lineaments, curvilinear features, and associated depression areas in Chaiyaphum Province, where are underlain by the Maha Sarakham Formation, by using remote sensing data interpretation correlated with the field survey in salt-crusted areas with saline-resistant crops (Figure 2.8). Moreover, various sizes of curvilinear features have a close relationship with salt domes like the previous studies (Hisao and Wichaidit, 1989; Supajanya et al., 1992).

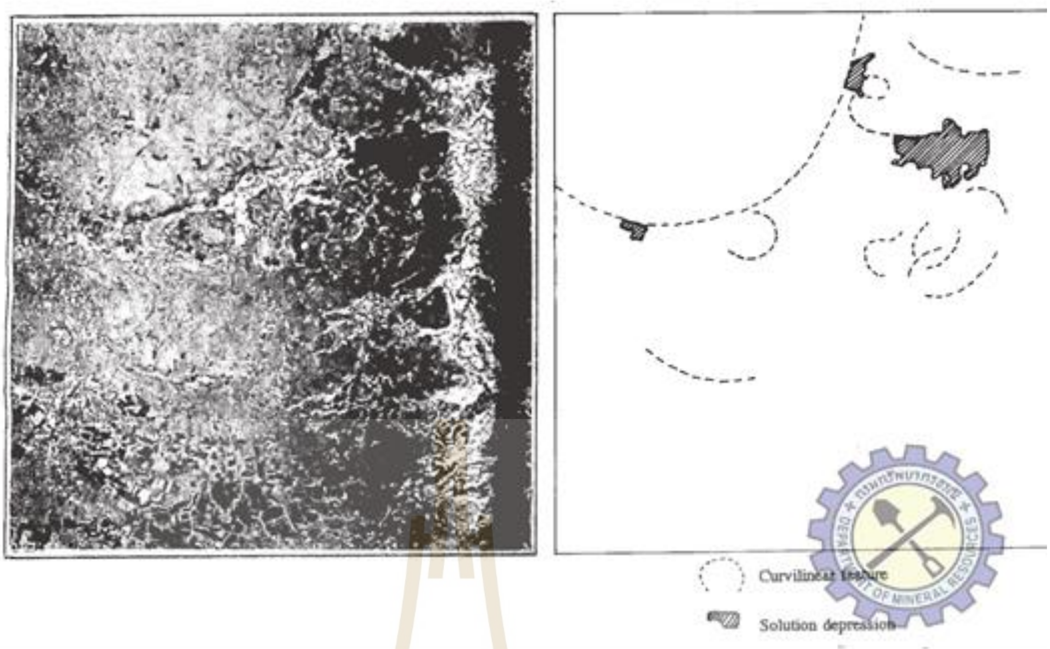

Figure 2.8 Interpretive curvilinear features and solution depression by using Radar images interpretation.

From Sarapirome et al. (1995).

Besides, from observing the physical characteristics of vegetation and soil, such as halophytic plants and the surficial salt crust that crumbles with a noisy crackling sound when stepped on, local salt-makers can select a potential area for salt-making (Thanaphattarapornchai, 2013). This skill that has been handed down for centuries is consistent with other surface expressions interpretations.

In the field conditions, the barren spots, stunted plants and the presence of white salt crusts or surface salt crystallization in as the results of evaporation, salt precipitation, and salt solution into the soil profile can indicate saline soils (FAO, 1988). Thus, they are significant indicators and levels of salinity and noticeable salt-making. The extent and frequency of bare spots are often an indication of the salt concentration in the soil. If the salinity level is not adequately high to cause barren places, the crop appearance may be irregular in vegetative vigour (FAO.org, www, 2013b).

Moreover, the integration of surface expression of salt and characteristic of salinized environments such as vegetation, indicator plant species, and salinity with surface expression of salt-making areas can be used for locating the potential salt-affected areas where are always correlated to ancient salt-making sites.

2.5 Remote sensing techniques for soil salinity and archaeological studies

2.5.1 Remote sensing applications for salt-affected soil detection

Remote sensing is a beneficial tool, which contributes to the detection of salt-related surface features (Qing, Yu, Li, and Deng, 2005, quoted in Meléndez-Pastor, Navarro-Pedreño, Koch, and Gómez, 2010). It offers the capability of rapid and synoptically monitoring of large areas (Wannakomol, 2005; Andrew and Ustin, 2008, quoted in Melendez-Pastor et al., 2010). Moreover, remote sensing is not limited by extremes in terrain or unsafe condition. Commonly, remote sensing should be integrated into the early stages of investigations and be combined with traditional mapping techniques (Wannakomol), and the other geospatial technology tools that can help much in mapping and monitoring soil properties, in particular, soil salinity.

Likewise, a variety of remote sensing data and techniques has been successfully used for mapping soil salinity to map salt-affected soils (Douaoui, Nicolas, and Walter, 2006; Farifteh, Farshad, and George, 2006; Mougenot, Pouget, and Epema, 1993). Especially when a salt-related symptom such as salt crusts is visible on the bare ground, in which case salinity is previously in an advanced stage of the salinization and the alkalinization process that the soil surface is already affected. The salinization process, which is a dynamic process and may vary seasonally, often starts in the subsoil and gradually develops upward. Salinity mapping can be more complicated when soil moisture affects the surface reflectance, especially in the visible portion of the spectrum. This mapping is usually based on the correlation between salt content in the soil and reflectance. Mapping scales vary according to the spatial and spectral resolutions of the sensors and the type of products generated. Additionally, satisfactory results have been obtained from bare soil with large salt contents.

In conclusion, remote sensing can be applied to salt-affected soil detection using remote sensing indexes such as NDSI and visual and automated image interpretation, such as supervised interpretation.

Remote sensing indexes

Ordinarily, remote sensing indexes such as salinity index (SI), normalized differential salinity index (NDSI), and brightness index (BI) are useful for predicting salinity and sodicity (Aldakheel, Elprince, and Al-Hussaini, 2005). Additionally, Khan, Rastoskuev, Sato, and Shiozawa (2005) proposed that the best classification results of salt-affected areas using salinity indexes could be achieved for the dry season. In the same way, in Thailand, salt crusts that are visible on the bare ground, typically occur in the dry season, where salt-makers start their salt-making activities.

Khan et al. (2005) studied monitoring irrigated saline soils of Faisalabad, Pakistan using GIS and remote sensing data acquired from the Indian Remote Sensing satellite (IRS-1B). Accordingly, they analyzed the effectiveness of several indicators for the presence of salts in the area in terms of salinity indexes; SI, NDSI, and NDVI. The best classification results could be achieved for the dry season, but not in wet or high-temperature periods.

The potential salt-affected area identification from image classification can be operated through NDSI (สุพรรณี ปลัดศรีช่วย, 2551; Wannakomol, 2005; Khan et al., 2005). The NDSI is basically the difference between the red and near-infrared band combination divided by the sum of the red and near-infrared band combination. The algorithm used is:

$$NDSI = (Red - NIR) / (Red + NIR) \tag{1}$$

Calculation in this way usually results in values between -1 and 1. The higher values indicate a more bare-soil presence.

Remotely sensed image interpretations

In visual image interpretation, the existence of salt is inferred from photographic elements and landscape features such as position in the landscape, drainage, condition, grey tone, the surroundings lithology, vegetation, and land use. However, salt detection is often satisfactory when aerial photographic interpretation is combined with satellite data analysis. The difference in surface reflectance helps separate salt-affected soils from non-affected ones. However, the detection of saline soils can be inaccurate by lack of specific absorption bands of some salt types, limited accessibility of satellite sensor data with the high spectral resolution, and unpredictability of saline soils in time and space (Metternicht and Zinck, 2003).

A variety of remote sensing data is available for salinity mapping and monitoring, then many researchers have applied some techniques together to map and monitor saline soils (Metternicht and Zinck, 2003). The application of remote sensing to soil properties quantitative evaluation was reviewed by Ben-Dor (2002). For the specific case of soil salinity and salt-affected soils, the literature reviews were reported by Metternicht and Zinck (2003) and Mougenot et al. (1993).

In Egypt, Masoud and Koike (2006) have monitored and detected salinization from changes in surface characteristics, expressed from vegetation indexes and tasseled cap transformations, and changes in radiometric thermal temperature, and linked its acceleration to a specific year.

Douaoui et al. (2006) illustrated the integration of electrical conductivity data and satellite images using geostatistical methods for better detection of salinity hazards.

In Israel, Ben-Dor, Patkin, Banin, and Karnieli (2002) processed hyperspectral airborne sensor data to yield quantitative maps of soil salinity. They studied a representative set of soil samples for laboratory determinations, with organic matter content, pH, and electrical conductivity, and this was followed by the selection of the most correlated spectral bands with the measured soil properties.

Howari, Goodell, and Miyamoto (2002) used supervised classification, spectral extraction, and matching techniques to investigate the types and occurrences of salts in the semiarid regions of the United States–Mexico border areas.

In China, Peng (1998) applied an approach combining Landsat TM data transforms with the depth and mineralization rate of groundwater to map soil salinity.

As for Northeast Thailand, Sarapirome et al. (1995) investigated geomorphology and geology of Chaiyaphum area, Thailand by using the air-borne radar images visual interpretation and field check. Besides, Wannakomol (2005) mapped the distribution of saline soil at the surface of the western part of the Khorat Basin. The study about the correlation of salt-related features visible in the remote sensing data, including Landsat 5 (TM), Landsat 7 (ETM+) and ASTER, developed assumptions on relationships between characteristic salt-related features in the remote sensing imagery and related subsurface condition. Then, this study outlined concepts on the development in soil salinity and investigated the differentiation between saline and non-saline soil by differences in their spectral properties.

2.5.2 Remote sensing applications for archaeological study

Most archaeologists applied remote sensing for the problem of finding, identifying, and archaeological mapping features. Naturally, there has been continued use of aerial photography. However, most researches have taken advantage of satellite imagery such as SPOT, Landsat, ASTER, IKONOS, QuickBird, and CORONA (Altaweel, 2005; Challis, 2007; De Laet, Paulissen, and Waelkens, 2007; Lasaponara and Masini, 2006).

Advances in GIS and remote sensing have promoted the creation of digital maps that now regularly include thousands of individual features spaced over large study areas. However, for practical application in archaeological projects, proposed the method to select the most applicable remote sensing data and analytical techniques for archaeological projects needs consideration about the resolutions of remote sensing data that relate to the physical environment of the study area in term of landscape types and archaeological site types (Parcak, 2009).

2.6 Spatial modeling

2.6.1 Concepts and theories

Logistic regression model (LR)

Regression can be considered a method to obtain the coefficients of empirical relationships from observations. Commonly regression approaches consist of linear regression, log-linear regression, and logistic regression. Ordinarily, logistic regression, a multivariate analysis model developed by McFadden (1973), is a statistical technique that involves one or more independent variables to predict the probability of a binary response (Hosmer and Lemeshow, 2000). Consequently, logistic regression aims to find the best model to describe the correlation between a dependent variable and multiple independent variables (Lee, 2005). The key to logistic regression is that the dependent variable is dichotomous. The independent variables in this model are predictors of the dependent variable and can be measured on a nominal, ordinal, interval, or ratio scale. The relationship between the dependent variable and independent variables is nonlinear. Logistic regression describes the correlation between a categorical or binary dependent variable and one or more continuous, categorical, or binary explanatory variables derived from samples and yielding the coefficient for each variable. Accordingly, the independent variables in this model can have a value of zero and one, representing the absence and presence of them. Model outcomes between zero and one show the potential of the ancient salt-making site occurrence. The general form of LR is as follows:

$$y = a + b_1x_1 + b_2x_2 + b_3x_3 \ldots + b_mx_m \quad (2)$$

$$y = \log_e \left[\frac{P}{1-P}\right] = \text{logit}(P) \tag{3}$$

$$P = \frac{e^y}{1+e^y} \tag{4}$$

Where $x_1, x_2, \ldots, x_m$ are explanatory or independent variables, and y is a linear combination function of the explanatory variables representing a linear relationship. The parameters $b_1, b_2, ., b_m$ are the regression coefficients to be estimated. If y is denoted as a binary response variable (0 or 1), value 1 ($y = 1$) means the presence of a site, and value 0 ($y = 0$) indicates the absence of a site. P refers to the probability of the occurrence of a site, i.e., $y = 1$. Function y is represented as logit (P), i.e., the log (to base e) of the odds or likelihood ratio that the dependent variable y is 1. The probability P is strictly increasing when the value of y increases. Regression coefficients $b_1, ., b_m$ show the contribution of each explanatory variable on probability value P. A positive sign means that the explanatory variable supports to increase the probability of change, and a negative sign implies the opposite effect. The statistical technique is a multivariate estimation method that examines the relative strength and significance of the factors.

Frequency ratio model (FR)

The frequency ratio is the ratio of occurrence probability to non-occurrence probability, for specific attributes. It can provide a simple geospatial evaluation tool to calculate the probabilistic correlation between dependent and independent variables, including multi-classified maps (Oh, Kim, Choi, and Lee, 2011). The frequency ratio approaches based on the observed relationships between an event, and each related factor is determined. The relationship analysis is the ratio of the area where the events occurred to the total area. A value of 1 indicates an average value, a value greater than 1 shows a high correlation, and a value less than 1 indicates a lower correlation (Oh, Lee, and Soedradjat, 2010). Application of the frequency ratio method is simple, and the results are easy to understand (Lee and Talib, 2005; Yilmaz, 2007). The frequency ratio model is applied to a variety of mappings namely, landslide susceptibility mapping, forest fire susceptibility mapping, urban prediction (Park, Jeon, and Choi, 2012), flood susceptibility mapping, and predictive site modeling (Clark and Hebert, 2008). In the case of ancient salt-making mound sites, frequency ratio approach is based on the observed relationships between the distribution of ancient salt-making site and each salt-making-related factor, to reveal the correlation between salt-making site locations and the factors in the study area.

A table will be constructed to contain each salt-making-related factor to calculate the frequency ratio. Then, the ratio salt-making occurrence and non-occurrence will be estimated for each range or type of factor, and the area ratio for each interval or kind of factor in the total area will be calculated. Finally, the frequency ratio for each range or type of factor will be calculated by dividing the salt-making-occurrence ratio by the area ratio. The calculation steps for a frequency ratio for a class of the salt-making site-related factors are below:

$$FR = \frac{A/B}{C/D} = \frac{E}{F} \tag{5}$$

Where A is the area of a class for the factor; B is the total area of the factor; C is the number of pixels in the class area of the factor; D is the number of total pixels in the study area; E is the percentage of area with respect to a class for the factor;

F is the percentage for the entire domain; and frequency ratio is the frequency ratio of a class for the factor.

After frequency ratio calculation, the ratios for each factor type are used to add for calculating the index. For a probability map, each factor's frequency ratio values with each factor given the fixed weight of 1 will be summed to the training area as:

$$I = Fr1 + Fr2 + \ldots\ldots + Frn \tag{6}$$

Where I is the probability index; *Fr* is the frequency ratio of a factor or rating of each factors' type, and *n* is the total number of input factors.

In the relation analysis, a value of 1 is an average value or mean. If the ratio is greater than 1, it means a higher correlation between an area and the specific factor's attribute; and if the value is less than 1, it means a lower correlation.

2.6.2 Previous studies on saline soil classification using spatial modeling

In Northeast Thailand, the spatial modeling with the integrated datasets of GIS data layers and remote sensing data is the principal procedure for salt-affected soil mapping or soil salinity potential area.

สมนึก ผ่องใส (2534) studied GIS technology and satellite image data for saline soil mapping in the Nam Sieo Watershed area, Maha Sarakham Province, and land ecosystem and soil fertility assessment in Muang Ubon Ratchathani District, Ubon Ratchathani Province. For spatial modeling, GIS database was composed of layers of geology, groundwater quality and its yield, land cover, and terrain. After rasterization and overlaying by using high salinity area criterion including the Maha Sarakham Formation underlies areas, low water quality and yield, the weak vegetation cover, the lower terrace location, the resultant map obtained has four classes of salinity. For reliability evaluation, the result with the existing saline soil map and field investigation were compared.

Mongkolsawat and Paiboonsak (2006) studied soil salinity potential area in the Northeast region. For providing the spatial distribution of severity classes of soil salinity, GIS data layers were used for overlay modeling with defined criteria. The data layers comprise the geologic formation, groundwater quality, and its yield, land cover, and landform. The salinity classes were randomly checked against the salt crust map performed by the Land Development Department.

ชรัตน์ มงคลสวัสดิ์, สถาพร ไพบูลย์ศักดิ์ และ บังอร ยมมรคา (2550) used GIS and remote sensing technology for setting up a saline soil database. Similarly, สุพรรณี ปลัดศรีช่วย (2551) evaluated the surface state of the Khorat Plateau by using the salinization relate-factors data layers and satellite data indexes, including the brightness index, normalized difference salinity index and the 1^{st} components of principal component analysis. The correlation between soil salinization and satellite indexes was performed to select the index to be used for the integration. The result indicated that the correlation between soil salinization and the normalized difference salinity index was high. The spatial model is an integration of geology, groundwater quality, and irrigation areas that occur in the low terrace and the area of high-normalized difference salinity index. The establishment of the GIS database for these layers was performed. Then, the overlay operation was undertaken with criteria showing the severity of salinity. The result obtained illustrates the distribution of soil salinity potential class in the combination of its acreage for each class.

2.6.3 Archaeological predictive modeling application

The analysis of the human site location in ancient times has always been an essential topic in archaeology. Moreover, the use of predictive modeling has made a significant role in this study. Predictive modeling is a technique that tries to predict the location of archaeological sites or materials in an area, based either on a sample of that region or on fundamental notions concerning human behavior (Kohler and Parker, 1986). Predictive modeling departs from the assumption that the location of archaeological remains in the landscape is not random, but is related to specific characteristics of the natural environment. The nature of these relations depends very much on the landscape characteristics involved, and the use that early people may have had for these characteristics, then it is assumed that particular portions of the landscape were more interesting for human activity than others. Nowadays the two primary purposes for applying predictive modeling in archaeology are: to archaeological site locations to guide future developments in the modern landscape and an archaeological heritage management application; to gain insight into past human behavior in the landscape for an academic research application (Kamermans, 2010).

Burke, Ebert, Cardille, and Dauth (2008) capitalized on the close relationship between primaeval huntsman and prey to acquire spatial models for the study of land-use patterns. They built upon a basic GIS model, including standard environmental variables adding a paleoethological variable in the form of range reconstructions for the locally dominant, prehistoric human prey species: *Equus hydruntinus*.

Espa, Benedetti, De Meo, Ricci, and Espa (2009) studied predictive modeling based on the combined use of statistics with GIS technology. The geographic information from remotely sensed data helped to identify the presence of unknown sites in the Cures Sabini archaeological area. Their study aimed to implement a GIS-based predictive model to produce probability maps of archaeological site locations by using Classification and regression trees (CART) model.

Vaughn and Crawford (2009) used binary logistic regression to identify potential archaeological areas in a portion of northwestern Belize. The predictive modeling procedure involves remotely sensed imagery, GIS data and techniques, and multivariate statistical approaches. Predictive variables signify both the pre-historic current landscape of the ancient Maya and the present-day physical scene. The predictive model identifies several regions of high archaeological probability, including areas that are unlikely to contain any archaeological remains. Results can be used to inform future field surveys in a more cost-efficient manner.

CHAPTER III

MATERIALS AND METHODS

The scope of this study will be focused on using logistic regression and the frequency ratio method for predicting ancient salt mining areas. The conceptual framework of the study is shown in Figure 3.1

As mention above, this study contains two research objectives: the first is to determine the relationship between physical and cultural characteristics of existing ancient salt-making sites and apply it to discovering potential sites. The second is to validate and compare the results of predicted ancient salt-making potential areas from two different methods; the logistic regression model and frequency ratio model. The research procedures in detail are described as follows:

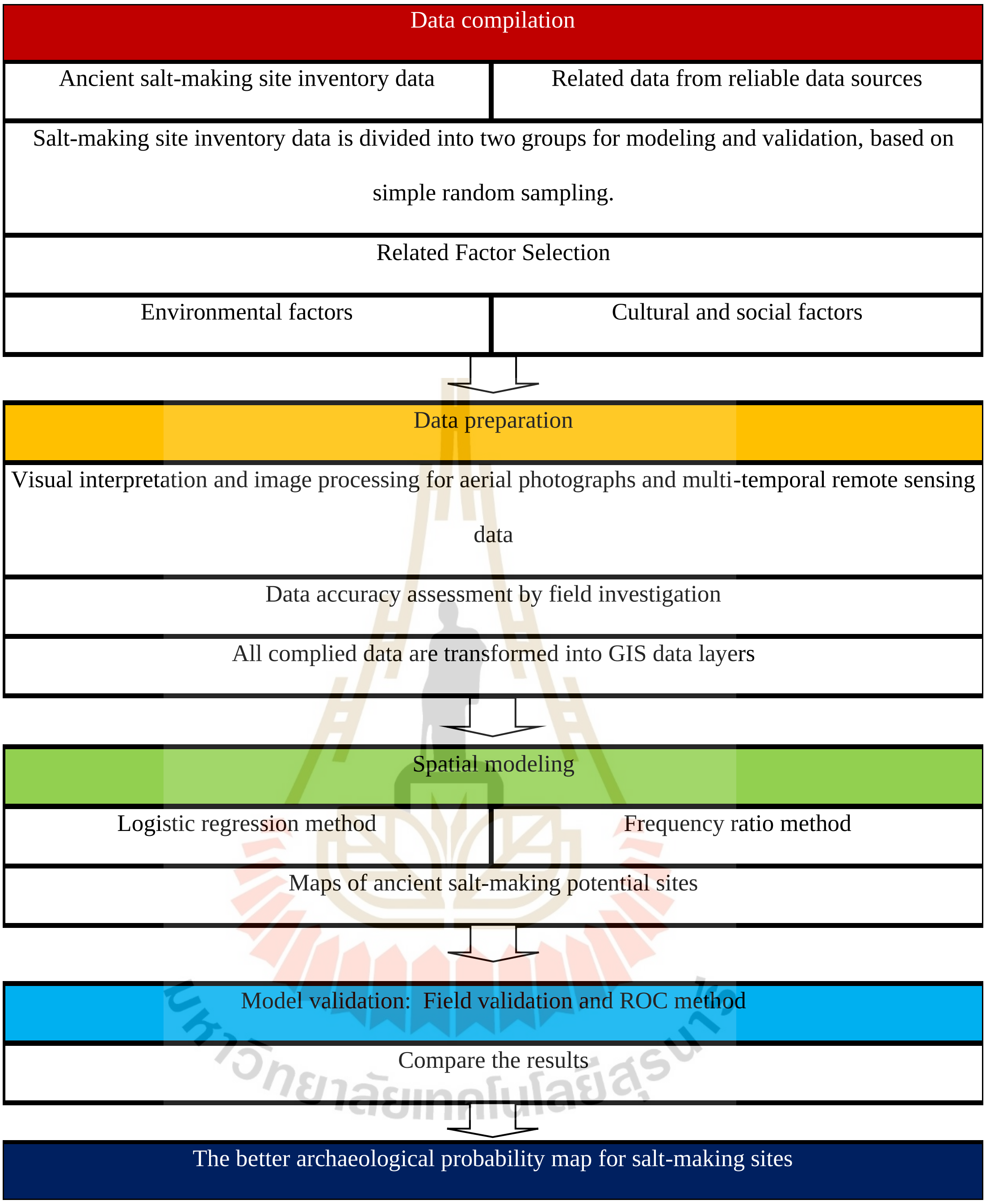

Figure 3.1 Conceptual flowchart of data processes for mapping the salt-making site probability.

3.1 Data collection and preparation

From the review in previous chapter, data from prior cultural studies such as archaeology, ethnography, ethnoarchaeology, anthropology, and historical documents in the study area and the vicinity where ancient salt-making sites located were used to analyze their locations and environment, sources, working behavior, and land-use patterns in ancient salt-making activities including relationships with the nearby ancient communities. Also, the surface expression analysis can indicate the environment or physical characteristics which dominate potential areas having salt source and capable of being developed to be ancient salt-making sites. Then, field data are acquired for more understanding the physical characteristics of existing ancient salt-making sites and the surroundings.

As mentioned above, it seems that several data factors are influencing how ancient people chose sites for salt mining. However, the data factor selection for the study can be constrained by their availability and difficulty in preparation. Because of these constraints, there are not many factors left as input for the analyses. To achieve the objectives of the study, the factors selected for this study were based entirely on theories of archaeology and geology (as comprehensively reviewed in Chapter II) including their recent availability, not gathering from any possible factors for subsequent statistical proving treatment. If results from statistical treatment were valid but not agreed with those back-up theories, it can be misled in applying them.

Nevertheless, for the LR model analysis, statistics were not ignored. It was used to reorganize data factors to be more statistically acceptable as much as possible, particularly the transformation of input data factors to be a normal distribution. This process might not be able to achieve a normal distribution of all data factors entirely, but the original data were transformed to be close to a normal distribution as much as possible. However, if the original data were better normal distributed than the transformed ones, they would be kept as they were for the input of the analysis. The test of normal distribution was operated on 411 points of existing ancient salt-making sites. It could assure that this method was timely optimal to achieve acceptable results from the analysis.

Data factors were selected in two groups, namely environmental and cultural and social factors. GIS and RS technology were applied to extracting and preparing data into contents and formats proper for the analysis of potential ancient site prediction. This analysis aimed to increase more chance to discover new ancient salt-making sites. It could be strongly related to the potential area of ancient people capable of being developed as salt-making sites. The factor data are described and discussed in the followings.

3.1.1 Related Factor Selection and their data preparation

From previous archaeological and anthropological researches in this region, the occurrence of ancient salt-making sites correlated highly with saline soil areas, traditional salt-making techniques, and settlement and water in the proximity. (ศรีศักร วัลลิโภดม, 2535; Nitta, 1992; Rivett and Higham, 2007). All selected factors were extracted to be variables used for spatial modeling. These variables were refined and manipulated to be a GIS data format fit for incorporation in modeling as shown in Table 3.1. The table shows a list of primary and secondary data as sources for data factor preparation.

Table 3.1 Details of the data used in this study.

Data	Scale/ Spatial resolution	Data type	Year	Source	Variables
Geological map	1:250,000	Polygon	2007	DMR	Locating on geologic formations
Geological structures and features	1:250,000	Line/polygon	2007	DMR	Distance to geological structures
Soil salinity map	1:50,000	Polygon	2007	LDD	Locating on salt crust area and saline wet belt
Terra-ASTER imageries	15 m	Grid	2002 to 2004	SUT	NDSI
Ancient salt-making site inventory map	-	Point	2011	FAD	Locations of salt mines
Ancient settlements	-	Point	2011	FAD	Distance to ancient settlements
Waterbody and stream	1:50,000	Line/polygon	2003	RTSD	Distance to water bodies and streams

They are described in the followings in terms of their influence on selecting areas to be ancient salt-mining sites.

Environmental factors:

Generally, a set of environmental factors relates to salt resource and its movement and accumulation in the soil. These factors are briefly described as follows:

1) Locating on the Maha Sarakham Formation (KTms) Quaternary sediments (Qa), and Terrace deposit quaternary (Qt)

Geologic materials are very variable in their elemental composition, and some formation can have higher salts than others. Thus, the kinds of geologic formations through which the drainage water passes importantly influence the composition and total concentration of salts (FAO.org, www, 2013a). As discussed in the previous chapter, the geology of the Maha Sarakham Formation in the Khorat Group contains layers of salts. Wherever in this Formation having shallow salt layer associated with structures tend to bring the salt up to the surface, that area has more chance to provide the higher potential of saline soil. Even though these areas have covered by thin Quaternary sediments of alluvium and terrace, they can still be identified as the potential areas.

Geologic map of the study area (กรมทรัพยากรธรณี, 2550) in the form of GIS data layer showing spatial distribution, the Maha Sarakham Formation was adopted to be used in the study. The study area falls into only the areas of the

Formation and thin Quaternary sediments overlaying on it. Therefore, the presence of potential area is firstly dependent on the binary decision whether the target area locates on the Formation or not. However, in varying units like the Maha Sarakham Formation, Quaternary alluvium and terrace deposit on top of the Formation, there are different potential as well. For the FR method, there is no problem applying information of these units to the analysis. But for the LR method, instead of using arbitrarily ordering scores for these units, FR index of each unit could be better to be applied as its score. This could be more reasonably objective transformation to the factor units.

2) Distance to geological structures

The studies of Hisao and Wichaidit (1989), Supajanya et al. (1992), นเรศ สัตยารักษ์ และ ทรงภพ พลจันทร์ (2533), and Sarapirome et al. (1995) revealed that geologic structures such as curvilinear, crack, and fault allow surface water flowing down to become saline water when reacting with underneath salt and evaporating up to be salt crystals. Shallow saline underground water can also be evaporated up to surface forming salt crystals. The spreading of the accumulation of these salt crystals can cause the occurrence of salt crust and saline soil in the areas nearby those structures. Additionally, the salt dome is also the structure associated with shallow salt underneath and is the area having high prone for salt to expose. Therefore, distance to these structures closely relates to the occurrence of salt crust or potential area. The area closer to the structures indicates a higher potential. GIS data layers of geologic structures (Wannakomol, 2005; กรมทรัพยากรธรณี, 2550; กรมทรัพยากรธรณี,

2553) were used in the model analysis. The visual interpretation of aerial photographs of the Land Development Department (กรมพัฒนาที่ดิน, 2555) was operated to cross-check the data. It is noticeable that geologic structures like cracks and faults will appear as lineaments in RS data interpretation due to lacking detectable offset movement.

Minimum distance to structures of each raster cell was extracted using Euclidian distance function of ArcGIS^{TM} software. The resulting raster layer was used as independent variable input for the regression analysis of the LR model.

For the FR analysis, the geological structure features were buffered to distances of 500,1,000, 1,500, 2,000 and 2,500 m based on the spreading of existing salt mines discovered in the previous archaeological field survey (กรมศิลปากร, 2534; สมเดช ลีลามโนธรรม, 2556).

3) Locating on salt crust area and saline wet belt

Related to the structures discussed above, salt crust area and saline wet belt are surficial evaporite areas and identified as actual potential areas for salt mining. This zone is evident by several discovered ancient salt mines which are always associated with these surface features. The Land Development Department prepared the data on the salt crust area and saline wert belt used in the model analysis. The areas can be indeed validated by field check. They always show almost non-vegetated or bare soil where is plenty of salt crystals on the ground and there are only a few kinds of salt-resist plants growing on it.

The data factor was classified to be nine classes. As same as geology data factor, for LR model analysis, each class of this data factor was scored using FR index.

4) NDSI

Due to having high reflectance, salt crust area is detectable using RS indexes. Based on several previous studies as reviewed in the previous chapter, the NDSI was selected to be the index expressing potential areas. A crop can scarcely stand on a salt-affected soil, even without surficial salt appearance. This situation causes it having more outstanding surface reflectance than that of the area with healthy vegetation and salt-free soil. However, using this index, the interpreted salt crust area can be confused with bare soil or some prepared ground areas after harvesting. It, therefore, can provide a more satisfactory result when aerial photographic interpretation is combined with satellite data analysis, especially indexes from satellite data. This reason is why the factor like geologic structures resulted from visual image interpretation was involved in the analysis. The NDSI in this study was derived from ASTER data and applied to the model analysis.

Remote sensing data used in this study were taken by the Advanced Spaceborne Thermal Emission and Reflection Radiometer (ASTER). The ASTER Level-1A data covering the study area was acquired on the dry season when the data can show outstanding reflectance of salt-affected soil. The dates of acquired data were December 7, 2001, December 23, 2001, January 1, 2002, December 6, 2002, January 17, 2002, February 2, 2002, December 17, 2004, and December 24, 2004, respectively. They consist of the image data without applying the corrections to the image data, thus maintaining original data values. Band 2 and 3N of the Visible and Near-Infrared (VNIR) with a spatial resolution of 15 m were applied to derive NDSI for further analysis in the models.

Cultural and social factors:

(1) Locations of salt mines

Locations of existing ancient salt mines in the study area were discovered by FAD's archaeologists (กรมศิลปากร, 2534; สมเดช ลีลามโนธรรม, 2556) and field investigation during this study. Figure 3.2 shows examples of ancient salt-making sites in the color aerial photograph and in the field. Only locations of 411 sites were discovered and used in the analysis. They were separated to be two groups of 289 for LR model building and for FR method to extract the frequency ratio of each data factor and the rests were for validation of the models. To work as a dependent variable in the regression model, the model needs the quantitative attribute of a salt mine. The data layer of presence or absence (binary codes) of ancient salt-making site location in the study area was generated to serve this purpose.

(a)


(b)

Figure 3.2 Example of salt-making sites from the visual interpretation and field survey at Ban Bing, Non Sung District, Nakhon Ratchasima Province. (a) Color aerial photograph of salt-making sites. (b) The landscape of sites in the field.

(2) Distance to ancient settlements.

Culturally, the distance to ancient settlements to the potential salt-affected area can actively control where the area should become mine. The distance should not be too far to walk back and forth in a day and should not be too close to disturb the living as same as the distance to geologic structure, the raster data layer of distance to the settlement was prepared from an ancient settlement data layer (กรมศิลปากร, 2554). Minimum distance to ancient settlements of each raster cell was extracted using Euclidian distance function of ArcGIS^{TM} software. The resulting raster layer was used as independent variable input for the regression analysis of the LR model.

The distance over 6,000 m from a settlement to a salt mine is too far for human walking ability to be back and forth in a day frequently. For the FR method, different ranges of the walking ability of human beings were separated to be <1,000, 1,000-2,000, 2,000-3,000, 3,000-4,000, 4,000-5,000 and >5,000 m. These ranges were applied to buffering distances from ancient settlements.

(3) Distance to water bodies and streams.

As known, the ancient salt-making process was very approximately related to distance to the source of water. The closer distance implies more potential salt-making because water is needed in the process. In the dry season, from January to May, the natural brine in salt-affected soil areas will crystallize into salt without difficulty because of appropriate climatic condition. After scratching the salt crust around the swamp, they dissolved it in the water, percolated, filtered, and boiled it in the vicinity. Firewood resource for boiling brine is located in the area near swamps as well. Today, some of the ancient salt-making sites in the lowland near the swamps are still used by local salt makers.

Again, the minimum distance to the water body of each raster cell was extracted using Euclidian distance function of ArcGIS™ software. The resulting raster layer was used as independent variable input for the regression analysis of the LR model.

For the FR analysis, the water body features were buffered to distances of 500, 1,000, 1,500, and 2,000 m as same as operating for distance to the ancient settlement.

3.1.2 Tools

The software employed for satellite image processing and spatial modeling in this study included:

- ArcGIS™ software
- ERDAS Imagine™ software
- IDRISI Selva software
- IBM SPSS™ software
- Microsoft Excel™ software

Equipment for the field survey included:

- Computer
- GPS
- Compass

3.1.3 Population / Samplings

There is no detailed ancient salt-making site data layer for Nakhon Ratchasima Province. Therefore, the map of salt-making site locations was prepared for this study, and the archaeological field survey confirmed this. In the ancient salt-making site inventory map, total *x* sites were identified in the study area, whereas (*x*-*y)* randomized numbers were generated and used as the test/validated salt-making sites. In other words, 30% of the total sites or the test sites were determined through randomization. The rests, 70% of the whole ancient salt-making sites or training sites were used in the analyses of FR and LR models. The test sites in the area were used only for validation of the analytical results (Figure 3.3).

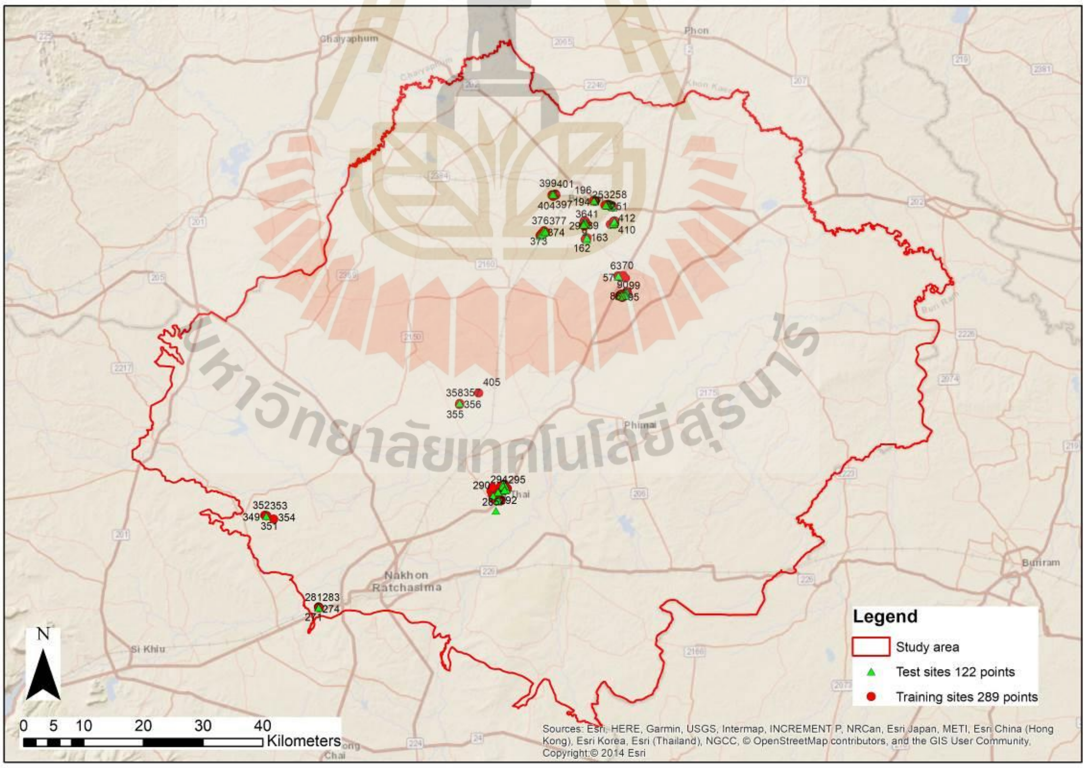

Figure 3.3 Distribution of existing ancient salt-making sites in the study area.

3.2 Using spatial modeling for ancient salt-making potential areas analysis

In the analysis, locations of salt-making sites are taken into consideration. More than 200 training sites in the form of points were used in the investigation. The site occurrence probability analysis was performed in the study area using the LR and FR methods. Accordingly, ancient salt-making sites and their related factors were considered to be variables responsible for the occurrence of sites. Likewise, in both methods, they were used to find the variable relationship specifically for each method and applied it to the finding operation of mining site occurrence probability. The result of the ancient mining site existence probability as a raster map of each method could be obtained.

3.2.1 Frequency ratio (FR) method

The spatial relationship between the event and each event-related factor can be analyzed by using the Frequency ratio method. This relationship is used to determine each factor's rating in the overlay analysis (Lee and Talib, 2005). For evaluating the contribution of each factor towards salt-making potential, salt-making site estimation group was overlaid with thematic data layers separately, then the frequency ratio of each factor's class was calculated in three steps. First, calculate the area ratio of salt-making site occurrence and non-occurrence in each factor's class. Then, calculate the area ratio of each factor's class to the total area of the factor. Finally, divide the salt-making occurrence ratio by the area ratio of each factor's class.

After the frequency ratio calculation, the ratio for each factor type was used for calculating the salt-making site probability index (SMSPI) by the use of the following equation.

$$\text{SMSPI} = Fr1(GF) + Fr2(GS) + Fr3(SC) + \text{Fr}4(NDSI) + Fr5(ARC) + Fr6(WA) \quad (8)$$

Where SMSPI is the salt-making site probability index; Fr_1 *to* Fr_6 is the frequency ratio or rating of each factor. A ratio value of 1 indicates an average value, a value greater than 1 shows a high correlation, and a value less than 1 indicates a lower correlation. The analysis was raster-based performance and resulted in a map showing SMSPI of each cell.

3.2.2 Logistic regression (LR) method

The inductive model of logistic regression analysis is the most basic predictive model that is used in various fields such as archaeology, ecology, wildlife biology, and soil for the binary response variable: presence or absence of the site in terms of probability mapping (Vaughn and Crawford, 2009). In general, the archaeological predictive model is the statistical and empirical relationship between the presence of archaeological evidence and the environmental factors such as soil type, elevation, slope, vegetation, water resources, geology, and landforms. Besides, this tool indicates the likelihood of encountering an archaeological site anywhere within a landscape. However, these are sometimes referred to as archaeological site probability maps or archaeological sensitivity maps because they show that some locations are more sensitive than others for cultural resources. These maps are beneficial for land-use planning and cultural resource management. If development projects can be modified to avoid zones where archaeological sites are predicted to occur, the result is more cost-effective planning. The reliability of these models is a function of their performance. Comparing a predicting model to archaeological field survey results can test this. Field-testing of a model is an essential component of demonstrating its reliability.

In the case of this research, logistic regression establishes a functional relationship between binary coded, presence or absence, of ancient salt-making site locations, as a dependent variable, and the various factors that have been identified as playing an important role in discovering the new ancient salt-making site, as a set of independent variables. These coefficients of the relationship serve as the weights in the algorithm, which were used in the analysis of GIS data layers to produce a map showing the likelihood of salt-making site probability. The *x* salt-making site-present pixels from the Fine Arts Department's database and related documents including additional field investigation were randomly selected to be (*x-y*) salt-making sites or test sites while the rests were used as training sites in the analysis. In this case, several training sites of existing ancient salt mines were 289 and of non-existing was 122 sites so that they could be consistent to samples used in the LR method.

It could be crucial to note that data of independent variables of all samples (existing salt-making sites) were checked and transformed to be normal distribution or as close as possible if required. The original data were compared to the transformed data using log10 and square root functions. The ones which were normal distribution or close to normal distribution the most were selected and then normalized for further input to the Ordinary Least Square (OLS) analysis. The selection of the better transformation method was fundamentally based on comparing skewness and the plot between expected normal and observed values. The original or transformed data with skewness closer to 0 is the better, while the more fit to a linear relationship between expected normal and observed values is the better. Multiple independent variables could have different normal distribution transformation methods. The specific methods were further applied to corresponding raster-based data layers of independent variables and then normalized before input to the regression model.

As known, geographic data have a spatial relationship among values of a variable according to the spatial arrangement of the values, called spatial autocorrelation (SA). The presence of significant SA proves the spatial dependency of data and encourage them to incorporate in the analysis. The spatial relationship expresses in three different ways, i.e. clustered, dispersed, and random. The Spatial Autocorrelation (Global Moran's I) was used in this study to check the spatial relationship of raster-based input data. If their spatial pattern is not random, they are valid for further spatial analysis (see Appendix A). If Moran’s I value is closer to 1 or -1, the data express a better correlation.

The Ordinary Least Square (OLS) function of ArcMap™ was used to estimate a set of model coefficients from samples. At the same moment, the Variance Inflation Factor (VIF) estimation was provided as well. The VIF measures redundancy of data among explanatory variables. Explanatory variables having VIF values larger than 7.5, or having too high redundant data with the former input variables should be removed (one by one) from the regression model (ESRI, 2012). A set of model coefficients from samples obtained from OLS was then used to calculate the salt-mining suitability using regression model for all cells in the study area by Raster Calculator tool within the GIS environment (Equation (2) in Chapter II). The data of independent variables as input to the calculation were obtained from the transformation process. Then logistic regression analysis (Equation (4) in Chapter II) of the salt-mining suitability raster layer was performed using the same tool so that the probability of the presence or non-presence in each cell of ancient salt-mining sites were able to estimate, resulting as a raster-based probability map.

As mentioned in Equation (2) in Chapter II, a set of variables accepted as influential predictors of salt-mining site occurrence for the logistic regression equations of the study are as follows:

The *P* value is the probability of ancient salt-making site occurrence, b_0 and b_1 to b_6 are the regression constant and regression coefficients that can be processed by using OLS analysis having a dependent variable (y), which is presented as binary code for existing or non-existing site. The predictive or explanatory variables consist of distance to geologic structures (GS), locating on salt crust area and saline wet belt (SC), NDSI, distance to ancient settlements (ARC), distance to water bodies (WA) and locating on the Maha Sarakham Formation and its related units or Geology (GF). To be able to determine the influence of each independent variable from a set of coefficients expressing their relationship to the existing salt-making sites, values of each independent variable were normalized to be between 0 and 1 before applying to OLS operation. This characteristic of it can be explained with supporting results from the FR method. The set of coefficients obtained from OLS analysis was then applied to regression analysis of transformed raster-based independent variables of the whole study area. The probability of site presence (P) ranges from 0 to 1 was then calculated as raster-based operation from the result of regression analysis and resulted in the probability map of ancient salt-making site occurrence.

The LR process can be generalized and displayed as a flowchart in Figure 3.4.

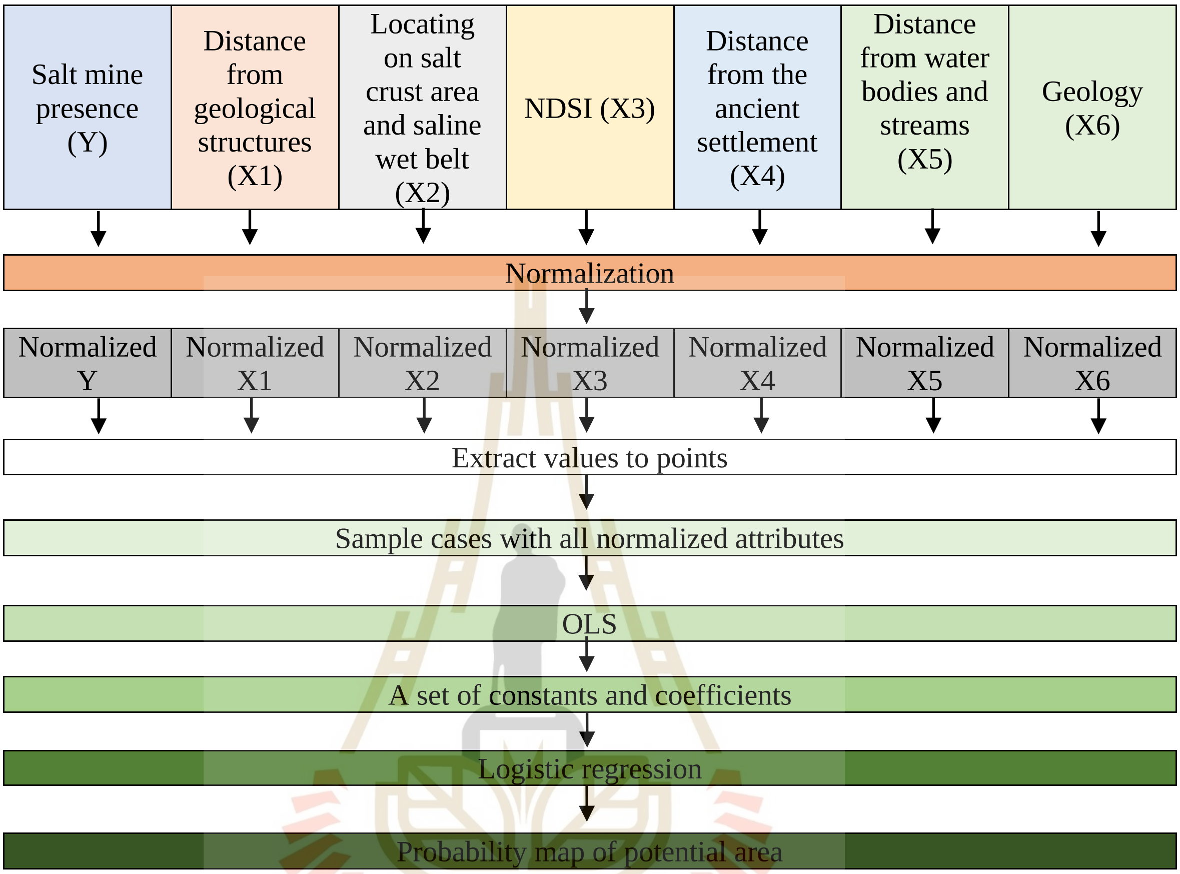

Figure 3.4 Flowchart for the LR method.

3.3 Validation and comparison of the model results

In this study, ancient salt-making site probability maps and a map showing SMSPI were prepared using the LR and FR models. The accuracy of each model result was evaluated by calculating relative operating characteristics (ROC) (Ozdemir, 2011). Then, the better model can be identified from the comparison of their ROCs.

CHAPTER IV

RESULTS AND DISCUSSIONS

The main results are described according to objectives of the study that has two parts, first of all as determination of the relationships between physical and cultural characteristics of existing ancient salt-making sites using the logistic regression model and frequency ratio and apply them to discovering potential sites and secondly as validation and comparison of the results of predicted ancient salt-making potential areas from these two different methods.

4.1 Factor data for modeling

The relevant factor data were listed and discussed in Chapter 3, how they could be related to or influence the locations of ancient salt mining sites. These include geology, distance to geologic structures, salt crust area and saline wet belts, NDSI, locations of salt mines, distance to ancient settlements, and distance to water bodies and streams. In order to determine the relationship of land and cultural characteristics to ancient salt-making sites, this set of factor data was prepared in the form of GIS data layers suitable for modeling operation. The result of data preparation is displayed in Figure 4.1. The training sites and validating/test sites were also shown in Figure 4.2.

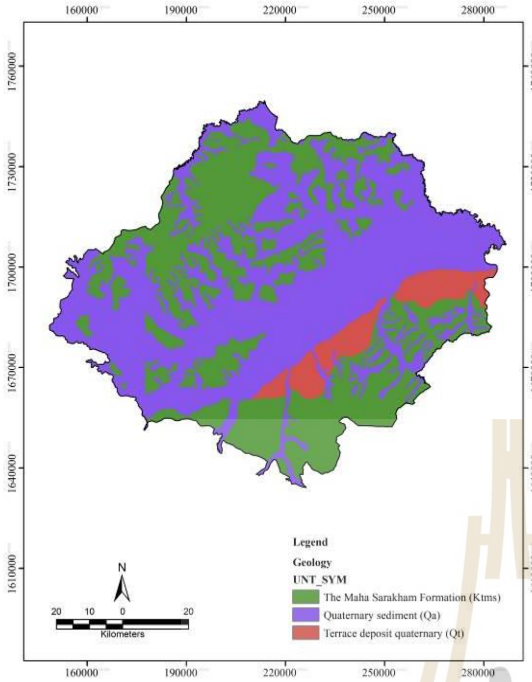

(a)

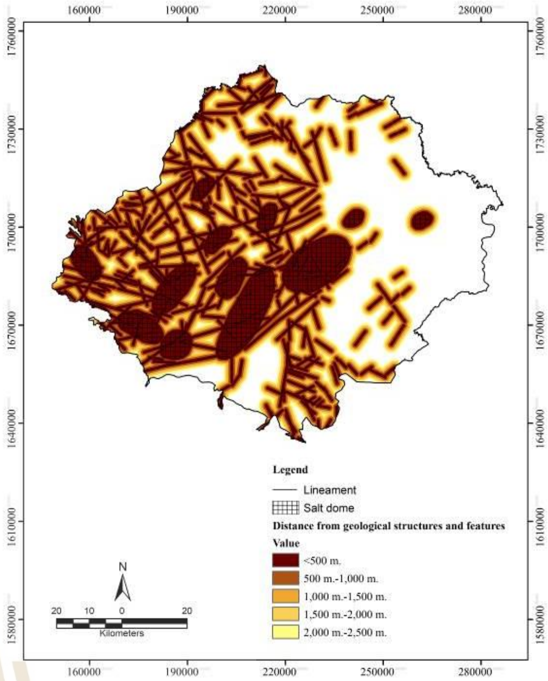

(b)

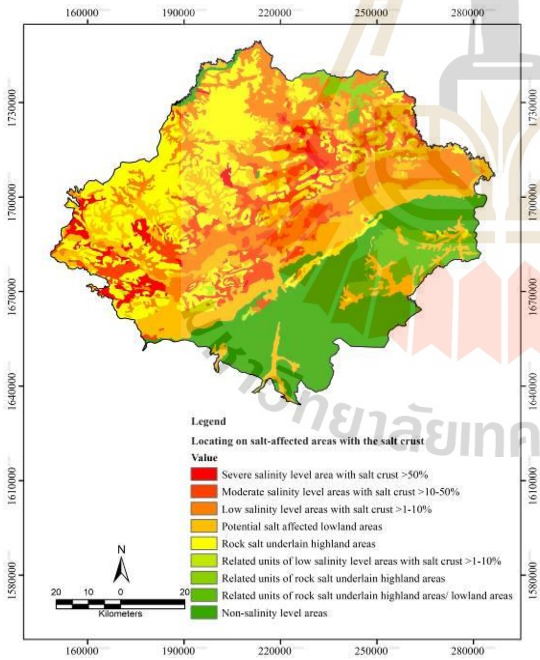

(c)

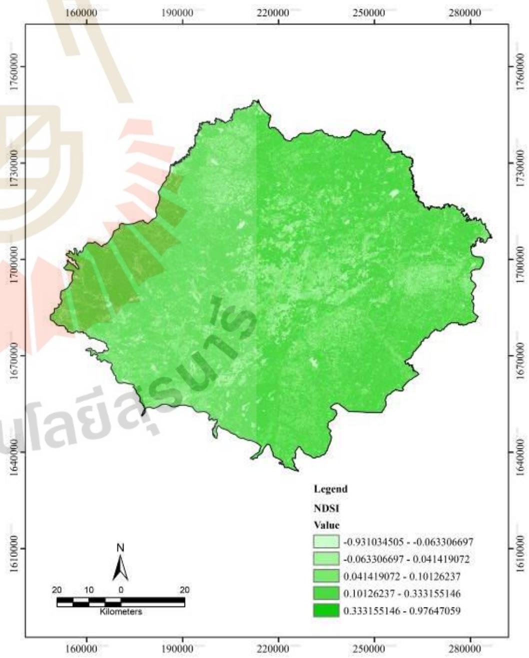

(d)

Figure 4.1 Factor maps in the form of GIS data layers. (a) Geology. (b) Distance to geologic structures. (c) Locating on salt crust area and saline wet belt. (d) NDSI. (e) Distance to ancient settlements. (f) Distance to water bodies and streams.

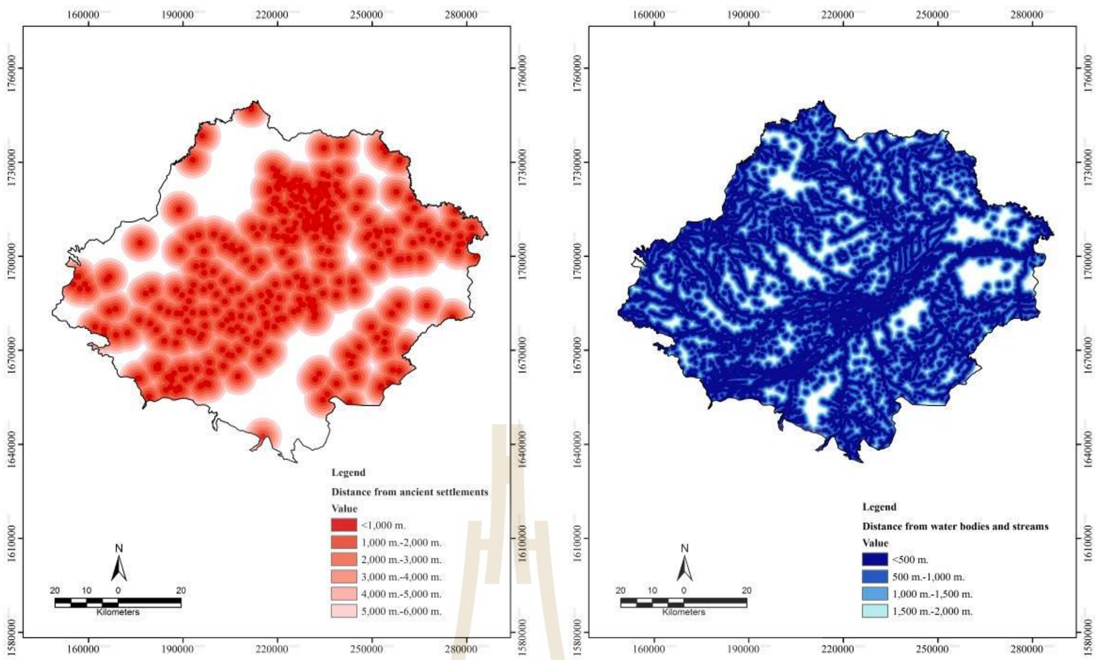

(e) (f)

Figure 4.1 (Continued) Factor maps in the form of GIS data layers.

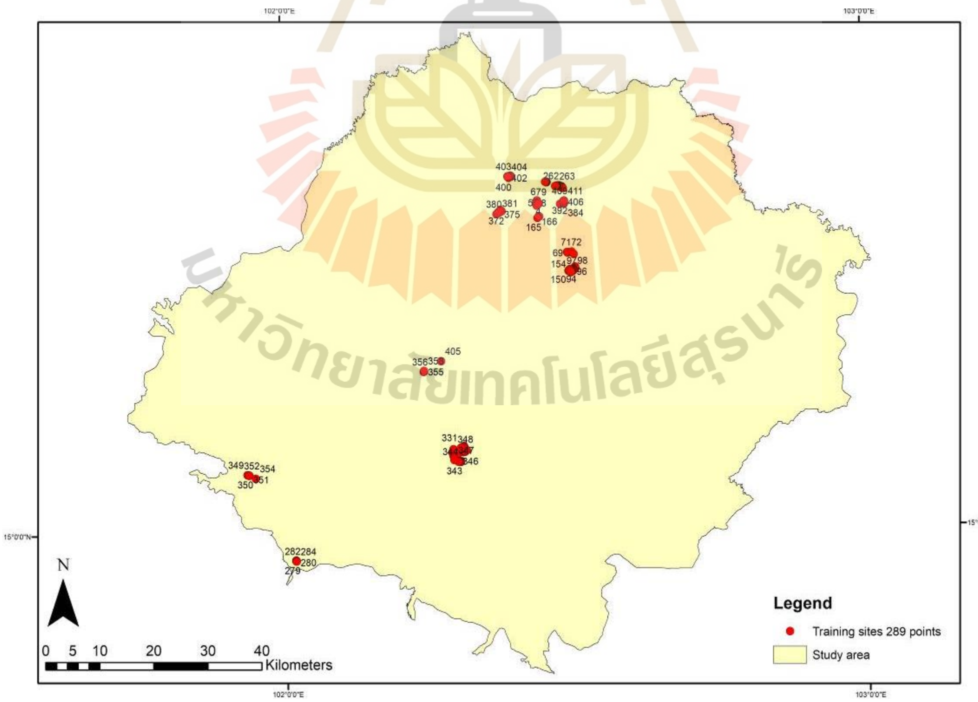

(a)

Figure 4.2 The training sites and test sites in the study area. (a) 289 training sites. (b) 122 test sites.

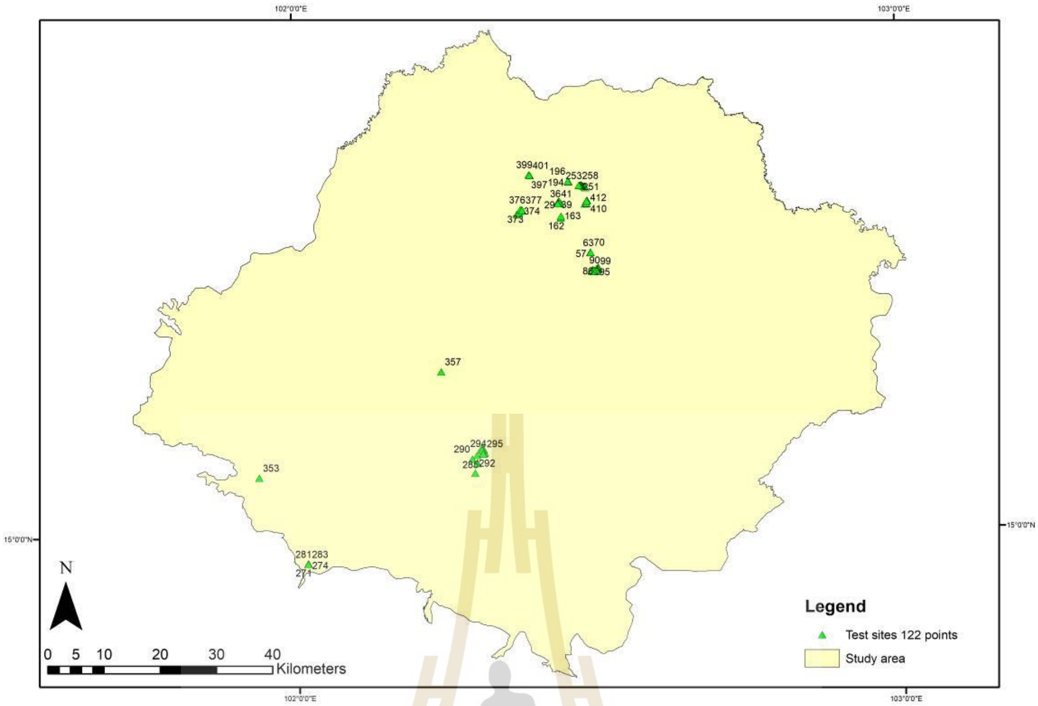

(b)

Figure 4.2 (Continued) The training sites and test sites in the study area.

4.2 Probability map of ancient salt-making sites from FR

The frequency ratios for all factors involved in the study are shown in Table 4.1. These FR values indicate the level of correlation between locations of the salt-making site to these factors. The higher value indicates a higher relation. The thematic maps of the six causative factors selected for the salt-making site probability map generation were assigned the frequency ratio for the respective classes using ArcGIS spatial analyst extension tool for the preparation of the final map. They were converted in the form of 15 x 15 m^2 grid cells to calculate a salt-making site probability index (SMSPI). The total number of cells in the study area is 40,743,414, and the number of salt-making site occurrence is 289. The relationship was used as each factor's rating in the overlay analysis.

Table 4.1 Frequency ratio of salt-making sites occurrence.

Factors	Class	Number of pixels in class		Ancient salt-making sites		FR
		Number	%	Number	%	
Geology (Locating on KTms, Qa, and Qt)	KTms	16,029,350	39.3421	39	13.4948	0.3430
	Qa	22,254,169	54.6202	250	86.5051	1.5837
	Qt	2,459,895	6.0375	0	0	0
Distance to geological structures	<500 m	13,111,629	44.2784	67	23.1833	0.5235
	500 m-1,000 m	6,783,532	22.9082	55	19.0311	0.8307
	1,000 m-1,500 m	4,588,845	15.4967	101	34.9480	2.2551
	1,500 m-2,000 m	2,986,007	10.0838	58	20.0692	1.9902
	>2,000 m	2,141,716	7.2326	8	2.7681	0.3827

Table 4.1 (Continued) Frequency ratio of salt-making sites occurrence.

Factors	Class	Number of pixels in class		Ancient salt-making sites		FR
		Number	%	Number	%	
Locating on salt crust area and saline wet belt	Severe salinity level areas with salt crust >50%	1,009,092	2.4767	49	16.9550	6.8457
	Moderate salinity level areas with salt crust >10 - 50 %	3,812,691	9.3578	121	41.8685	4.4741
	Low salinity level areas with salt crust >1 - 10 %	7,437,380	18.2542	47	16.2629	0.8909
	Potential salt affected lowland areas	8,852,590	21.7277	12	4.1522	0.1911
	Rock salt underlain highland areas	8,942,146	21.9475	60	20.7612	0.9459
	Related units of low salinity level areas with salt crust >1 - 10 % / rock salt underlain highland areas	74,007	0.1816	0	0	0
	Related units of rock salt underlain highland areas/ low salinity level areas with salt crust >1 - 10 %	488,278	1.1984	0	0	0
	Related units of rock salt underlain highland areas/ lowland areas	1,679,088	4.1211	0	0	0
	Non-salinity level areas	8,447,953	20.7346	0	0	0

Table 4.1 (Continued) Frequency ratio of salt-making sites occurrence.

Factors	Class	Number of pixels in class		Ancient salt-making sites		FR
		Number	%	Number	%	
NDSI value	-0.931 to -0.063	272,500	0.6688	0	0	0
	-0.063 to 0.041	3,321,823	8.1530	10	3.4602	0.4244
	0.041 to 0.101	11,341,735	27.8369	203	70.2422	2.5233
	0.101 to 0.333	25,807,262	63.3408	76	26.2975	0.4151
	0.333 to 0.976	184	0.0004	0	0	0
Distance to ancient settlements	<1000 m	4,459,150	15.3782	251	86.8512	5.6476
	1,000 m-2,000 m	7,973,725	27.4988	33	11.4186	0.4152
	2,000 m-3,000 m	7,084,430	24.4319	0	0	0
	3,000 m-4,000 m	5,452,374	18.8035	0	0	0
	4,000 m-5,000 m	4,026,869	13.8874	4	1.3840	0.0996
	>5,000 m	3,105,640	10.7103	1	0.3460	0.0323
Distance to water bodies and streams	<500 m	20,419,357	55.8554	116	40.1384	0.7186
	500 m-1,000 m	10,983,883	30.0455	79	27.3356	0.9098
	1,000 m-1,500 m	5,154,255	14.0990	73	25.2595	1.7915
	>1,500 m	2,298,989	6.2886	21	7.2664	1.1554

A total number of pixels in the study area: 40,743,414 pixels.

Number of salt-making site points: 289

FR = % salt-making occurrence points / % number of pixels

For geology factor or locating on the Maha Sarakham Formation (KTms), Quaternary alluvial sediments (Qa), and Quaternary terrace deposit (Qt), it was found that majority of the study area falls in Quaternary alluvial sediments followed by the Maha Sarakham Formation and the least on Quaternary terrace deposit. From the calculation of frequency ratio, the relationship between salt-making site occurrence and geology shows that the frequency ratio was highest in Quaternary alluvial sediments (FR = 1.58) and was lowest in Quaternary terrace deposit (FR = 0). The frequency ratio of the Maha Sarakham Formation and Quaternary terrace deposit was lower than 1.0, which indicates a low salt-making site occurrence probability. The frequency ratio of Quaternary alluvial sediments was greater than 1.0, indicating a high salt-making site occurrence probability. The result allows to reasonably conclude that the most probability class was Quaternary alluvial sediments. This situation could be explained that Quaternary alluvial sediments are always situated in low land area and associated with water or wet area. Additionally, it is more frequently situated on the thinner burden of rock salt layer. The lowest FR values (FR = 0) belong to Terrace deposit, which mostly contains gravel, sand, silt, clay, and laterite. FR value shows a very low correlation with salt-making site occurrences. Then, a very low probability of salt-making site occurrence in this class could be expected.

In the case of distance to geologic structures, the frequency ratio was the highest in the range of 1,000 to 1,500 m and the lowest in distance above 2,000 m. In the ranges of 1,000 to 1,500 m and 1,500 to 2,000 m, the ratio was greater than 1.0, indicating a high probability of salt-making occurrence, and for distance below 1,000 m and distance above 2,000 m, the ratio was lower than 1.0, indicating a low probability. This result can be explained that the salt-making probability based on this factor may be strongly affected by other factors.

In the study area, locating on salt crust area and saline wet belt (salt-affected areas with salt crust) is the major controlling factor for salt-making site occurrence. From the results of FR calculations, the area of this factor shows the highest FR values, and therefore, the most susceptible class belongs to severe salinity level areas with salt crust >50% (FR = 6.85). The frequency ratio was the lowest (FR = 0) in four classes i.e. related units of low salinity level areas with salt crust >1 - 10 % / rock salt underlain highland areas, related units of rock salt underlain highland areas/ low salinity level areas with salt crust >1 - 10 %, related units of rock salt underlain highland areas/ lowland areas, and Non-salinity level areas. Their FR values were very low then the very low probability of salt-making site occurrence in these classes could be expected. For severe salinity level areas with salt crust >50% and moderate salinity level areas with a salt crust >10%, the ratios were greater than 1.0, indicating a high salt-making site occurrence probability. For classes of low salinity level areas with salt crust <10 %, potential salt-affected lowland areas, rock salt underlain highland areas, and non-salinity level areas, the ratios were lower than 1.0, indicating a low probability of salt-making site occurrence. This result confirms that the salt-making occurrence probability increases with the increasing percentage of salt crust in salt-affected areas.

The NDSI of the study area ranges from -0.931 to 0.976 and was classified into 5 classes namely, -0.931 to -0.063, -0.063 to 0.041, 0.041 to 0.101, 0.101 to 0.333, and 0.333 to 0.976 based on Natural Breaks (Jenk's) method. It was found that the majority of the area falls in the category of 0.101 to 0.333, followed by 0.041 to

0.101, -0.063 to 0.041, -0.931 to -0.063, and 0.333 to 0.976. For NDSI values below 0.041 and above 0.101, the frequency ratio was lower than 1.0, indicating a low salt-making occurrence probability and for NDSI values between 0.041 to 0.101, the ratio was greater than 1.0, indicating a high salt-making occurrence probability. This result shows that the high salt-making occurrence probability is related to the specific NDSI range.

The next factor considered is the distance to ancient settlements. This factor ranges from 0 – 6,000 m and is classified into six classes. Majority of salt-making sites (86.85%) in the area have occurred close to the ancient settlements within a distance of 1,000 m, and only thirty-eight salt-making sites (13.15%) have taken place beyond 1,000 m and up to 6,000 m. Hence, distance to ancient settlements has taken as the basis for ancient salt-making sites occurrence because the nearby salt-making sites are the salt productive workspace of local salt makers. For distances above 1,000 m, the frequency ratio was lower than 1.0, indicating a low salt-making site occurrence probability. For distances below 1,000 m, the frequency ratio was greater than 1.0, indicating a high salt-making occurrence probability. This result revealed that the salt-making occurrence probability is high in the right distance to ancient settlements.

Distance to water bodies and streams ranged from 0 – 2,000 m and was classified into three classes. Majority of salt-making site (55.86%) in the area have occurred close to the water bodies and streams within a distance of 500 m, and only 21 salt-making sites (6.29%) have taken place beyond 1,500 m. In the case of this factor, from 1,000 to 2,000 m the ratio was greater than 1.0, indicating a high probability of salt-making occurrence probability, and for distances below 1,000 m, the ratio was lower than 1.0, indicating a low salt-making occurrence probability. As same as the distance to ancient settlements, this result revealed that the high salt-making occurrence probability is related to the specific distance range from water bodies and streams.

The result of frequency ratio calculation in the map shows that the SMSPI has a minimum value of 1229.44, and a maximum value of 55354.98, with an average value of 15875.45 and a standard deviation of 10251.95. If the SMSPI value was high, there was a higher probability of salt-making site occurrence. A lower value indicates a lower probability. During the overlay analysis, the SMSPI was calculated by summation of each factor's frequency ratio value. The final salt-making site prediction map was prepared based on SMSPI in 5 classes, from very low to very high, using standard deviation method to generate the class breaks that provides the best information which is suitable to compare to other methods (Ayalew and Yamagishi, 2005 quoted in Samdrup Dorji, 2016 pp. 127). The salt-making occurrence probability map using the FR model is displayed in Figure 4.3. The covering area percentage of each probability class is shown in Table 4.2.

Table 4.2 Salt-making probability classes, SMSPI, and coverage area percentage using the FR model.

Salt-making Probability Classes	SMSPI	% of Area
Very low probability	1,229.4407 - 10,645.2550	39.8098
Low probability	10,645.2550 - 20,891.1184	38.8967
Moderate probability	20,891.1184 - 31,136.9819	9.9811
High probability	31,136.9819 - 41,382.8453	8.7339
Very high probability	41,382.8453 - 55,354.9844	2.5784

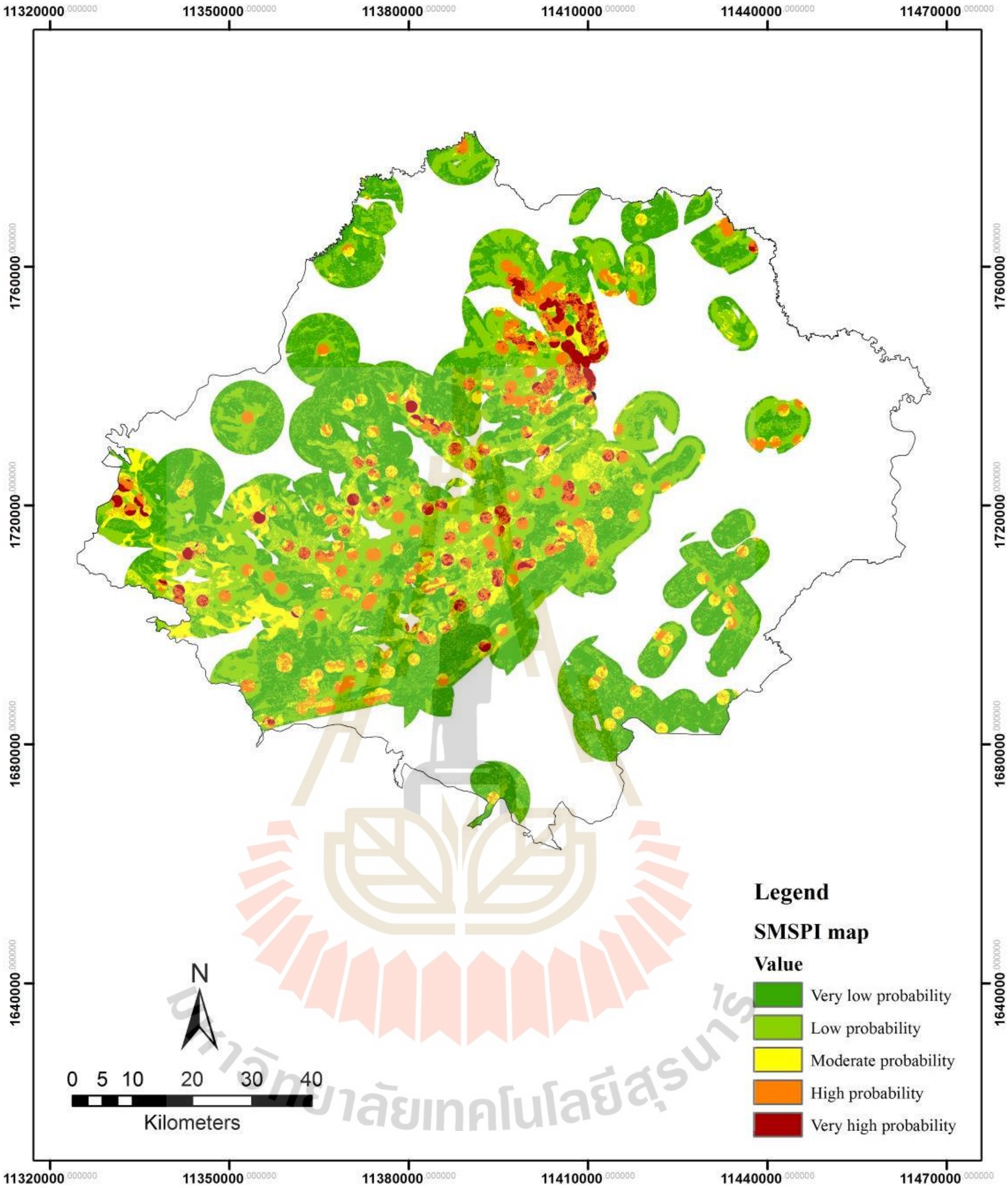

Figure 4.3 Salt-making occurrence probability map using the FR model.

4.3 Probability map of ancient salt-making sites from LR

As mentioned in the previous chapter, GIS data layers of factors could work well in the FR method. However, for the LR model, their normal distribution transformation was required to reduce inaccuracy and increase the analytical result acceptability. Working on 411 samples, the methods that could transform data of independent variables to be normal distribution or closest to be were tested and selected as a result shown in Table 4.3. More details of the tests can be seen in Appendix A. So, the better method was selected based on skewness and the plot between expected normal and observed values. The original or transformed data with skewness closer to 0 is the better, while the more fit to a linear relationship between expected normal and observed values is the better.

Table 4.3 The skewness of data based on the method used for data transformation of each variable (shaded cell is the selected transformation method for the variable).

Independent variables	**Original data**	**Transform method**	
		Log10	**SQRT**
	Skewness	**Skewness**	**Skewness**
X1	4.571	-0.542	2.157
X2	0.612	-0.228	0.238
X3	-0.694	-1.950	-1.145
X4	2.665	0.273	1.543
X5	0.923	-1.017	-0.062
X6	-1.406	-1.498	-1.653

The results of spatial autocorrelation of input data were all clustered pattern with positive Moran's I (see Appendix B). The results were appropriately consistent with their characteristics in nature. This indicated that they were proved to have significant spatial autocorrelation and valid as the input of spatial modelling.

The OLS was operated from samples of existing and non-existing ancient salt-mining sites to obtain a set of coefficients expressing the relationship of the dependent and independent variables. The resulting relationship is shown in Table 4.4.

Table 4.4 A set of coefficients expressing the relationship between the dependent and independent variables, including the Variance Inflation Factor (VIF).

Variables	Coefficient	VIF*
Constant	1.7409	-
X1 Distance to geologic structures and features	-0.2009	1.1074
X2 Locating on salt crust area and saline wet belt	0.4692	1.2700
X3 NDSI	-0.3771	1.0301
X4 Distance to ancient settlements	-1.9362	1.1915
X5 Distance to water bodies and streams	0.4397	1.2544
X6 Geology	0.2894	1.1070

*The VIF measures redundancy among explanatory variables. As a rule of thumb, explanatory variables associated with VIF values larger than about 7.5 should be removed (one by one) from the regression model (ESRI, 2012).

From Table 4.4, the constant means that when each independent variable has a value of 0 the dependent variable or suitability to be ancient mining site is 1.7409. For coefficients, the higher values, either positive or negative, provide comparatively higher influence among independent variables. The minus means that the area with a higher value of that variable can have less chance to be suitable site while vice versa for the positive.

Look at the coefficients, the outstanding highest influence among variables is the distance to ancient settlements (-1.9362), in a negative direction. It is followed by the locating on salt crust area and saline wet belt and the distance to water bodies and streams. This indicates that the area with a lower value of the distance to ancient settlements could have more chance to be higher suitable. This expression is consistent with the FR method. The class that shows the highest frequency ratio (5.6476) falls into <1,000 m, the lowest class.

Area locating on the more highly salt-affected area has higher site suitability. This can be confirmed that the area with salt crust >50% shows the highest FR (6.8457). Compared to other variables, it shows moderate influence in a positive direction on site suitability and not much different from the distance to water bodies and NDSI. Distance to the water body acts almost the same as locating on the salt-affected area. The longer distance indicates higher suitability. It is consistent with the result of the FR method. The classes of 1,000-1,500 m and 1,500-2,000 m have the highest FR of 1.7915 and 1.1554. This can be explained that area too close to the water body might have frequent floods that can dilute the salt crust, if present, and make it not concentrate enough for the making process. Salt making site too close to the water body can give more chance to contaminate water used for other purposes.

Very low NDSI (0.041 to 0.101), having FR as 2.5233, which is the highest among classes. This is reasonable because the lower NDSI from this class carries minus values, indicating so high vegetation dominating of the area that cannot be suitable as a site.

For distance to geologic structure, the highest FR (2.2551) is at the class of 1,000-1,500 m which is the moderate distance. The reason could be that the referent data used was in so small scale that could have positional inaccuracy.

From the Table, VIF value of each variable is much lower than 7.5 and indicates that there is statistically no data redundancy among independent variables.

This relationship was applied to the estimation of the dependent variable all over the area by further input into the logistic regression model for site occurrence probability estimation. The result of the estimation was the probability map classified to be five classes using the standard deviation method and is displayed in Figure 4.4. The covering area percentage of each probability class is shown in Table 4.5.

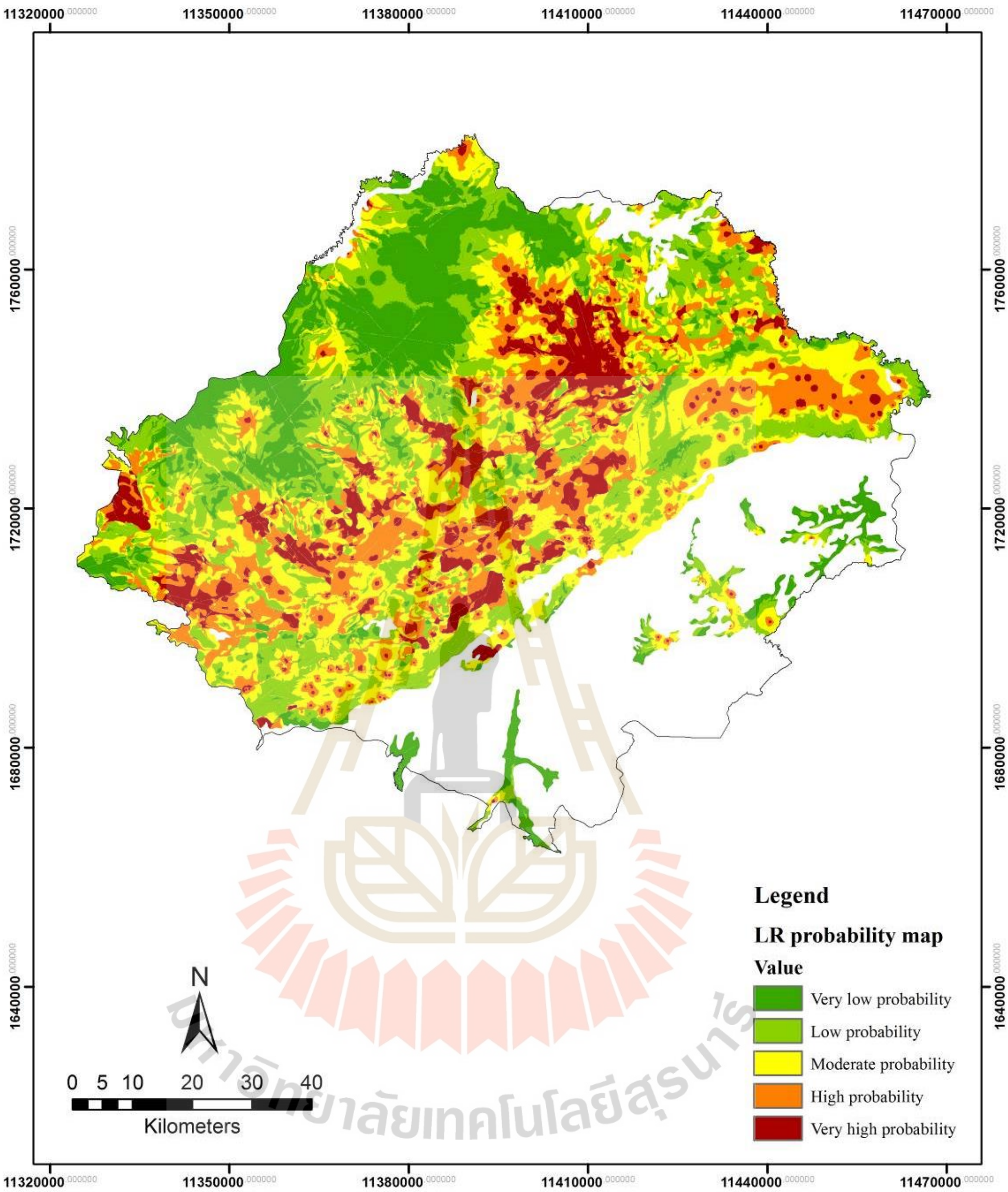

Figure 4.4 Salt-making occurrence probability map using the LR model.

Table 4.5 Salt-making probability classes and coverage area percentage using the LR model.

Salt-making Probability Classes	Value	% of Area
Very low probability	0.3858 - 0.4198	17.3341
Low probability	0.4198 - 0.5514	26.7167
Moderate probability	0.5514 - 0.6172	26.3623
High probability	0.6172 - 0.6830	19.3488
Very high probability	0.6830 - 0.8624	10.2380

4.4 Validation and comparison of model results

Visual comparison of the two probability maps could not be fairly operated because of the difference in the continuity of their input data and numerical range of entire probability values. All input data of FR were spatially categorized to be classes and then analyzed. Therefore, FR values remain category characteristics. The same characteristics hardly appear on the LR probability map, which resulted mainly from continuous input data. No-data area of FR probability map presents the areas out of classes of input data.

Meanwhile, no-data of the LR probability map occurred in non-salinity area where there is no chance for salt-making activity and marked as an error when transformed by using the log10 function. The area with error data was ignored in LR analysis. Nevertheless, if only areas with topmost probability are considered, they are quite consistent in these two maps.

According to the above discussion, it is the reason why the method like Receiver Operating Characteristics (ROC) was required to operate for their result accuracy assessment and comparison. The results of the probability maps were validated by the ROC curves as results displayed in Figure 4.5. The area under the curve (AUC) for each model is a global statistical accuracy for each model.

For LR probability map, the ROC curve has an AUC of 0.908. Meanwhile, the ROC curve of FR probability map has an AUC of 0.810. It means that both of them rank a random positive example higher than a random negative example 50% of the time. From a rough guide for classifying the accuracy of a diagnostic test in the traditional academic point system (Tape, 2019), it appears that the result of LR method was excellent acceptable and of the FR method was good. More confirmably, from 122 test sites in the area were used for validation the result maps, 106 sites fall into high and very high probability classes of FR probability map, and 117 sites were found in high and very high probability class of LR probability map (Figure 4.6).

The LR method provides a better result when comparing to result from the FR method. Practically, the resulting probability maps should be used as a lead to discover new sites.

During this study, several sites have been newly discovered. Totally 23 newly discovered sites were overlaid on the probability maps (Figure 4.7-4.8). It appears that they fall into moderate to very high probability classes of both maps. This discovery helps confirm that the models and their results are valid and applicable to serve the objectives of the study.

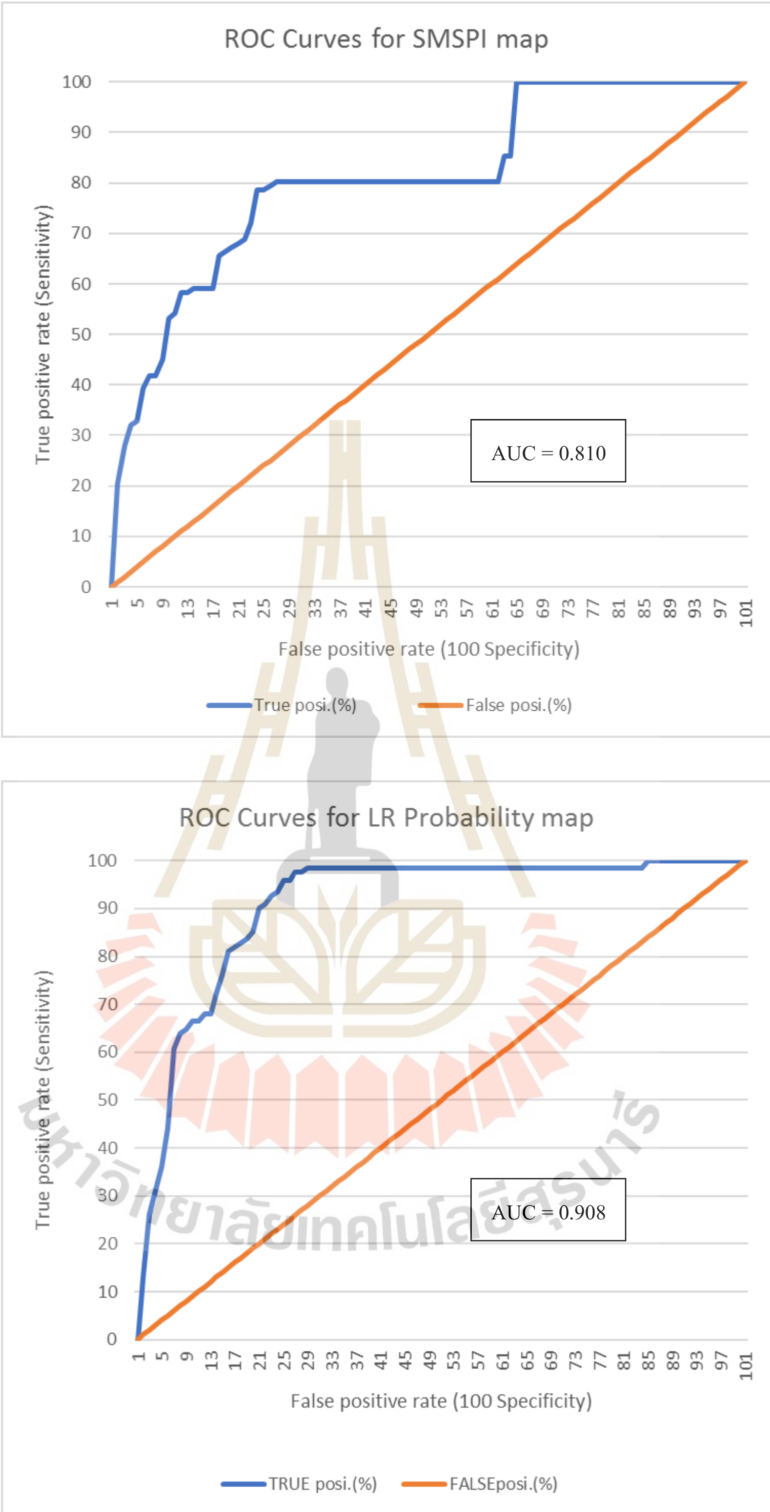

Figure 4.5 ROC curves for ancient salt-making site probability map validation.

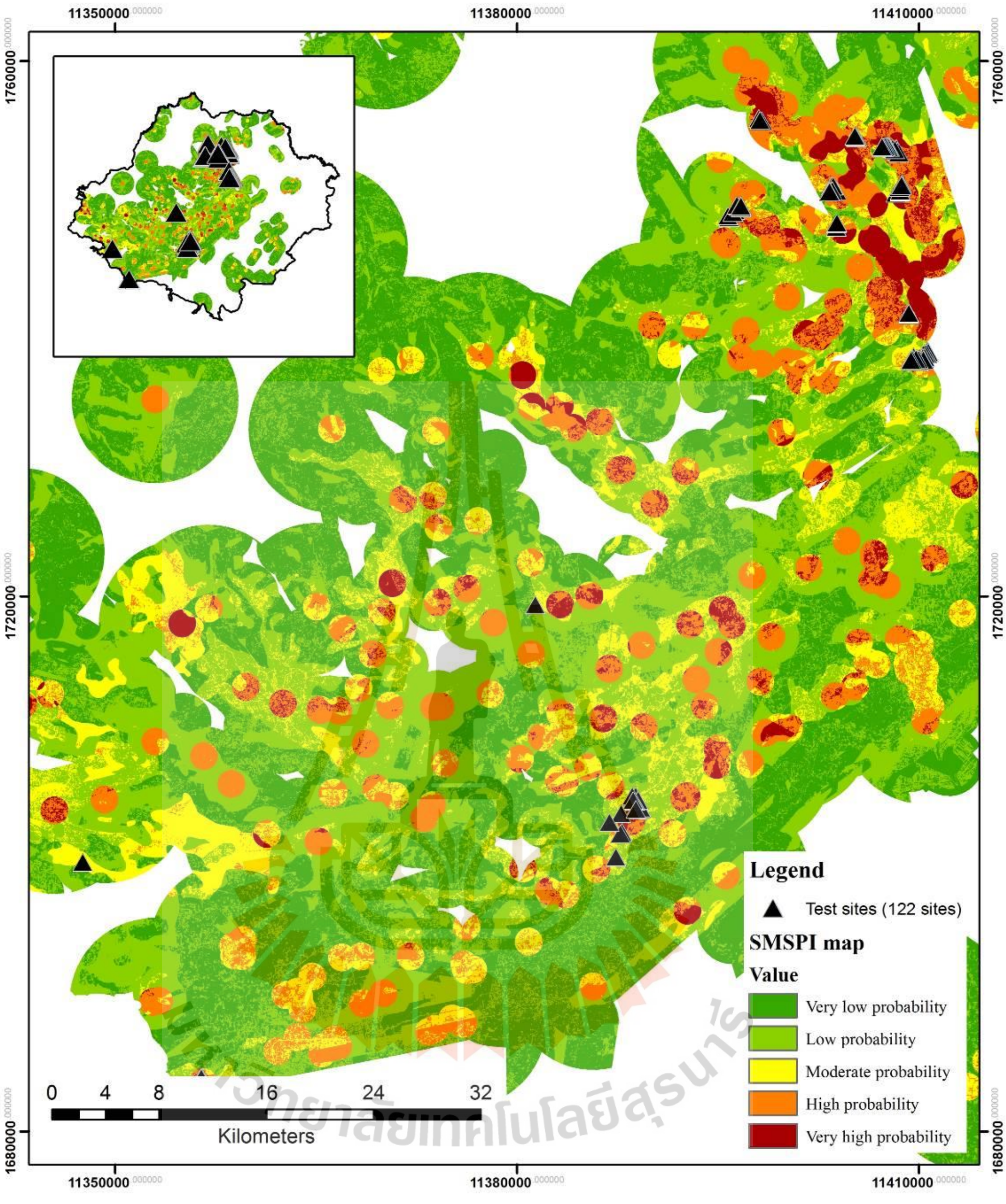

(a)

Figure 4.6 122 Test sites showing in salt-making occurrence probability maps of FR and LR models.

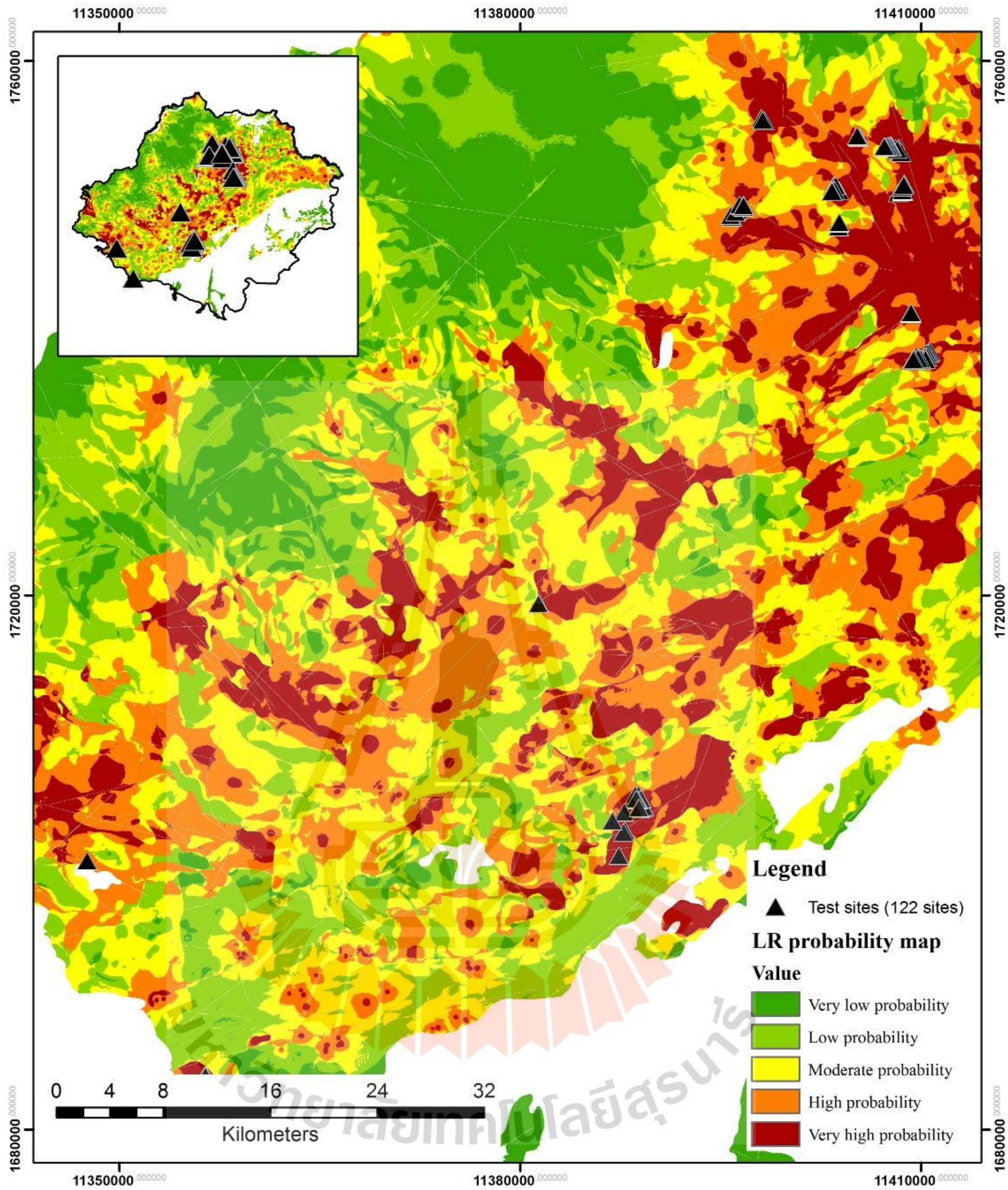

(b)

Figure 4.6 (Continued) 122 Test sites showing in salt-making occurrence probability maps of FR and LR models.

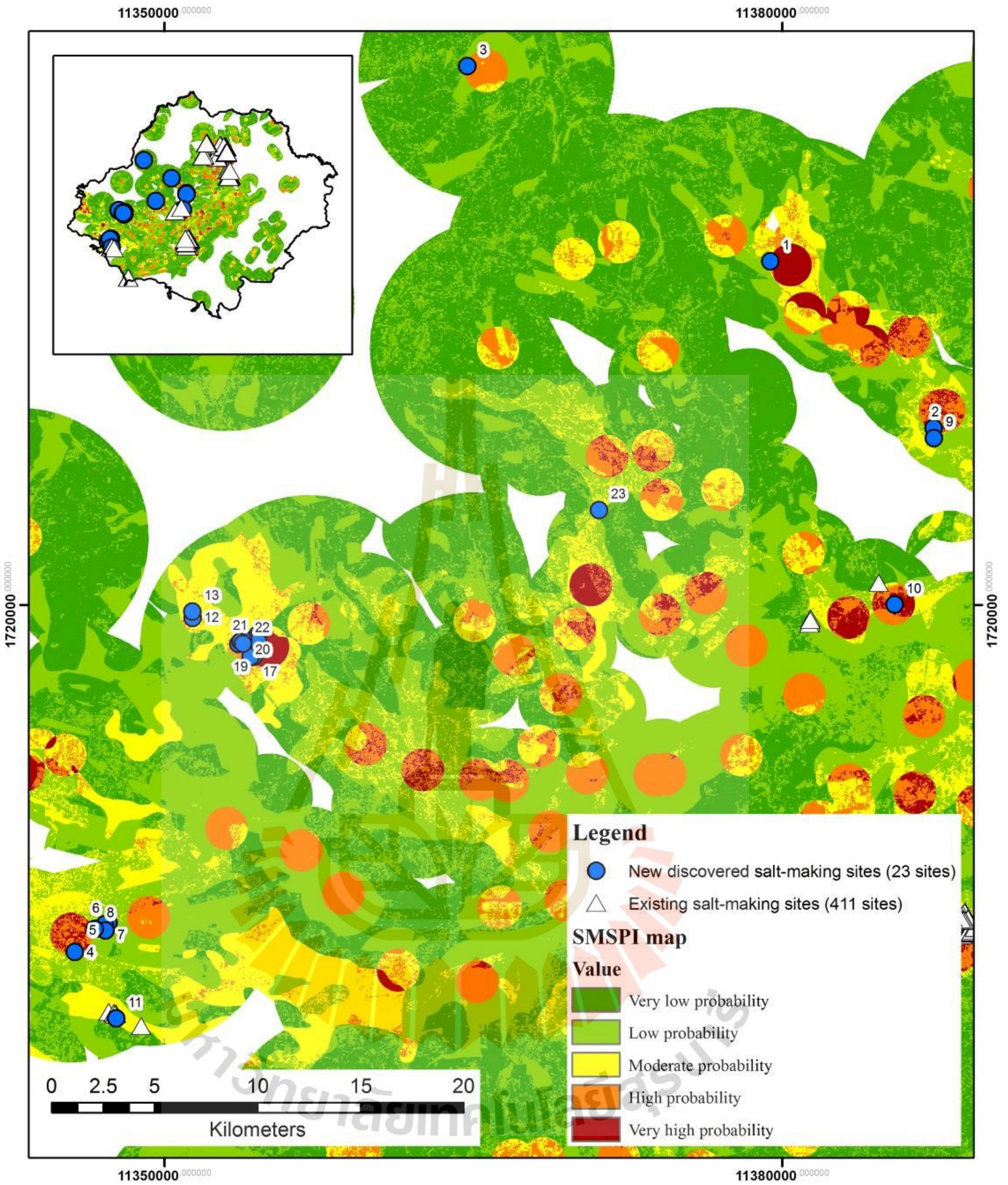

Figure 4.7 The distribution of newly discovered salt-making sites over FR probability maps.

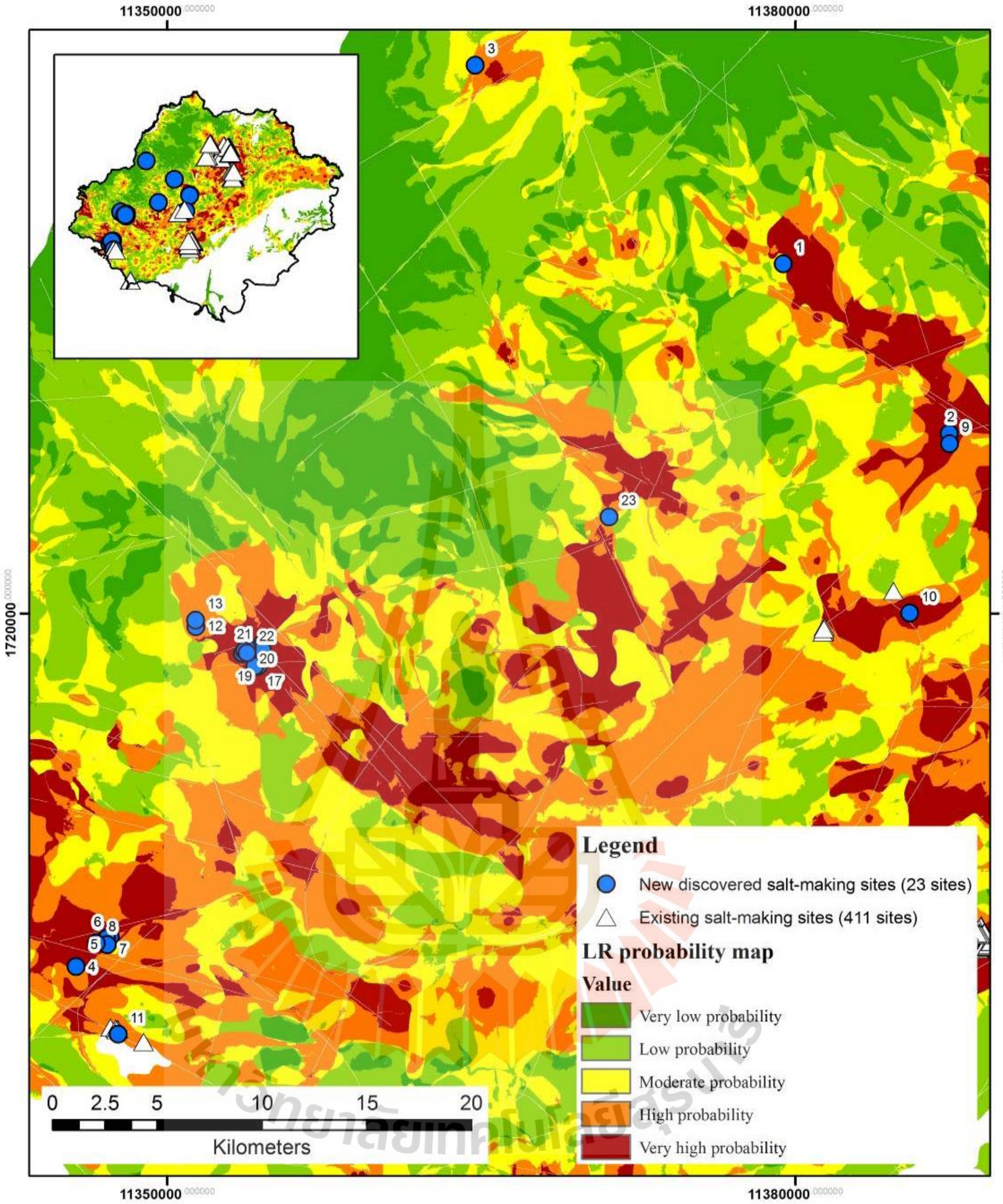

Figure 4.8 The distribution of newly discovered salt-making sites over LR probability maps.

CHAPTER V

CONCLUSION AND RECOMMENDATION

The information on the potential area to discover the ancient salt-mining site is required for land-use planning and development in any area. It helps protect the archaeological treasure of the nation from accidental damage in land use development. It also supports effective planning for archaeological site development and conservation. From the archaeological record, the study area of this research, Nakhon Ratchasima province, was identified to be a very high potential area of very active ancient salt mining. The study, therefore, aims at identifying those potential areas using two methods of spatial modelling, i.e. FR and LR, resulted in two maps of probability of ancient salt-making occurrence. The area with higher probability in the map should be considered more restricted to land-use development for other purposes or more promising in new discovering ancient salt-making sites.

From the set of coefficients showing the relationship among variables in regression model which is a part of LR, it revealed that the distance from ancient settlements was the most influential factor, followed by the locating on salt crust area and saline wet belt and the distance to water bodies and streams. The variable of the distance from ancient settlements displayed a negative relationship with the presence of ancient mining sites. This indicates that the area with its lower values could have more chance to be higher suitable or discoverable. This indication is opposite to the locating on salt crust area and saline wet belt and the distance to water bodies and streams which are influential factors in a positive direction. The relationship from this method was fully supported by or consistent with the results of the FR method, as discussed in Chapter 4. The results have been very consistent with the studies on the archaeology of salt production by Nitta (1992, 1997), Rivett and Higham (2007), and ศรีศักร วัลลิโภดม (2535) and on ethnoarchaeology of salt-making by Thanaphattarapornchai (2013).

Using the ROC method, both probability maps were validated. The results appeared that both of them were highly acceptable. The LR method provides a better result when comparing to result from the FR method. It can be concluded that both methods are fruitfully applicable and valid to serve the objectives of the study.

There are some limitations in this study that can turn to be recommendations for further study. This include:

(1) Availability of factors influencing the presence of ancient salt mine was very limited. The factors selected for this study were completely based on theories of archaeology and geology including their recent availability, not gathering from any possible factors for subsequent statistical proving treatment. Even though the statistical data transformation was applied to original data of variables in this study, the results were still not able to comply with trendy rules. For future research, it could be worth trying when having more samples of salt-making sites or changing the study area.

(2) Factor like spatially electrical conductivity might be a valid factor. However, the available ones in this area were hitherto collected in scattered areas.

Their poor spatial distribution and consistency become the problem. In some other areas, EC data could be effective to apply.

(3) Some secondary data should be carefully refined to improve the accuracy of the analysis. It is recommended that, for example, a geologic structure, which is the original data to determine distance, should be reinterpreted in the proper scale. This could increase the accuracy and confidence in the analysis.

(4) The study revealed that varying categorization of input data for the FR model could affect the final result. More classes categorized could provide higher result accuracy. Also, their classes should be added up to cover the entire area of the study so that the result can be more comparable to the result from LR.

(5) Apart from the presence and absence of salt-making sites working as the dependent variable in LR, the mound volume at sites can be applied as well. The volume surely implies how active the sites could be in the past. However, the data are not available recently. Field investigation on this information could take great time, effort, and budget. However, it would be an interesting benefit if the model result of applying the volume can be compared to the result of this study.

(6) The resulting probability maps should be used as a lead to discover new sites. Then, those new sites should be added in the model input data to rerun the models and result shall be observed. The better result could be expected.

(7) The models should be applied to other potential areas. If the study results are valid, it can be confirmed that they are valid models for universal application.

REFERENCES

REFERENCES

กรมทรัพยากรธรณี. (2550). แผนที่ธรณีวิทยาจังหวัดนครราชสีมา – กรมทรัพยากรธรณี. [On-line]. Available: https://www.dmr.go.th/download/pdf/NorthEast/korat.pdf.

กรมทรัพยากรธรณี. (2553). **การจำแนกเขตเพื่อการจัดการด้านธรณีวิทยาและทรัพยากรธรณีจังหวัดนครราชสีมา**. กรุงเทพฯ: จันวาณิชย์ ซีเคียวริตี้พริ้นท์ติ้ง.

กรมพัฒนาที่ดิน. (2555). กรมพัฒนาที่ดิน (LDD) – ระบบการบริหารจัดการตัดสินใจเชิงพื้นที่. [On-line]. Available: http://eis.ldd.go.th/lddeis/PLM.aspx

กรมศิลปากร. (2534). **แหล่งโบราณคดีประเทศไทย เล่ม 4 (ภาคตะวันออกเฉียงเหนือตอนล่าง) เอกสารกองโบราณคดีหมายเลข 3/2533**. กรุงเทพฯ : กรมศิลปากร.

กรมศิลปากร. (2544). **รายงานเบื้องต้นการสำรวจแหล่งโบราณคดีในพื้นที่ทุ่งกุลาร้องไห้**. กรุงเทพฯ: กรมศิลปากร.

กรมศิลปากร. (2554). **ระบบภูมิสารสนเทศแหล่งมรดกทางศิลปวัฒนธรรม.** [On-line]. Available: http://gis.finearts.go.th/fineart/.

ชรัตน์ มงคลสวัสดิ์, สถาพร ไพบูลย์ศักดิ์ และ บังอร ยมมรคา. (2550). **ระบบฐานข้อมูลดินเค็มภาคตะวันออกเฉียงเหนือ.** ขอนแก่น: มหาวิทยาลัยขอนแก่น.

ชลิต ชัยครรชิต. (2540). ยุคเหล็กในประเทศไทย: พัฒนาการทางเทคโนโลยีและสังคม. ใน **การประชุมทางวิชาการโครงการเมธีวิจัยอาวุโส สกว.** กรุงเทพฯ: ศูนย์มานุษยวิทยาสิรินธร (องค์การมหาชน).

ชาร์ลส ไฮแอม และ รัชนี ทศรัตน์. (2542). **สยามดึกดำบรรพ์ ยุคก่อนประวัติศาสตร์ถึงสมัยสุโขทัย** . กรุงเทพฯ: บริษัท อมรินทร์พริ้นติ้งแอนด์พับลิชชิ่ง จำกัด (มหาชน).

นเรศ สัตยารักษ์ และ ทรงภพ พลจันทร์. (2533). เกลือหินใต้ที่ราบสูงโคราช. ใน **การประชุมวิชาการกรมทรัพยากรธรณี**. กรุงเทพฯ: กรมทรัพยากรธรณี.

สมเดช ลีลามโนธรรม. (2556). พัฒนาการของชุมชนโบราณบริเวณลุ่มน้ำลำสะแทด ก่อนพุทธศตวรรษที่ 19 : กรณีศึกษาแหล่งโบราณคดีบ้านกระเบื้อง อำเภอบัวใหญ่ จังหวัดนครราชสีมา และการสำรวจพื้นที่โดยรอบ. วิทยานิพนธ์ปริญญามหาบัณฑิต สาขาวิชาโบราณคดีสมัยประวัติศาสตร์บัณฑิตวิทยาลัย มหาวิทยาลัยศิลปากร.

สมนึก ผ่องใส. (2534). การวิเคราะห์ภาพถ่ายดาวเทียมแลนแซทและการใช้ระบบสารสนเทศทางภูมิศาสตร์เพื่อการทำแผนที่ดินเค็มและแผนที่ระบบนิเวศของพื้นที่ในภาคตะวันออกเฉียง

เหนือ. วิทยานิพนธ์ปริญญามหาบัณฑิต สาขาวิชาปฐพีศาสตร์ บัณฑิตวิทยาลัย มหาวิทยาลัยขอนแก่น.

สุพรรณี ปลัดศรีช่วย. (2551). การประเมินสถานภาพพื้นผิวเพื่อแสดงศักยภาพความเป็นเกลือของดินในที่ราบสูงโคราชด้วยข้อมูลจากดาวเทียมและระบบสารสนเทศภูมิศาสตร์. วิทยานิพนธ์ ปริญญามหาบัณฑิต สาขาวิชาการรับรู้จากระยะไกล บัณฑิตวิทยาลัย มหาวิทยาลัยขอนแก่น.

ศรีศักร วัลลิโภดม. (2535). เกลืออีสาน. **เมืองโบราณ.** 18 (1): 71-123.

Aldakheel, Y.Y., Elprince, A.M., and AI-Hosaini, A.I. (2005). Mapping of salt affected soils of irrigated lands in arid regions using remote sensing and GIS. **The 2nd International Conference on Recent Advances in Space Technologies (RAST 2005)**. Istanbul: (n.p).

Altaweel, M. (2005). The use of ASTER satellite imagery in archaeological contexts. **Archaeological Prospection**. 12: 151-166.

Andrew, M., Ustin, S. (2008). The role of environmental context in mapping invasive plants with hyperspectral image data. **Remote Sensing of Environment**. 112: 4301-4317. Quoted in Meléndez-Pastor, I., Navarro-Pedreño, J., Koch, M., and Gómez, I. (2010). Applying imaging spectroscopy techniques to map saline soils with ASTER images. **Geoderma**. 158 (1-2): 55-65.

Antonites, A. (2013). Archaeological salt production at the Baleni spring, Northeastern South African **Archaeological Bulletin**. 68 (198): 105–118.

Arunin, S. (1992). Strategies for utilizing salt-affected land in Thailand. In **Proceedings of the International Symposium on Strategies for Utilizing Salt Affected Lands** (pp 26-37). Bangkok: Land Development Department.

Ayalew, L., and Yamagishi, H. (2005). The application of GIS-based logistic regression for landslide susceptibility mapping in the Kakuda-Yahiko

Mountains, Central Japan. **Geomorphology**. 65 (1-2): 15-31. Quoted in Dorji, S. (2016). **Wildfire susceptibility analysis in Bhutan using geoinformatics technology.** M.S. thesis, Suranaree University of Technology.

Ben-Dor, E. (2002). Quantitative remote sensing of soil properties. **Advances in Agronomy.** 75:173-243.

Ben-Dor, E., Patkin, K., Banin, A., and Karnieli, A. (2002). Mapping of several soil properties using DAIS-7915 hyperspectral scanner data - a case study over clayey soils in Israel. **International Journal of Remote Sensing**. 23 (6): 1043-1062.

British Columbia Association of Professional Archaeologists. (2012). **BCAPA Standard of Practice Defining Site Boundaries in the Field** [Online]. Available: https://www.bcapa.ca/wp-content/uploads/Site_Boundary_SOP-Mar2012.pdf.

Burke, A., Ebert, D., Cardille, J., and Dauth, D. (2008). Paleoethology as a tool for the development of archaeological models of land-use: the Crimean Middle Palaeolithic. **Journal of Archaeological Science**. 35: 894-904.

Cawte, Hayden and Bhadravarma Bongsasip. (2009) Ethnoarchaeological investigations of household salt-making in Northeast Thailand: A scalar hypothesis for prehistoric production. Paper presented at the 19th Indo-Pacific Prehistory Association Congress, December 3, 2009, Hanoi.

Challis, K. (2007). Archaeology’s Cold War windfall: The CORONA programme and lost landscapes of the Near East. **Journal of the British Interplanetary Society**. 60: 21-27.

Clark, K., and Hebert, J. (2008). **Determining the Factors that Form the Basis of the Relationship between Clinker Deposits and Archaeological Sites in Southeast Montana.** [On-line]. Available: http://web.pdx.edu/~jduh/courses/Archive/ geog492s08/Projects/KClark&JHebert.pdf.

De Laet, V., Paulissen, E., and Waelkens, M. (2007). Methods for the extraction of archaeological features from very high-resolution Ikonos-2 remote sensing imagery, Hisar (southwest Turkey). **Journal of Archaeological Science**. 34: 830-841.

Dorji, S. (2016). **Wildfire susceptibility analysis in Bhutan using geoinformatics technology.** M.S. thesis, Suranaree University of Technology.

Douaoui, A.E.K., Nicolas, H., and Walter, C. (2006). Detecting salinity hazards within a semiarid context by means of combining soil and remote sensing data. **Geoderma**. 134: 217-230.

Duke, B.J., Carter, A.K., and Chang, N.J. (2010). The Excavation of Iron Age Working Floors and Small-Scale Industry at Ban Non Wat, Thailand. **Papers from the Institute of Archaeology**, 20: 123-130.

ESRI. (2012). ArcGIS Desktop: Release 10.1 [Computer software] Redlands, CA: Environmental Systems Research Institute.

Espa, G., Benedetti, R., De Meo, A., Ricci, U., and Espa, S. (2009). GIS based models and estimation methods for the probability of archaeological site location. **Journal of Cultural Heritage**. 7: 147-155.

FAO. (1988). Salt-affected soils and their management. **Bulletin No. 39.** Rome: FAO.

FAO. (2013a). **Origin, classification, and distribution of salt-affected soils** [On-line]. Available: https://www.fao.org/docrep/x5871e/x5871e03.htm.

FAO. (2013b). **Saline soils and their management** [On-line]. Available: https://www.fao.org/docrep/x5871e/x5871e04.htm.

Farifteh, J., Farshad, A., and George, R.J. (2006). Assessing salt-affected soils using remote sensing, solute modeling, and geophysics. **Geoderma**. 130: 191-206.

Gouletquer, P. and Welter, O. (2015). Techniques of salt making: from China (Yangtze River) to their world context. In R. Brigand and O. Welter (eds). **Archaeology of Salt** (pp 13-28). Leiden: Sidestone Press.

Halliwell, A., Yankowski, A., and Chang, N. (2016) Gendered labor in pottery and salt production in northeast Thailand. In S-E. Kelly, T. Ardren (eds). **Gendered Labor in Specialized Economies** (pp 117-157). Boulder: Univ Press Colorado.

Higham, C.F.W. (1977). The late prehistory of the southern Khorat Plateau, North East Thailand with particular reference to Roi Et Province. In W. Casparie, I. C. Glover, and G.-J. Bartstra (eds). **Modern Quaternary Research in Southeast Asia** 3 (pp 103-41). Rotterdam: Balkema.

Higham, C.F.W. (1996). **The Bronze age of Southeast Asia**. Cambridge: Cambridge University Press.

Hisao, F., and Pichai Wichaidit. (1989). Salt and sinkhole - corrosion as a principal factor governing topography and mass movement in Northeast Thailand. **Southeast Asian Studies**. 27(1): 3-34.

Hoi, E. (2011). Salt of the Early Civilizations: Case Studies on China. **Penn History Review**. 18(2): 68-99.

Hosmer, D.W., and Lemeshow, S. (2000). **Applied Logistic Regression**. (2nd ed). NewYork: John Wiley and Sons.

Howari, F.M., Goodell, P.C., and Miyamoto, S. (2002). Spectral properties of salt crusts formed on saline soils. **Journal of Environmental Quality**. 31(5): 1453-1461.

Kamermans, H. (2010). The Application of Predictive Modelling in Archaeology: Problems and Possibilities. In F.Niccolucci and S.Hermon (eds). Beyond the artifact – Digital Interpretation of the Past - Proceedings of CAA2004 – Prato (pp 273-277). Budapest: Archaeolingua.

Khan, N.M., Rastoskuev, V.V., Sato, Y., and Shiozawa, S. (2005). Assessment of hydrosaline land degradation by using a simple approach of remote sensing indicators. **Agriculture Water Management**. 77: 96-109.

Kohler, T.A., and Parker, S.C. (1986). Predictive models for archaeological resource location. In M. B. Schiffer (ed). **Advances in archaeological method and theory** 9 (pp. 397-452). New York: Academic Press.

Lasaponara, R., and Masini, N. (2006). Identification of archaeological buried remains based on the normalized difference vegetation index (NDVI) from QuickBird satellite data. **IEEE Geoscience and Remote Sensing Letters.** 3: 325-328.

Lee, S. (2005). Application of logistic regression model and its validation for landslide susceptibility mapping using GIS and remote sensing data. **International Journal of Remote Sensing**. 26: 1477-1491.

Lee, S., and Talib, J.A. (2005). Probabilistic landslide susceptibility and factor effect analysis. **Environmental geology**. 47: 982-990.

Masoud, Alaa A., and Koike, K. (2006). Arid land salinization detected by remotely-sensed landcover changes: A case study in the Siwa region, NW Egypt.

Journal of Arid Environments. 66(1): 151-167.

McFadden, D. (1973). Conditional logit analysis of quantitative choice behavior. In P. Zarembka (ed). **Frontiers in econometrics** (pp 105-142). New York: Academic Press.

Meléndez-Pastor, I., Navarro-Pedreño, J., Koch, M., and Gómez, I. (2010). Applying imaging spectroscopy techniques to map saline soils with ASTER images. **Geoderma**. 158(1-2): 55-65.

Metternicht, G., and Zinck, J. (2003). Remote sensing of soil salinity: potentials and constraints. **Remote Sensing of Environment**. 85: 1-20.

Mongkolsawat C., and Paiboonsak, S. (2006) **GIS application to spatial distribution of soil salinity potential in Northeast Thailand**. Khon Kaen: Geoinformatics Center for the Development of Northeast Thailand, Khon Kaen University.

Monjai, D. (2007). Landform associated with the Maha Sarakham Formation, the Phu Thok Formation and salt diapir in the Khorat Plateau, Northeastern Thailand. In **Proceedings of the International Conference on Geology of Thailand: Towards Sustainable Development and Sufficiency Economy (GEOTHAI' 07)** (pp 145-150). Bangkok: Department of Mineral Resources.

Mougenot, B., Pouget, M., and Epema, G.F. (1993). Remote sensing of salt-affected soils. **Remote Sensing Reviews**. 7: 241-259.

National Register of Historic Places. 1997. **How to complete the National Register registration form U.S. Department of the Interior, National Park Service National Register, History and Education.** Washington D.C.: Government Printing Office.

Nitta, E. (1992). Ancient industries, ecosystem and environment: special reference to the Northeast of Thailand. **Historical Science Reports, Kagoshima University**. 39: 61-80.

Nitta, E. (1997). Iron smelting and salt-making industries in Northeast Thailand. **Bulletin of the Indo-Pacific Prehistory Association**. 16: 153-60.

Oh, H.-J., Kim, Y.-S., Choi, J.-K., and Lee, S. (2011). GIS mapping of regional probabilistic groundwater potential in the area of Pohang City, Korea. **Journal of Hydrology**. 399: 158-172.

Oh, H.-J., Lee, S., and Soedradjat, G. (2010). Quantitative landslide susceptibility mapping at Pemalang area, Indonesia. **Environmental Earth Sciences.** 60 (6): 1317-1328.

Ozdemir, A. (2011). GIS-based groundwater spring potential mapping in the Sultan Mountains (Konya, Turkey) using frequency ratio, weights of evidence and logistic regression methods and their comparison. **Journal of Hydrology**. 411(2011): 290-308.

Parcak, S.H. (2009). **Satellite remote sensing for archaeology**. New York: Routledge.

Park, S., Jeon, S., and Choi, C. (2012). Mapping urban growth probability in South Korea: comparison of frequency ratio, analytic hierarchy process, and logistic regression models and use of the environmental conservation value assessment. **Landscape and Ecological Engineering**. 8(1): 17-31.

Peng, W. (1998). Synthetic analysis for extracting information on soil salinity using remote sensing and GIS: a case study of Yanggao basin in China. **The Journal of Environmental Management**. 22(1): 153-159.

Qing, K., Yu, R., Li, X., and Deng, X. (2005). Application of spectral angle mapping model to rapid assessment of soil salinization in arid area. In **Proceeding of International Geoscience and Remote Sensing Symposium (IGARSS)** 4 (pp 2355-2357). Seoul: Institute of Electrical and Electronics Engineers (IEEE). Quoted in Meléndez-Pastor, I., Navarro-Pedreño, J., Koch, M., and Gómez, I. (2010). Applying imaging spectroscopy techniques to map saline soils with ASTER images. **Geoderma**. 158(1-2): 55-65.

Rivett, P., and Higham, C.F.W. (2007). The archaeology of salt production. In C.F.W. Higham, A. Kijngam, and S.Talbot (eds). **The origins of the civilization of Angkor: the excavation of Noen U-Loke and Non Muang Kao 2** (pp 589-593). Bangkok: Prachachon.

Sarapirome, S., Tassanasorn, A., and Suwanwerakamtorn, R. (1995). Using radar images as a tool to study geomorphology and geology of the Chaiyaphum area, Thailand. In **International Conference on Geology, Geotechnology and Mineral Resources of Indochina (Geo-Indo'95)** (pp 135-144). (n.p.).

Seifert, D.J. (1995). **Defining Boundaries for National Register Properties. National Register Bulletin 21**. **U.S. Department of the Interior, National Park Service.** Washington D.C.: Government Printing Office.

Shrestha, D.P., and Farshad, A. (2008). Chapter 13. Mapping Salinity Hazard: An Integrated Application of Remote Sensing and Modeling-Based Techniques. In G. Metternicht, and J. A. Zinck (eds). **Remote Sensing of Soil Salinization: Impact on Land Management** (pp 257-272). Boca Raton: CRC Press.

Sukchan, S., and Yamamoto, Y. (2002). Classification of salt-affected areas using remote sensing and GIS. In **JIRCAS Working Report 2002**. 30: 15-19.

Supajanya, T., Vichapan, K., and Sri-israporn, S. (1992). Surface expression of shallow salt dome in Northeast Thailand. In C. Piancharoen (ed). **National Conference on Geologic Resources of Thailand: Potential for Future Development** (pp 89-95). Bangkok: Department of Mineral Resources.

Sutton, M.Q. (2016). **Archaeology The Science of the Human Past** (4th ed). Newyork: Routledge.

Takaya, Y., Hattori, T., and Pichai, W. (1984). Soil Salinization in the Khorat Plateau. **Original paper submitted to Mekhong's Secretariat**. Quoted in Hisao, F., and Pichai Wichaidit. (1989). Salt and sinkhole - corrosion as a principal factor governing topography and mass movement in Northeast Thailand. **Southeast Asian Studies**. 27(1): 3-34.

Tape, T.G. (2019). The Area Under a ROC Curve [On-line]. Available: http://gim.unmc.edu/dxtests/roc3.htm.

Thanaphattarapornchai, M. (2013). Traditional salt-making techniques and a virtual museum: a case study of Ban Marum, Non Sung District, Nakhon Ratchasima Province, Thailand. In A. Denes and P. Davis (eds). **Safeguarding intangible cultural heritage in the Asia-Pacific: proceedings from the ICH and Museums Field School Alumni Seminar 2012** (pp 183-207). Bangkok: Kletthai.

Vaughn, S., and Crawford, T. (2009). A predictive model of archaeological potential: An example from northwestern Belize. **Applied Geography**. 29: 542-555.

Wannakomol, A. (2005). Soil and groundwater salinization problems in the Khorat Plateau, NE Thailand - integrated study of remote sensing, geophysical and field data. Ph.D. Dissertation, Free University.

Wongsomsak, S. (1986). Salinization in Northeast Thailand. **Southeast Asian Studies**. 24(2): 133-153. Quoted in Wannakomol, A. (2005). **Soil and groundwater salinization problems in the Khorat Plateau, NE Thailand - integrated study of remote sensing, geophysical and field data**. Ph.D. Dissertation, Free University.

Yankowski, A. (2014). Photos: Thailand Salt Production [On-line]. Available: http://andreayankowski.com/v3/photos2. html?page=2

Yankowski, A., and Kerdsap, P. (2013). Salt-making in Northeast Thailand – An Ethnoarchaeological Study in Tambon Phan Song Khram, Nakhon Ratchasima Province, Northeast Thailand. **Silpakorn University Journal of Social Sciences, Humanities, and Arts** 13(1): 231-252.

Yilmaz, I. (2007). GIS based susceptibility mapping of karst depression in gypsum: a case study from Sivas basin (Turkey). **Engineering Geology**. 90: 89-103.

Integrated Application of Remote Sensing and Modeling-Based Techniques. In G. Metternicht, and J.A. Zinck (eds). **Remote Sensing of Soil Salinization: Impact on Land Management** (pp 257-272). Boca Raton: CRC Press.

APPENDICES

APPENDIX A

DATA TRANSFORMATION

1) Distance to geological structures (X1)

Original

Case Processing Summary

	Cases					
	Valid		Missing		Total	
	N	Percent	N	Percent	N	Percent
x1_origin	411	100.0%	0	0.0%	411	100.0%

Descriptives

			Statistic	Std. Error
x1_origin	Mean		1428.972632	87.76766822
	95% Confidence Interval for Mean	Lower Bound	1256.441860	
		Upper Bound	1601.503404	
	5% Trimmed Mean		1142.057320	
	Median		1181.580000	
	Variance		3166000.233	
	Std. Deviation		1779.325781	
	Minimum		.0000000000	
	Maximum		14407.10000	
	Range		14407.10000	
	Interquartile Range		938.9320000	
	Skewness		4.571	.120
	Kurtosis		24.675	.240

Tests of Normality

	Kolmogorov-Smirnov[a]			Shapiro-Wilk		
	Statistic	df	Sig.	Statistic	df	Sig.
x1_origin	.289	411	.000	.512	411	.000

a. Lilliefors Significance Correction

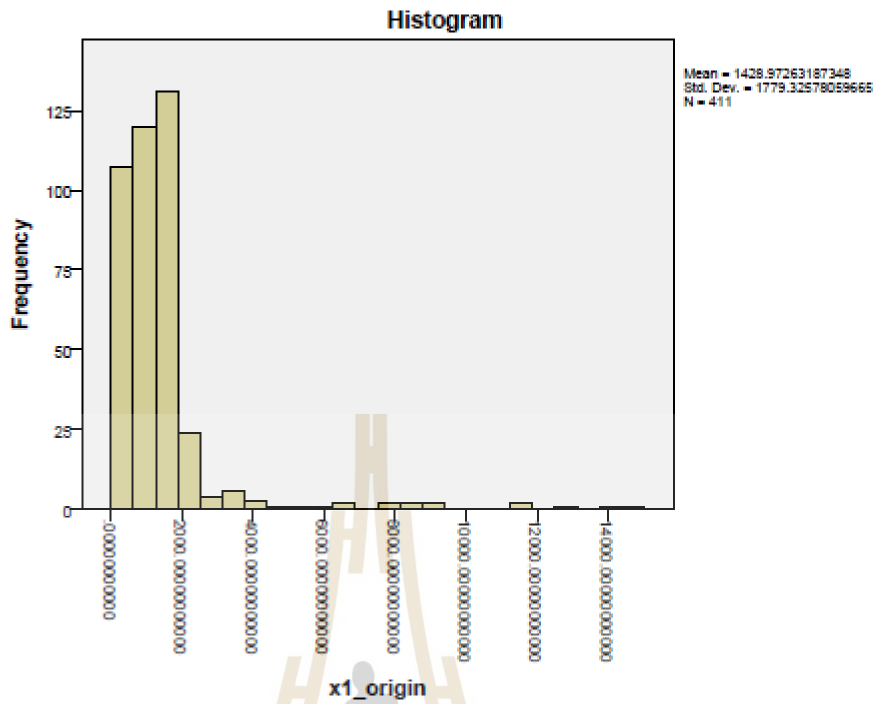
Histogram
Mean = 1428.97263187348
Std. Dev. = 1779.32578059665
N = 411
Frequency
125
100
75
50
25
0
.000000000
2000.000000000
4000.000000000
6000.000000000
8000.000000000
10000.000000000
12000.000000000
14000.000000000
x1_origin

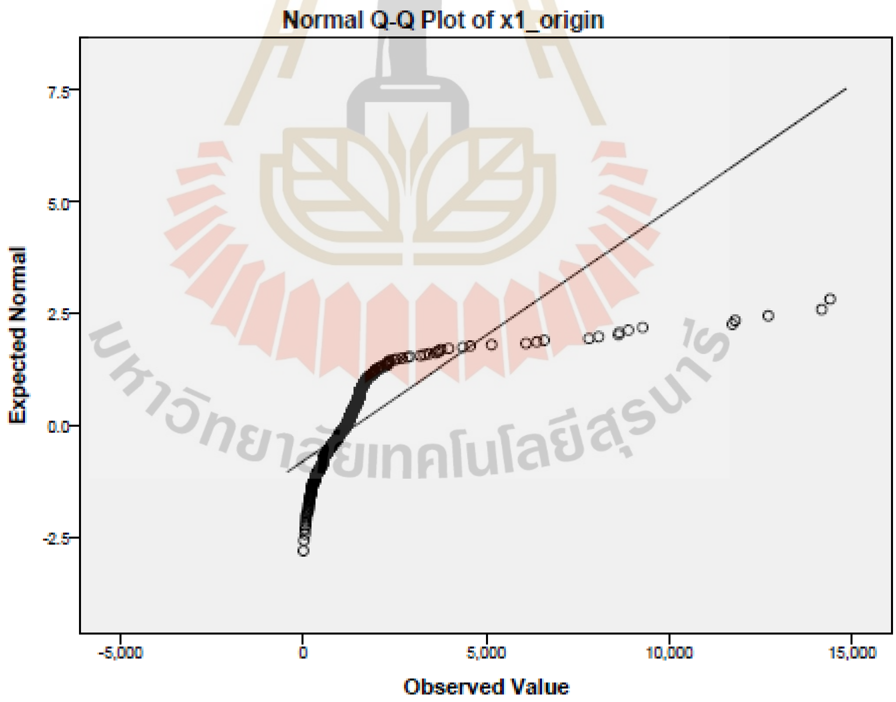
Normal Q-Q Plot of x1_origin
Expected Normal
7.5
5.0
2.5
0.0
-2.5
-5,000
0
5,000
10,000
15,000
Observed Value

Log 10

Case Processing Summary

	Cases					
	Valid		Missing		Total	
	N	Percent	N	Percent	N	Percent
log_x1_new	410	99.8%	1	0.2%	411	100.0%

Descriptives

			Statistic	Std. Error
log_x1_new	Mean		2.9843	.01942
	95% Confidence Interval for Mean	Lower Bound	2.9461	
		Upper Bound	3.0225	
	5% Trimmed Mean		2.9906	
	Median		3.0725	
	Variance		.155	
	Std. Deviation		.39328	
	Minimum		1.18	
	Maximum		4.16	
	Range		2.98	
	Interquartile Range		.41	
	Skewness		-.542	.121
	Kurtosis		2.287	.240

Tests of Normality

	Kolmogorov-Smirnov[a]			Shapiro-Wilk		
	Statistic	df	Sig.	Statistic	df	Sig.
log_x1_new	.115	410	.000	.937	410	.000

a. Lilliefors Significance Correction

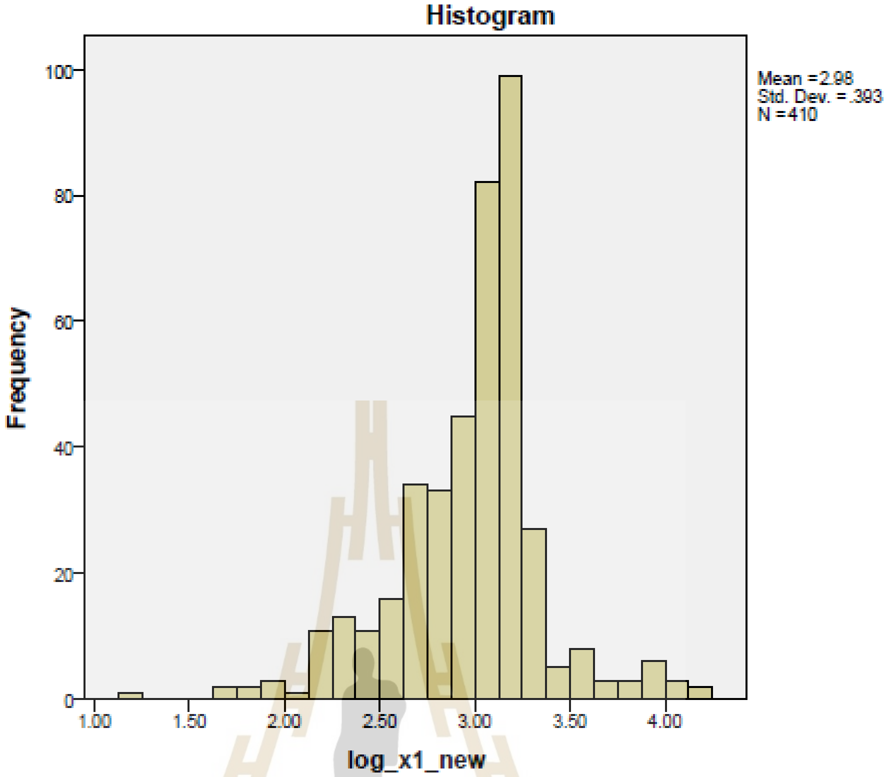
Histogram
Mean =2.98
Std. Dev. =.393
N =410
Frequency
0
20
40
60
80
100
1.00
1.50
2.00
2.50
3.00
3.50
4.00
log_x1_new

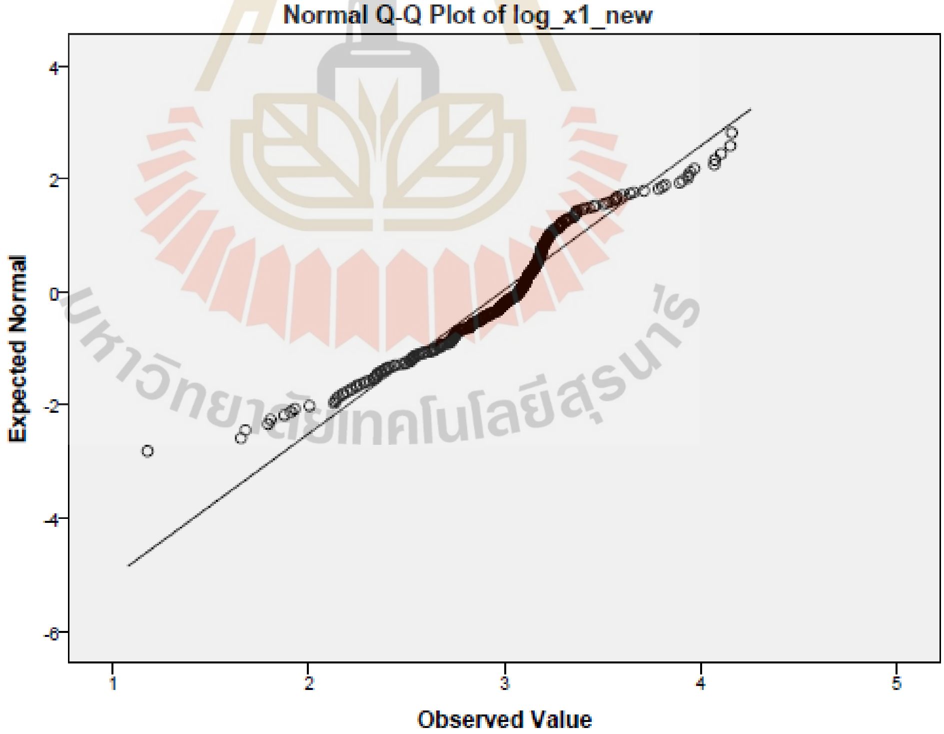
Normal Q-Q Plot of log_x1_new
Expected Normal
4
2
0
-2
-4
-6
1
2
3
4
5
Observed Value

SQRT

Case Processing Summary

	Cases					
	Valid		Missing		Total	
	N	Percent	N	Percent	N	Percent
SQRT_X1_origin	411	100.0%	0	0.0%	411	100.0%

Descriptives

			Statistic	Std. Error
SQRT_X1_origin	Mean		30.3286	.98970
	95% Confidence Interval for Mean	Lower Bound	28.3831	
		Upper Bound	32.2741	
	5% Trimmed Mean		28.8686	
	Median		33.6019	
	Variance		402.574	
	Std. Deviation		20.06425	
	Minimum		.00	
	Maximum		120.06	
	Range		120.06	
	Interquartile Range		17.80	
	Skewness		1.003	.120
	Kurtosis		3.554	.240

Tests of Normality

	Kolmogorov-Smirnov[a]			Shapiro-Wilk		
	Statistic	df	Sig.	Statistic	df	Sig.
SQRT_X1_origin	.150	411	.000	.870	411	.000

a. Lilliefors Significance Correction

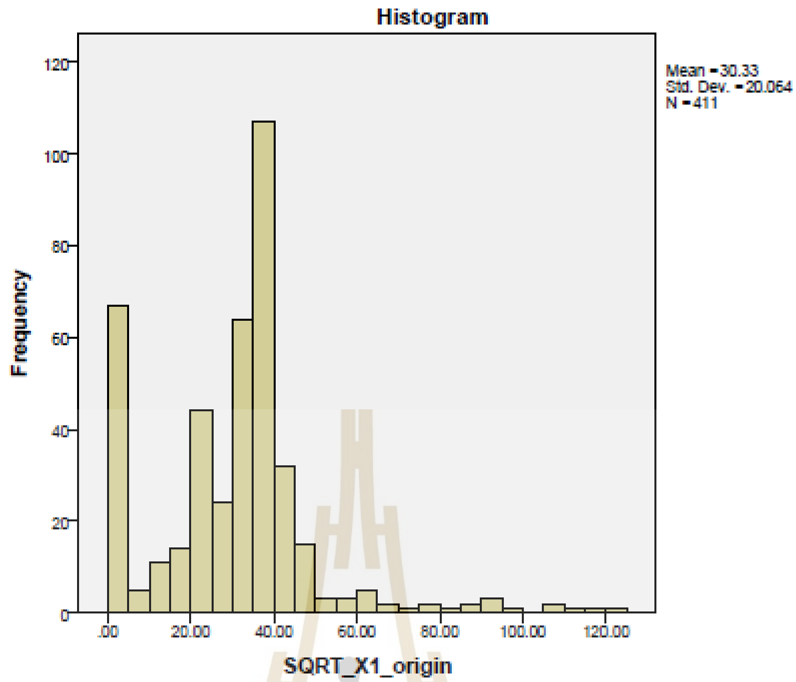
Histogram
Mean = 30.33
Std. Dev. = 20.064
N = 411
Frequency
0
20
40
60
80
100
120
.00
20.00
40.00
60.00
80.00
100.00
120.00
SQRT_X1_origin

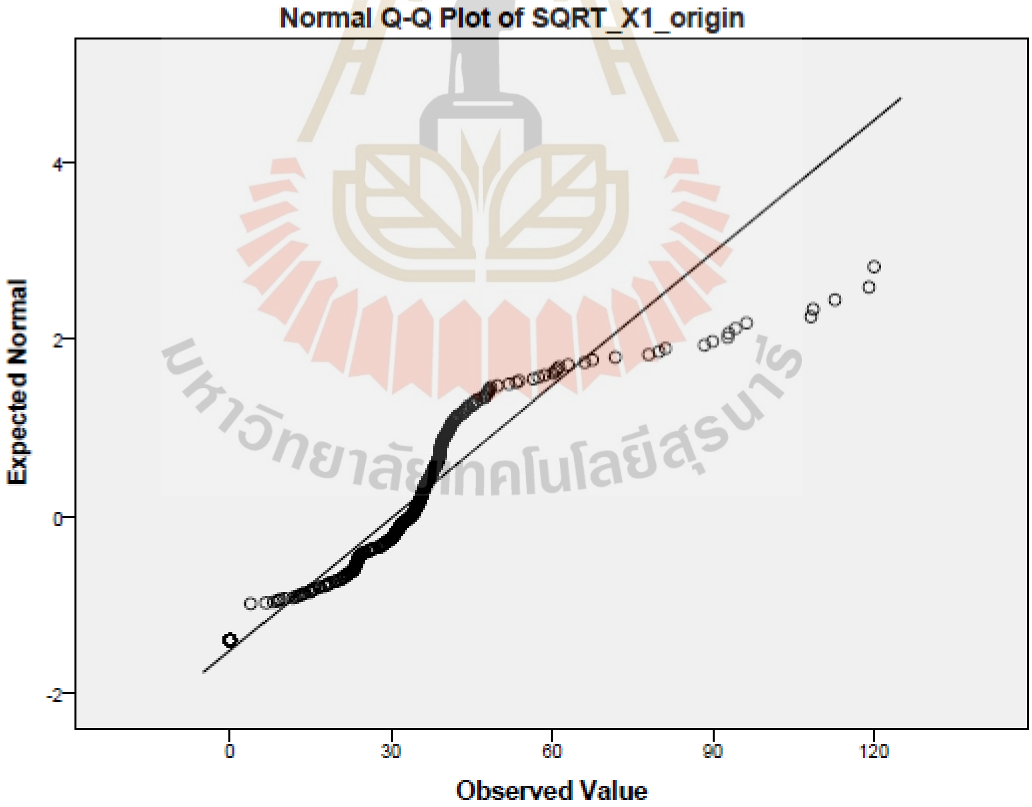
Normal Q-Q Plot of SQRT_X1_origin
Expected Normal
-2
0
2
4
0
30
60
90
120
Observed Value

2) Locating on salt crust area and saline wet belt (X2)

<u>Original</u>

Case Processing Summary

	Cases					
	Valid		Missing		Total	
	N	Percent	N	Percent	N	Percent
x2_origin	411	100.0%	0	0.0%	411	100.0%

Descriptives

			Statistic	Std. Error
x2_origin	Mean		2.486893209	.1115292674
	95% Confidence Interval for Mean	Lower Bound	2.267652674	
		Upper Bound	2.706133745	
	5% Trimmed Mean		2.385720857	
	Median		.8979600000	
	Variance		5.112	
	Std. Deviation		2.261047887	
	Minimum		.0000000000	
	Maximum		6.680230000	
	Range		6.680230000	
	Interquartile Range		3.464517000	
	Skewness		.612	.120
	Kurtosis		-1.118	.240

Tests of Normality

	Kolmogorov-Smirnov[a]			Shapiro-Wilk		
	Statistic	df	Sig.	Statistic	df	Sig.
x2_origin	.336	411	.000	.788	411	.000

a. Lilliefors Significance Correction

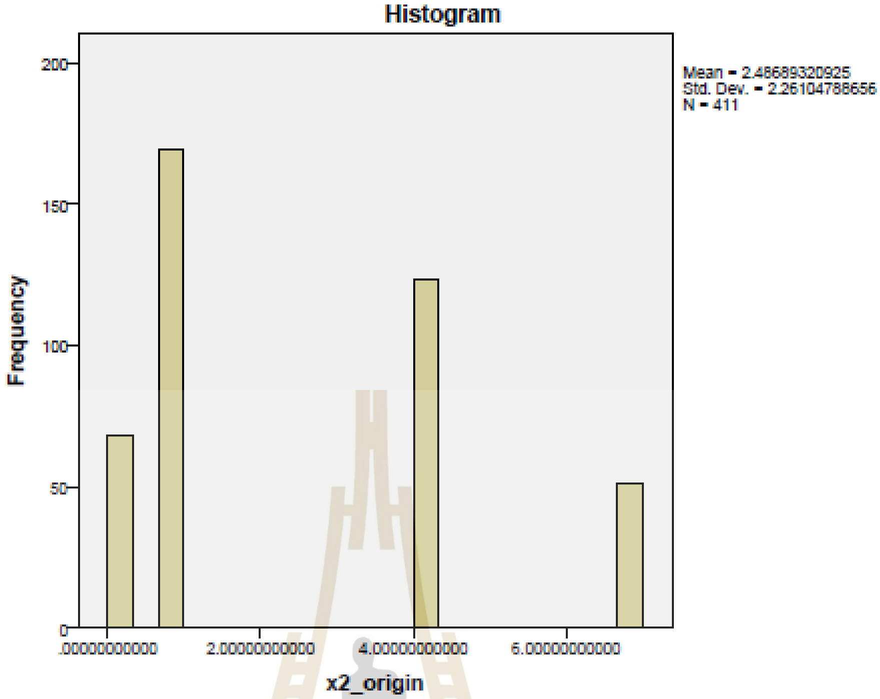
Histogram
Mean = 2.48689320925
Std. Dev. = 2.26104788656
N = 411
Frequency
200
150
100
50
0
.000000000000
2.000000000000
4.000000000000
6.000000000000
x2_origin

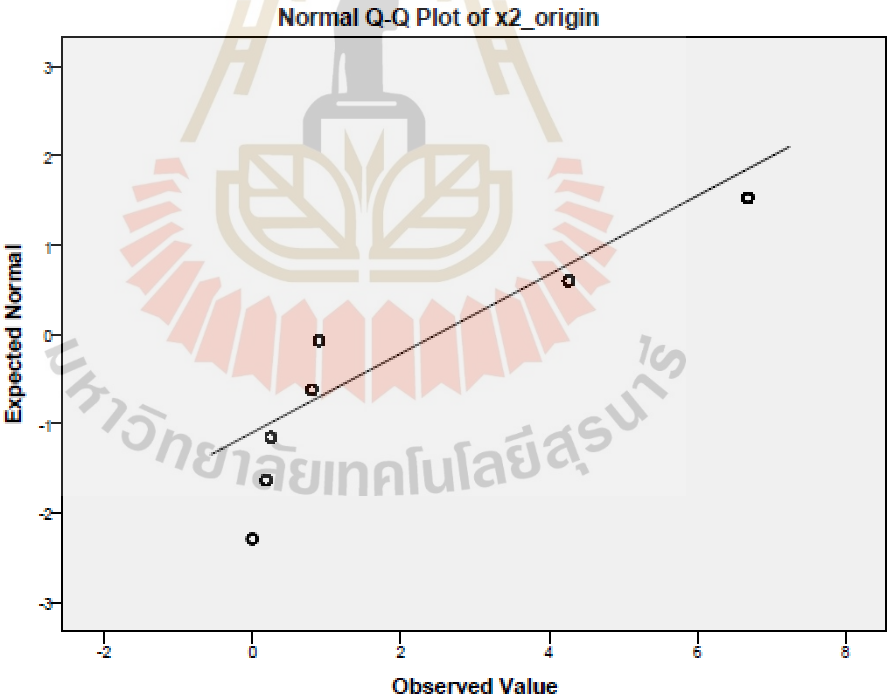
Normal Q-Q Plot of x2_origin
Expected Normal
3
2
1
0
-1
-2
-3
-2
0
2
4
6
8
Observed Value

Log 10

Case Processing Summary

	Cases					
	Valid		Missing		Total	
	N	Percent	N	Percent	N	Percent
Log_X2_origin	388	94.4%	23	5.6%	411	100.0%

Descriptives

			Statistic	Std. Error
Log_X2_origin	Mean		.2521586148	.0236096344
	95% Confidence Interval for Mean	Lower Bound	.2057394109	
		Upper Bound	.2985778186	
	5% Trimmed Mean		.2681563450	
	Median		-.0467430087	
	Variance		.216	
	Std. Deviation		.4650558647	
	Minimum		-.6084333303	
	Maximum		.8247914155	
	Range		1.433224746	
	Interquartile Range		.7673091878	
	Skewness		-.228	.124
	Kurtosis		-1.303	.247

Tests of Normality

	Kolmogorov-Smirnov[a]			Shapiro-Wilk		
	Statistic	df	Sig.	Statistic	df	Sig.
Log_X2_origin	.290	388	.000	.814	388	.000

a. Lilliefors Significance Correction

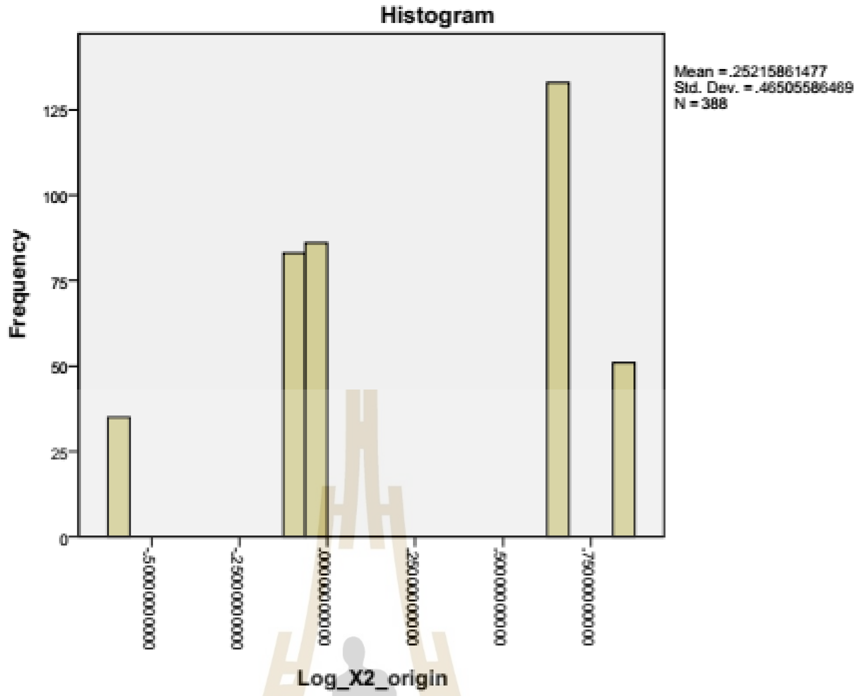
Histogram
Mean =.25215861477
Std. Dev. =.46505586469
N = 388
Frequency
Log_X2_origin

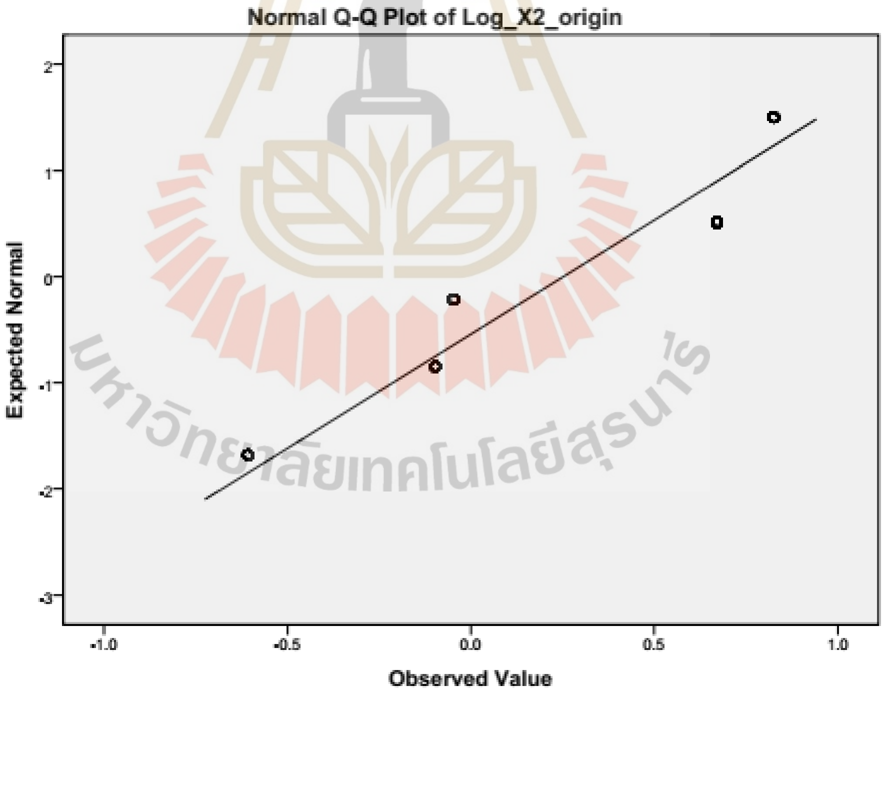
Normal Q-Q Plot of Log_X2_origin
Expected Normal
Observed Value

SQRT

Case Processing Summary

	Cases					
	Valid		Missing		Total	
	N	Percent	N	Percent	N	Percent
SQRT_X2_origin	411	100.0%	0	0.0%	411	100.0%

Descriptives

			Statistic	Std. Error
SQRT_X2_origin	Mean		1.3862	.03713
	95% Confidence Interval for Mean	Lower Bound	1.3132	
		Upper Bound	1.4592	
	5% Trimmed Mean		1.3819	
	Median		.9476	
	Variance		.567	
	Std. Deviation		.75278	
	Minimum		.00	
	Maximum		2.58	
	Range		2.58	
	Interquartile Range		1.17	
	Skewness		.238	.120
	Kurtosis		-1.392	.240

Tests of Normality

	Kolmogorov-Smirnov[a]			Shapiro-Wilk		
	Statistic	df	Sig.	Statistic	df	Sig.
SQRT_X2_origin	.297	411	.000	.849	411	.000

a. Lilliefors Significance Correction

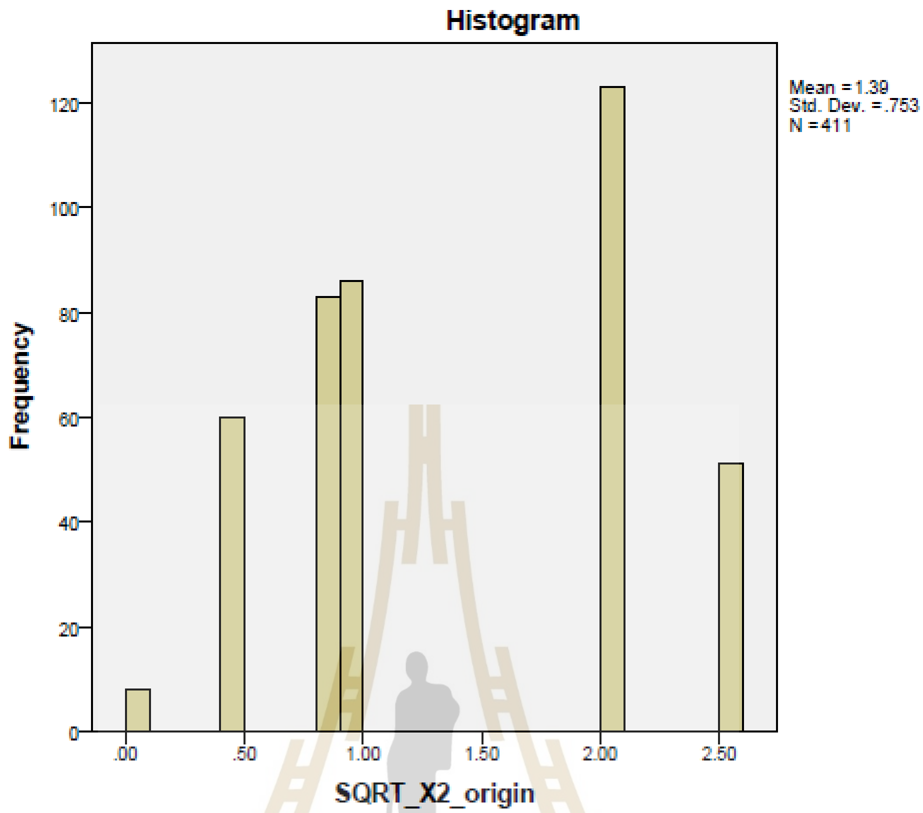
Histogram
Mean = 1.39
Std. Dev. = .753
N = 411
Frequency
120
100
80
60
40
20
0
.00
.50
1.00
1.50
2.00
2.50
SQRT_X2_origin

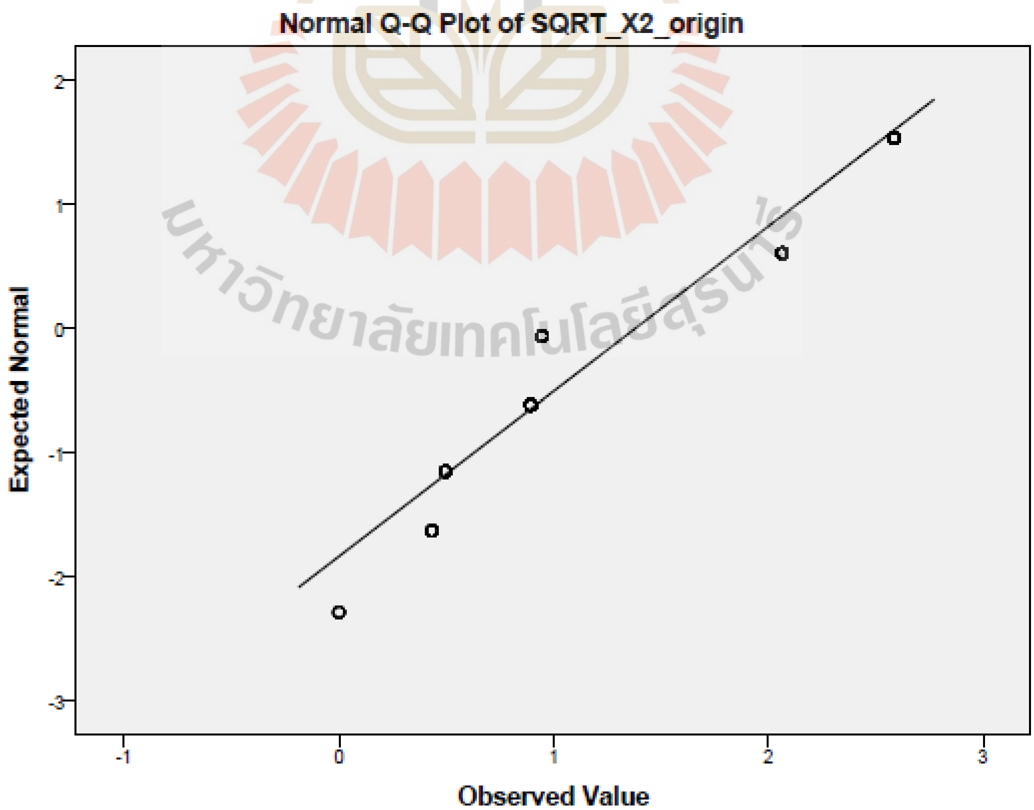
Normal Q-Q Plot of SQRT_X2_origin
Expected Normal
2
1
0
-1
-2
-3
-1
0
1
2
3
Observed Value

3) NDSI (X3)

Original

Case Processing Summary

	Cases					
	Valid		Missing		Total	
	N	Percent	N	Percent	N	Percent
x3_origin	411	100.0%	0	0.0%	411	100.0%

Descriptives

			Statistic	Std. Error
x3_origin	Mean		.0905446699	.0015103200
	95% Confidence Interval for Mean	Lower Bound	.0875757329	
		Upper Bound	.0935136068	
	5% Trimmed Mean		.0914284669	
	Median		.0925926000	
	Variance		.001	
	Std. Deviation		.0306189211	
	Minimum		-.0612245000	
	Maximum		.1690140000	
	Range		.2302385000	
	Interquartile Range		.0362433000	
	Skewness		-.694	.120
	Kurtosis		2.308	.240

Tests of Normality

	Kolmogorov-Smirnov[a]			Shapiro-Wilk		
	Statistic	df	Sig.	Statistic	df	Sig.
x3_origin	.057	411	.003	.971	411	.000

a. Lilliefors Significance Correction

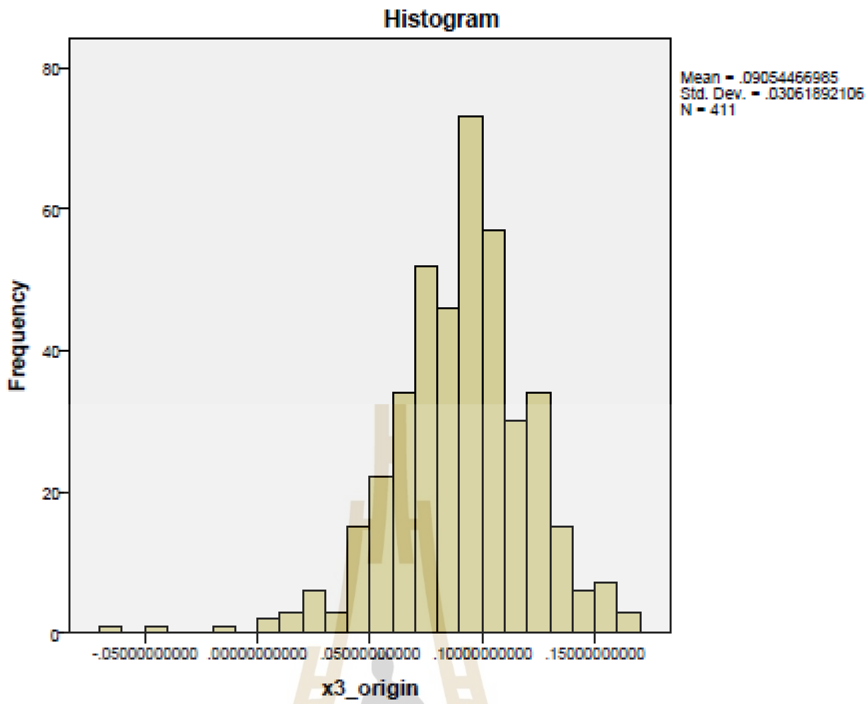
Histogram
Mean = .09054466985
Std. Dev. = .03061892106
N = 411
Frequency
80
60
40
20
0
-.05000000000
.00000000000
.05000000000
.10000000000
.15000000000
x3_origin

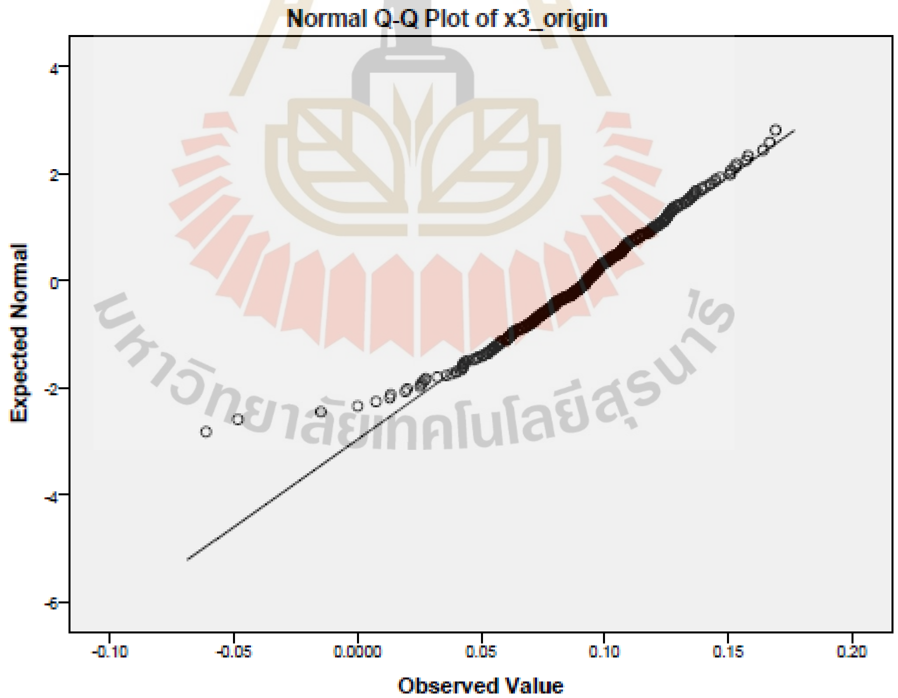
Normal Q-Q Plot of x3_origin
Expected Normal
4
2
0
-2
-4
-6
-0.10
-0.05
0.0000
0.05
0.10
0.15
0.20
Observed Value

Log 10

Case Processing Summary

	Cases					
	Valid		Missing		Total	
	N	Percent	N	Percent	N	Percent
Log_X3_origin	407	99.0%	4	1.0%	411	100.0%

Descriptives

			Statistic	Std. Error
Log_X3_origin	Mean		-1.0640	.00834
	95% Confidence Interval for Mean	Lower Bound	-1.0804	
		Upper Bound	-1.0476	
	5% Trimmed Mean		-1.0497	
	Median		-1.0320	
	Variance		.028	
	Std. Deviation		.16831	
	Minimum		-2.13	
	Maximum		-.77	
	Range		1.36	
	Interquartile Range		.17	
	Skewness		-1.950	.121
	Kurtosis		7.063	.241

Tests of Normality

	Kolmogorov-Smirnov[a]			Shapiro-Wilk		
	Statistic	df	Sig.	Statistic	df	Sig.
Log_X3_origin	.116	407	.000	.868	407	.000

a. Lilliefors Significance Correction

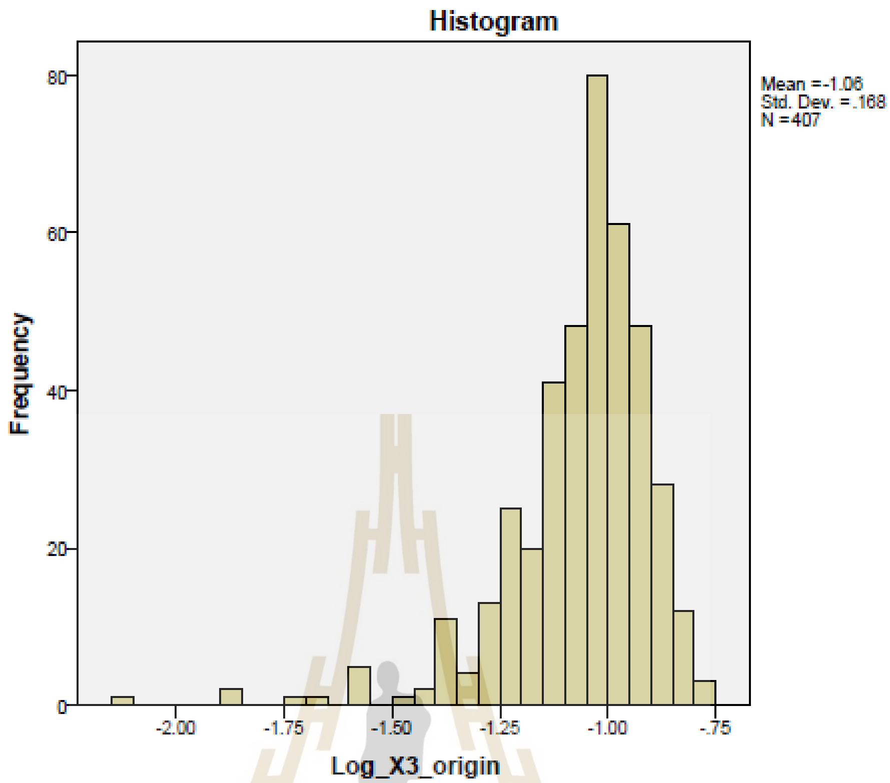

Histogram
Mean =-1.06
Std. Dev. =.168
N =407
Frequency
0
20
40
60
80
-2.00
-1.75
-1.50
-1.25
-1.00
-.75
Log_X3_origin

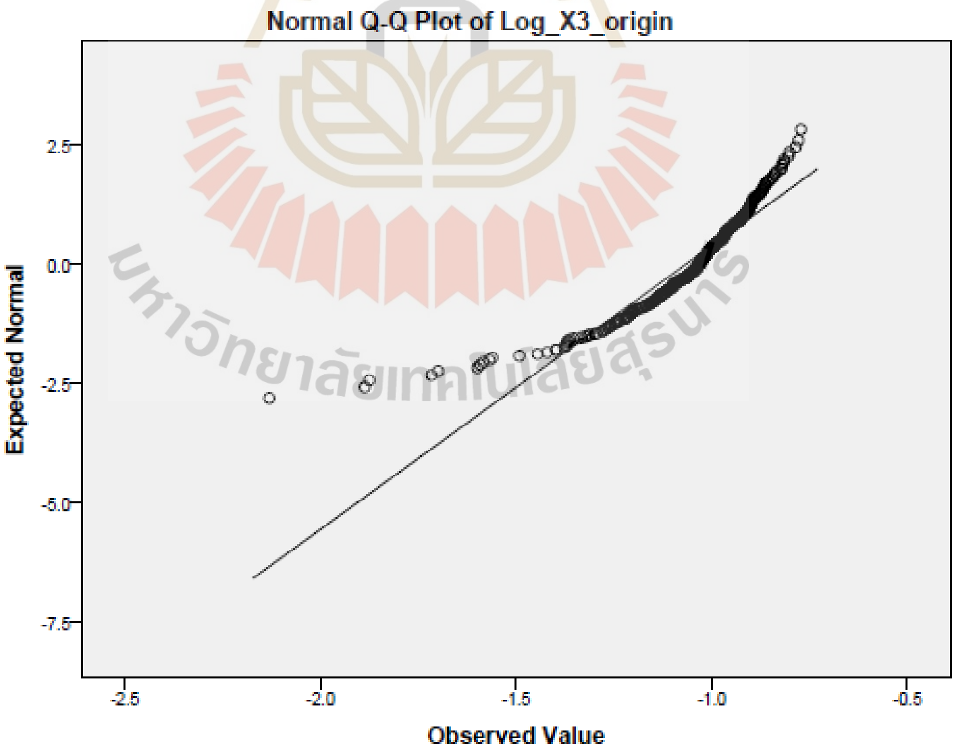

Normal Q-Q Plot of Log_X3_origin
Expected Normal
2.5
0.0
-2.5
-5.0
-7.5
-2.5
-2.0
-1.5
-1.0
-0.5
Observed Value

SQRT

Case Processing Summary

	Cases					
	Valid		Missing		Total	
	N	Percent	N	Percent	N	Percent
SQRT_X3_origin	408	99.3%	3	0.7%	411	100.0%

Descriptives

			Statistic	Std. Error
SQRT_X3_origin	Mean		.2980	.00258
	95% Confidence Interval for Mean	Lower Bound	.2929	
		Upper Bound	.3031	
	5% Trimmed Mean		.3008	
	Median		.3047	
	Variance		.003	
	Std. Deviation		.05211	
	Minimum		.00	
	Maximum		.41	
	Range		.41	
	Interquartile Range		.06	
	Skewness		-1.145	.121
	Kurtosis		3.443	.241

Tests of Normality

	Kolmogorov-Smirnov[a]			Shapiro-Wilk		
	Statistic	df	Sig.	Statistic	df	Sig.
SQRT_X3_origin	.084	408	.000	.944	408	.000

a. Lilliefors Significance Correction

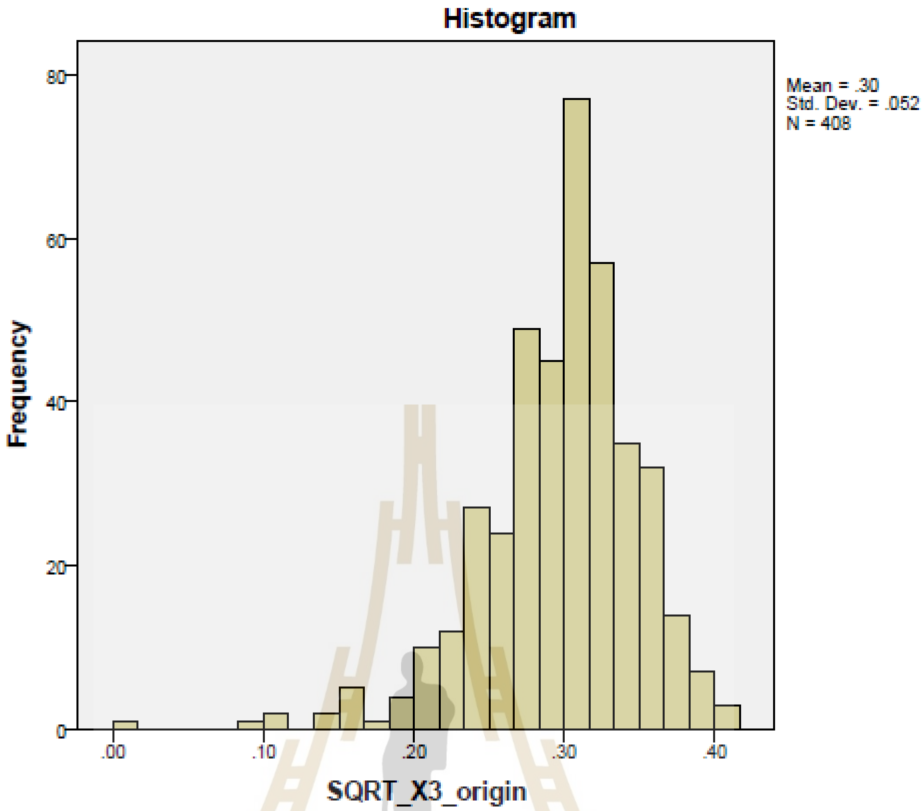
Histogram
Mean = .30
Std. Dev. = .052
N = 408
Frequency
80
60
40
20
0
.00
.10
.20
.30
.40
SQRT_X3_origin

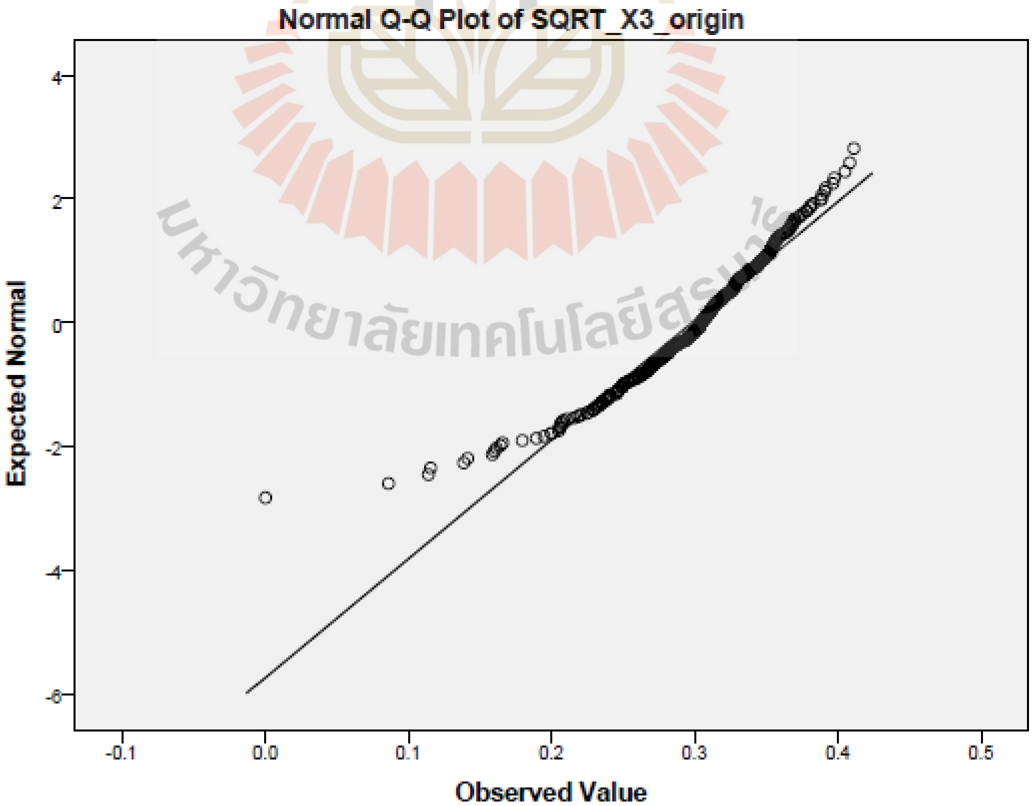
Normal Q-Q Plot of SQRT_X3_origin
Expected Normal
4
2
0
-2
-4
-6
-0.1
0.0
0.1
0.2
0.3
0.4
0.5
Observed Value

4) Distance to ancient settlements (X4)

<u>Original</u>

Case Processing Summary

	Cases					
	Valid		Missing		Total	
	N	Percent	N	Percent	N	Percent
x4_origin	411	100.0%	0	0.0%	411	100.0%

Descriptives

			Statistic	Std. Error
x4_origin	Mean		1596.131589	111.3182614
	95% Confidence Interval for Mean	Lower Bound	1377.305842	
		Upper Bound	1814.957336	
	5% Trimmed Mean		1261.882328	
	Median		725.7580000	
	Variance		5093011.435	
	Std. Deviation		2256.770133	
	Minimum		67.08200000	
	Maximum		14578.30000	
	Range		14511.21800	
	Interquartile Range		1233.092000	
	Skewness		2.665	.120
	Kurtosis		8.060	.240

Tests of Normality

	Kolmogorov-Smirnov[a]			Shapiro-Wilk		
	Statistic	df	Sig.	Statistic	df	Sig.
x4_origin	.277	411	.000	.639	411	.000

a. Lilliefors Significance Correction

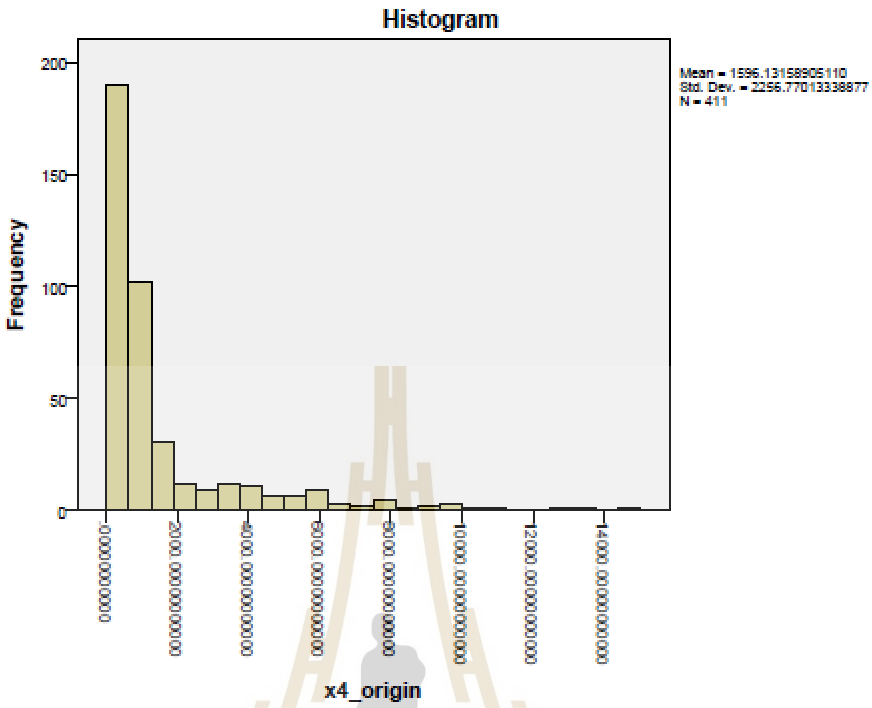
Histogram
Mean = 1596.13158905110
Std. Dev. = 2256.77013338877
N = 411
Frequency
x4_origin

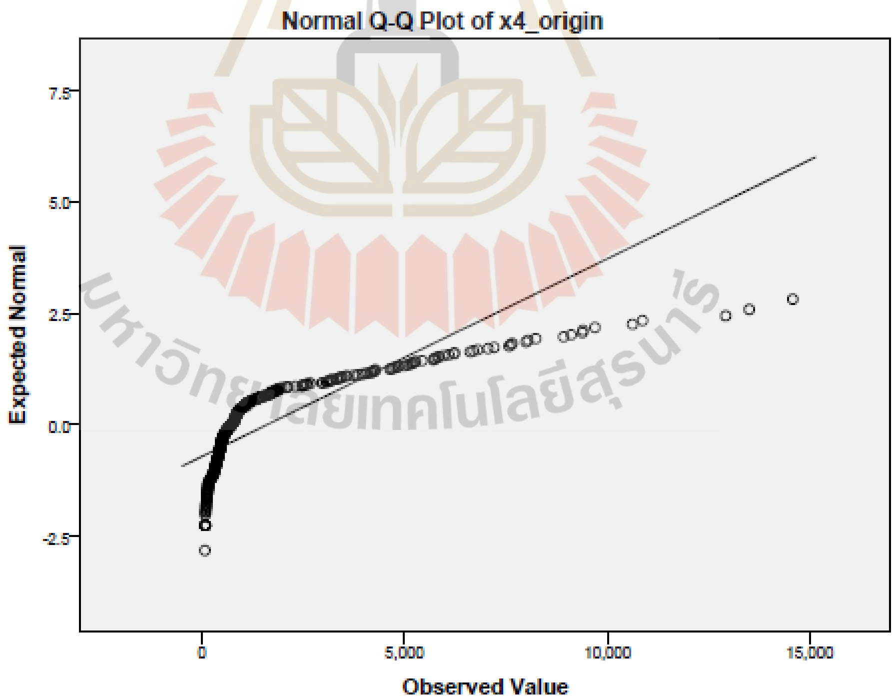
Normal Q-Q Plot of x4_origin
Expected Normal
Observed Value

Log 10

Case Processing Summary

	Cases					
	Valid		Missing		Total	
	N	Percent	N	Percent	N	Percent
Log_X4_origin	411	100.0%	0	0.0%	411	100.0%

Descriptives

			Statistic	Std. Error
Log_X4_origin	Mean		2.9012	.02480
	95% Confidence Interval for Mean	Lower Bound	2.8525	
		Upper Bound	2.9500	
	5% Trimmed Mean		2.8966	
	Median		2.8608	
	Variance		.253	
	Std. Deviation		.50274	
	Minimum		1.83	
	Maximum		4.16	
	Range		2.34	
	Interquartile Range		.61	
	Skewness		.273	.120
	Kurtosis		-.253	.240

Tests of Normality

	Kolmogorov-Smirnov[a]			Shapiro-Wilk		
	Statistic	df	Sig.	Statistic	df	Sig.
Log_X4_origin	.086	411	.000	.975	411	.000

a. Lilliefors Significance Correction

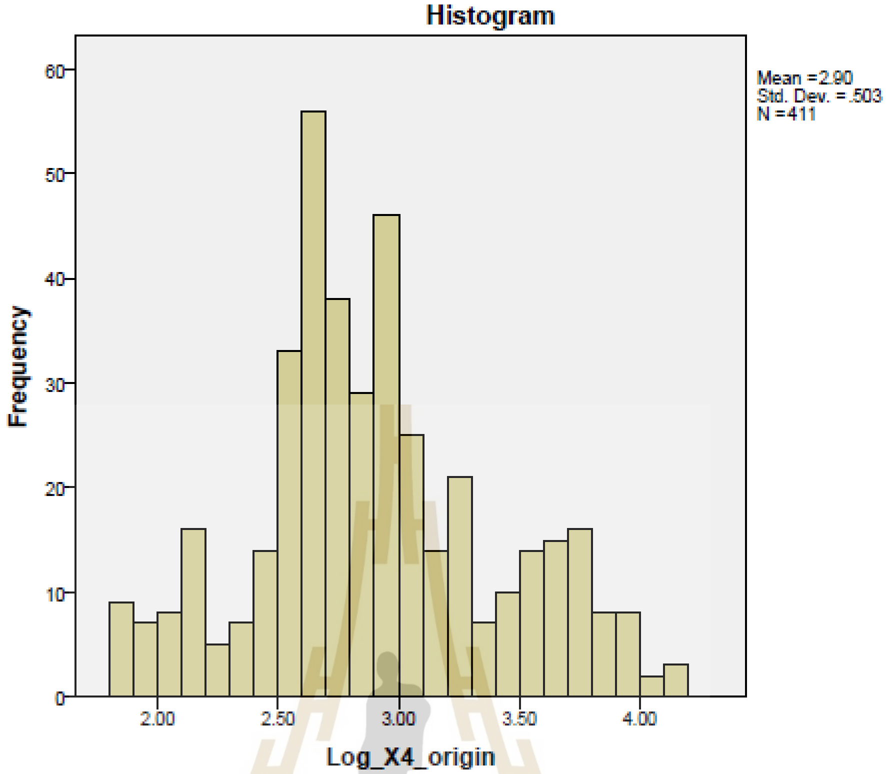
Histogram
Mean =2.90
Std. Dev. =.503
N =411
Frequency
0
10
20
30
40
50
60
2.00
2.50
3.00
3.50
4.00
Log_X4_origin

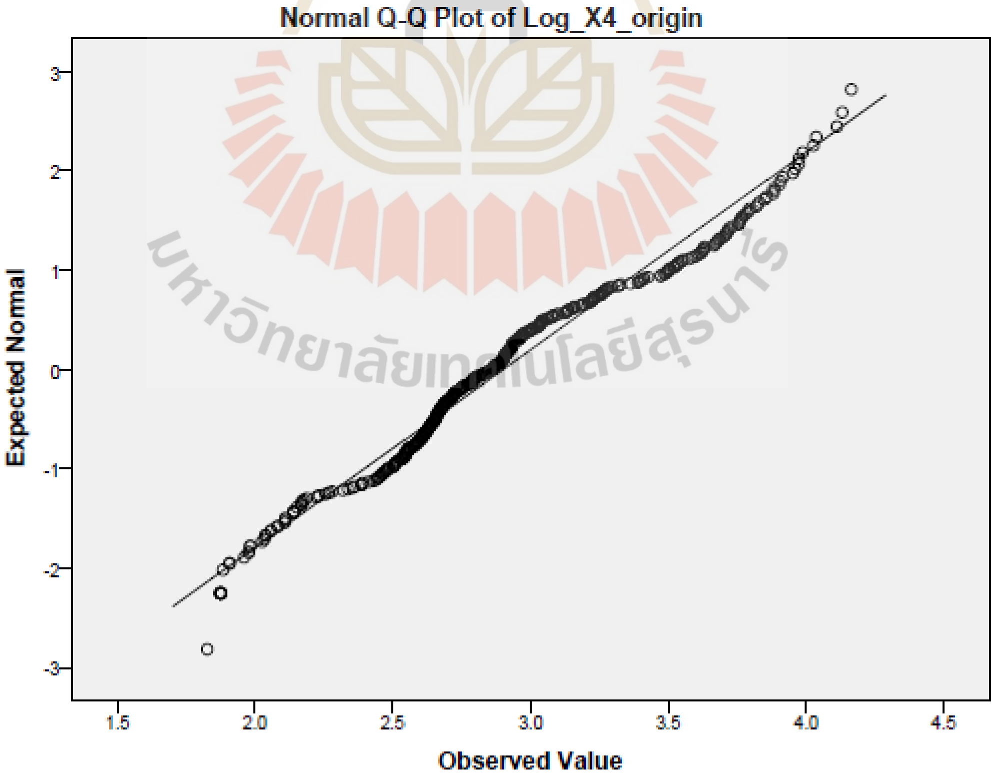
Normal Q-Q Plot of Log_X4_origin
Expected Normal
3
2
1
0
-1
-2
-3
1.5
2.0
2.5
3.0
3.5
4.0
4.5
Observed Value

SQRT

Case Processing Summary

	Cases					
	Valid		Missing		Total	
	N	Percent	N	Percent	N	Percent
SQRT_X4_origin	411	100.0%	0	0.0%	411	100.0%

Descriptives

			Statistic	Std. Error
SQRT_X4_origin	Mean		33.5805	1.06894
	95% Confidence Interval for Mean	Lower Bound	31.4792	
		Upper Bound	35.6818	
	5% Trimmed Mean		31.5240	
	Median		26.9399	
	Variance		469.622	
	Std. Deviation		21.67076	
	Minimum		8.19	
	Maximum		120.74	
	Range		112.55	
	Interquartile Range		20.35	
	Skewness		1.543	.120
	Kurtosis		2.017	.240

Tests of Normality

	Kolmogorov-Smirnov[a]			Shapiro-Wilk		
	Statistic	df	Sig.	Statistic	df	Sig.
SQRT_X4_origin	.197	411	.000	.832	411	.000

a. Lilliefors Significance Correction

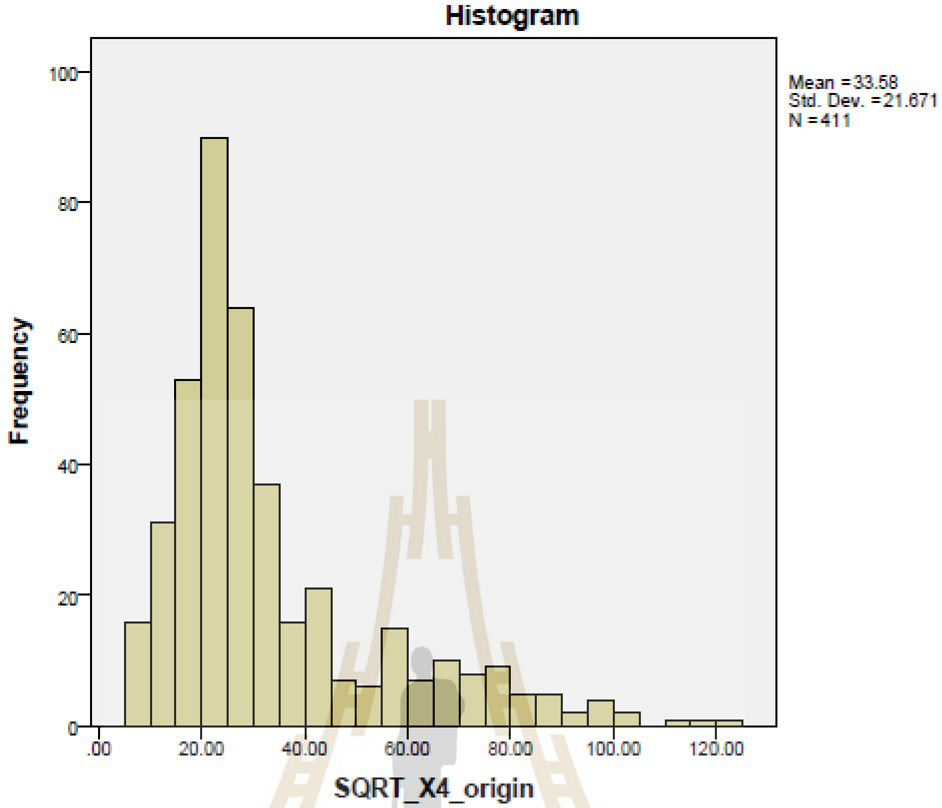
Histogram
Mean =33.58
Std. Dev. =21.671
N =411
Frequency
SQRT_X4_origin

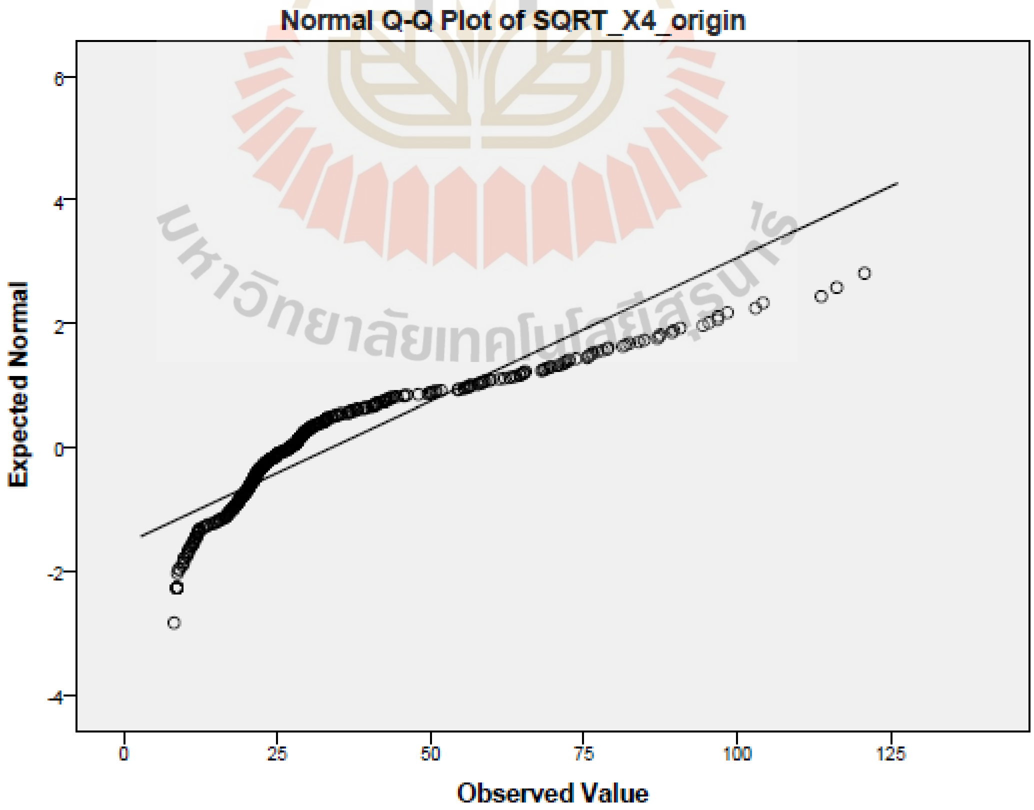
Normal Q-Q Plot of SQRT_X4_origin
Expected Normal
Observed Value

5) Distance to water bodies and streams (X5)

Original

Case Processing Summary

	Cases					
	Valid		Missing		Total	
	N	Percent	N	Percent	N	Percent
x5_origin	411	100.0%	0	0.0%	411	100.0%

Descriptives

			Statistic	Std. Error
x5_origin	Mean		721.9465039	25.93712510
	95% Confidence Interval for Mean	Lower Bound	670.9601635	
		Upper Bound	772.9328443	
	5% Trimmed Mean		694.7727680	
	Median		636.3960000	
	Variance		276493.862	
	Std. Deviation		525.8268369	
	Minimum		.0000000000	
	Maximum		3333.010000	
	Range		3333.010000	
	Interquartile Range		782.2460000	
	Skewness		.923	.120
	Kurtosis		1.763	.240

Tests of Normality

	Kolmogorov-Smirnov[a]			Shapiro-Wilk		
	Statistic	df	Sig.	Statistic	df	Sig.
x5_origin	.103	411	.000	.928	411	.000

a. Lilliefors Significance Correction

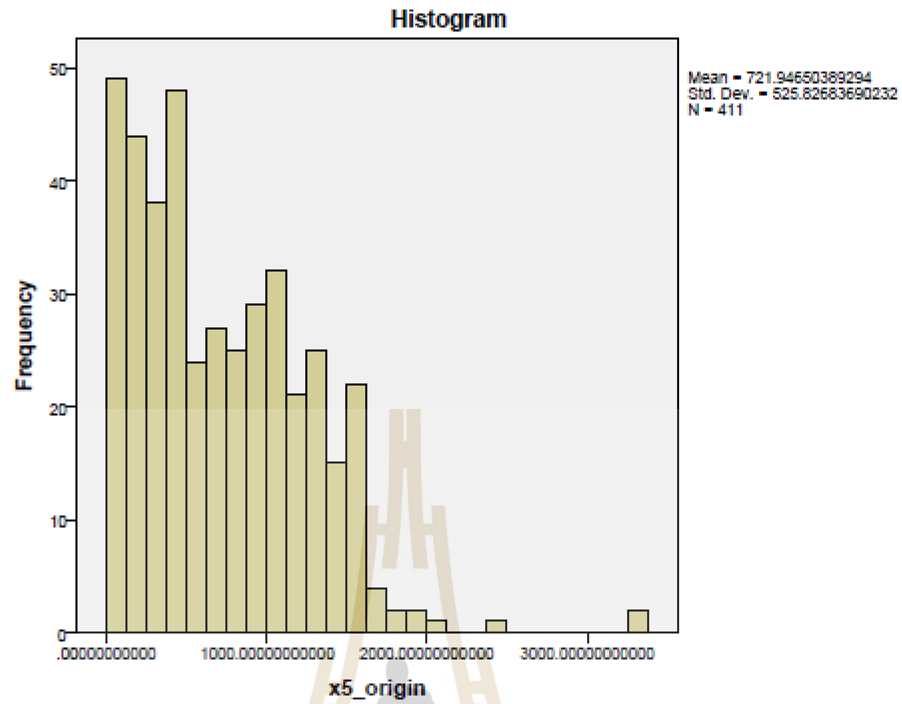
Histogram
Mean = 721.94650389294
Std. Dev. = 525.82683690232
N = 411
Frequency
50
40
30
20
10
0
.000000000000
1000.000000000000
2000.000000000000
3000.000000000000
x5_origin

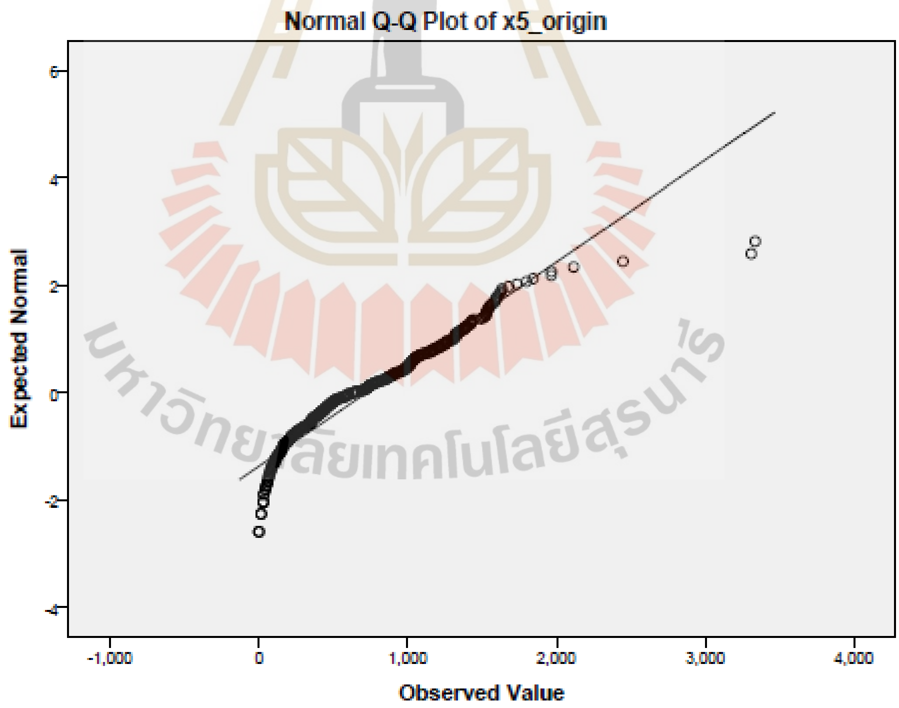
Normal Q-Q Plot of x5_origin
Expected Normal
6
4
2
0
-2
-4
-1,000
0
1,000
2,000
3,000
4,000
Observed Value

<u>Log 10</u>

Case Processing Summary

	Cases					
	Valid		Missing		Total	
	N	Percent	N	Percent	N	Percent
Log_X5_origin	408	99.3%	3	0.7%	411	100.0%

Descriptives

			Statistic	Std. Error
Log_X5_origin	Mean		2.7000	.02181
	95% Confidence Interval for Mean	Lower Bound	2.6571	
		Upper Bound	2.7429	
	5% Trimmed Mean		2.7311	
	Median		2.8075	
	Variance		.194	
	Std. Deviation		.44058	
	Minimum		1.18	
	Maximum		3.52	
	Range		2.35	
	Interquartile Range		.57	
	Skewness		-1.017	.121
	Kurtosis		.663	.241

Tests of Normality

	Kolmogorov-Smirnov[a]			Shapiro-Wilk		
	Statistic	df	Sig.	Statistic	df	Sig.
Log_X5_origin	.116	408	.000	.919	408	.000

a. Lilliefors Significance Correction

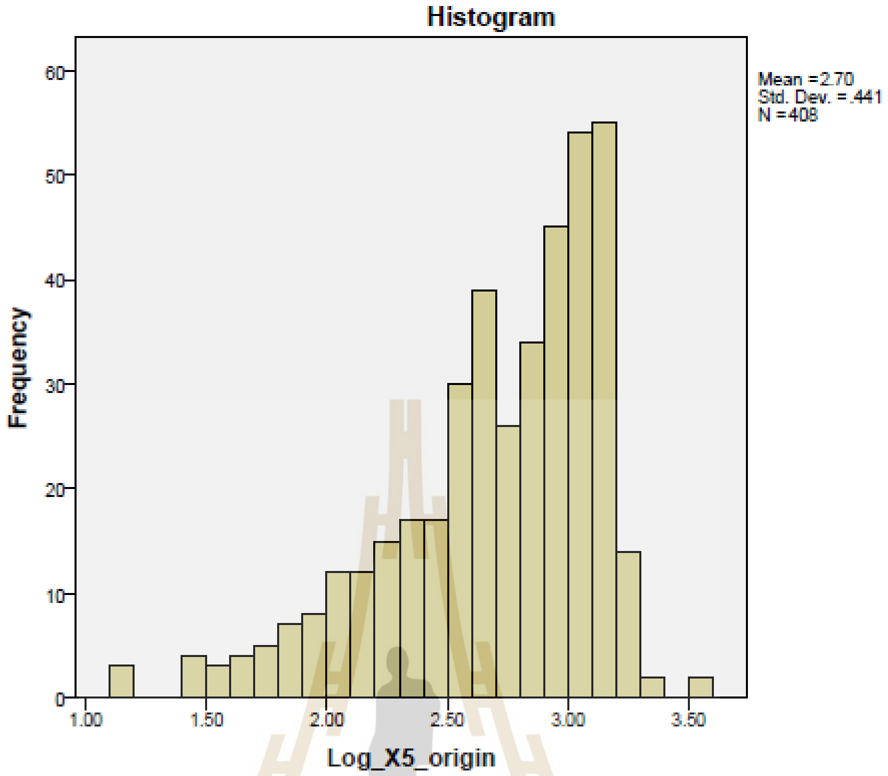
Histogram
Mean =2.70
Std. Dev. =.441
N =408
Frequency
Log_X5_origin
0
10
20
30
40
50
60
1.00
1.50
2.00
2.50
3.00
3.50

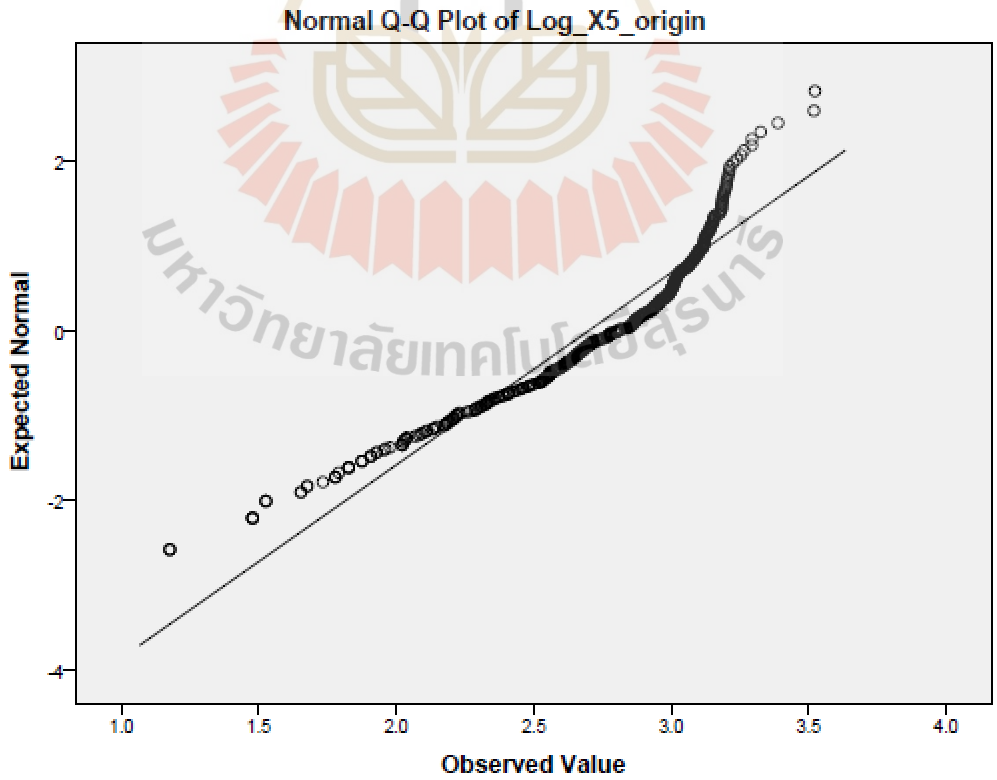
Normal Q-Q Plot of Log_X5_origin
Expected Normal
Observed Value
2
0
-2
-4
1.0
1.5
2.0
2.5
3.0
3.5
4.0

SQRT

Case Processing Summary

	Cases					
	Valid		Missing		Total	
	N	Percent	N	Percent	N	Percent
SQRT_X5_origin	411	100.0%	0	0.0%	411	100.0%

Descriptives

			Statistic	Std. Error
SQRT_X5_origin	Mean		24.7702	.51415
	95% Confidence Interval for Mean	Lower Bound	23.7595	
		Upper Bound	25.7809	
	5% Trimmed Mean		24.8339	
	Median		25.2269	
	Variance		108.647	
	Std. Deviation		10.42340	
	Minimum		.00	
	Maximum		57.73	
	Range		57.73	
	Interquartile Range		15.78	
	Skewness		-.062	.120
	Kurtosis		-.569	.240

Tests of Normality

	Kolmogorov-Smirnov[a]			Shapiro-Wilk		
	Statistic	df	Sig.	Statistic	df	Sig.
SQRT_X5_origin	.070	411	.000	.981	411	.000

a. Lilliefors Significance Correction

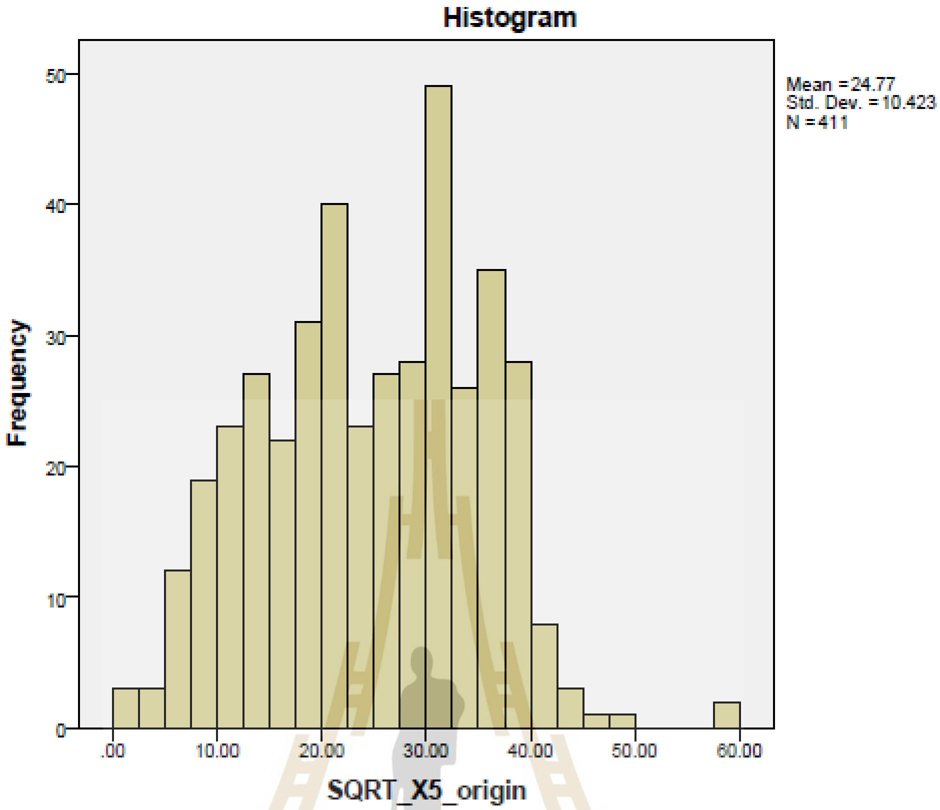
Histogram
Mean = 24.77
Std. Dev. = 10.423
N = 411
Frequency
50
40
30
20
10
0
.00
10.00
20.00
30.00
40.00
50.00
60.00
SQRT_X5_origin

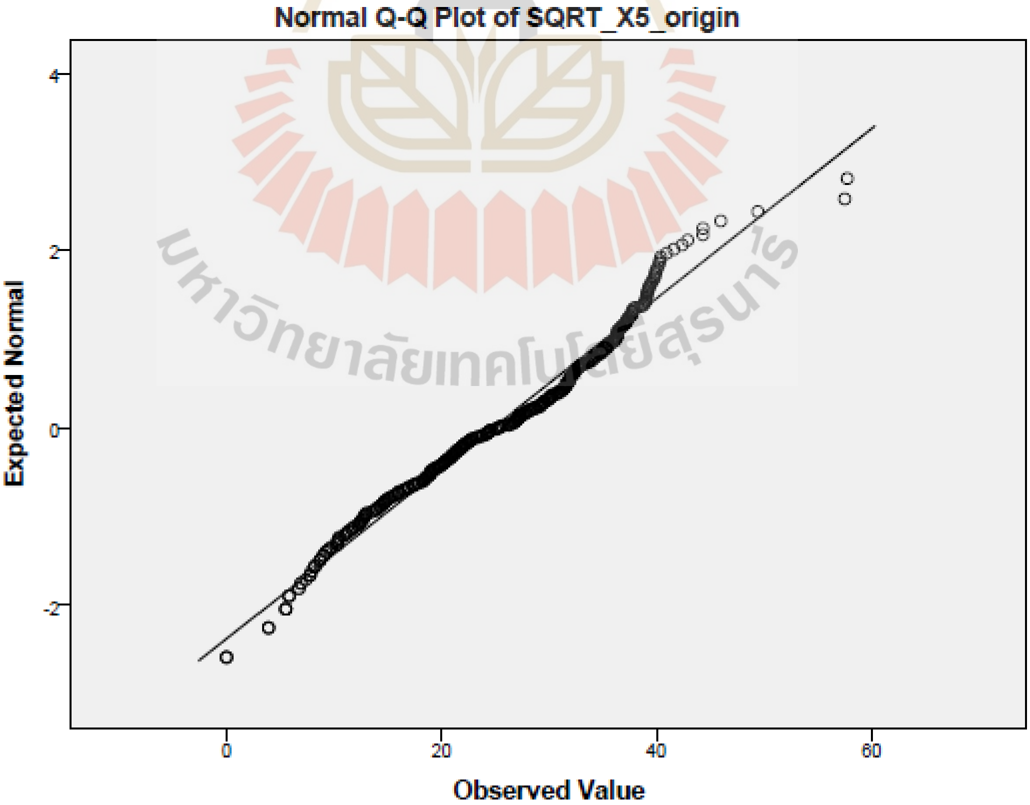
Normal Q-Q Plot of SQRT_X5_origin
Expected Normal
4
2
0
-2
0
20
40
60
Observed Value

6) Geology (X6)

Original

Case Processing Summary

	Cases					
	Valid		Missing		Total	
	N	Percent	N	Percent	N	Percent
x6_origin	411	100.0%	0	0.0%	411	100.0%

Descriptives

			Statistic	Std. Error
x6_origin	Mean		1.318540063	.0268618266
	95% Confidence Interval for Mean	Lower Bound	1.265735975	
		Upper Bound	1.371344151	
	5% Trimmed Mean		1.365252281	
	Median		1.603640000	
	Variance		.297	
	Std. Deviation		.5445734349	
	Minimum		.0000000000	
	Maximum		1.603640000	
	Range		1.603640000	
	Interquartile Range		.0000000000	
	Skewness		-1.406	.120
	Kurtosis		.026	.240

Tests of Normality

	Kolmogorov-Smirnov[a]			Shapiro-Wilk		
	Statistic	df	Sig.	Statistic	df	Sig.
x6_origin	.483	411	.000	.522	411	.000

a. Lilliefors Significance Correction

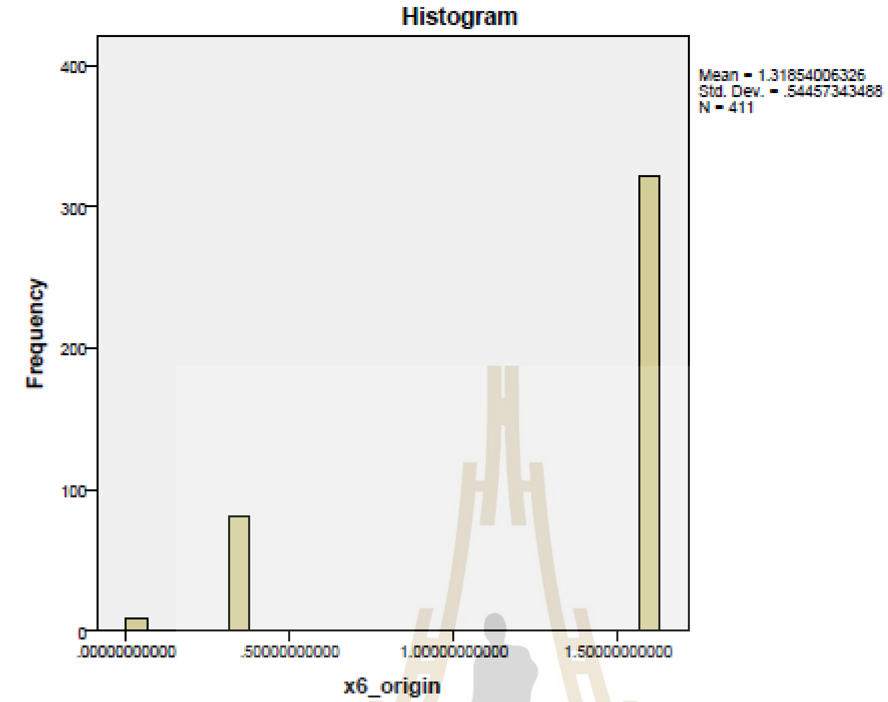
Histogram
Mean = 1.31854006326
Std. Dev. = .54457343488
N = 411
Frequency
400
300
200
100
0
.00000000000
.50000000000
1.00000000000
1.50000000000
x6_origin

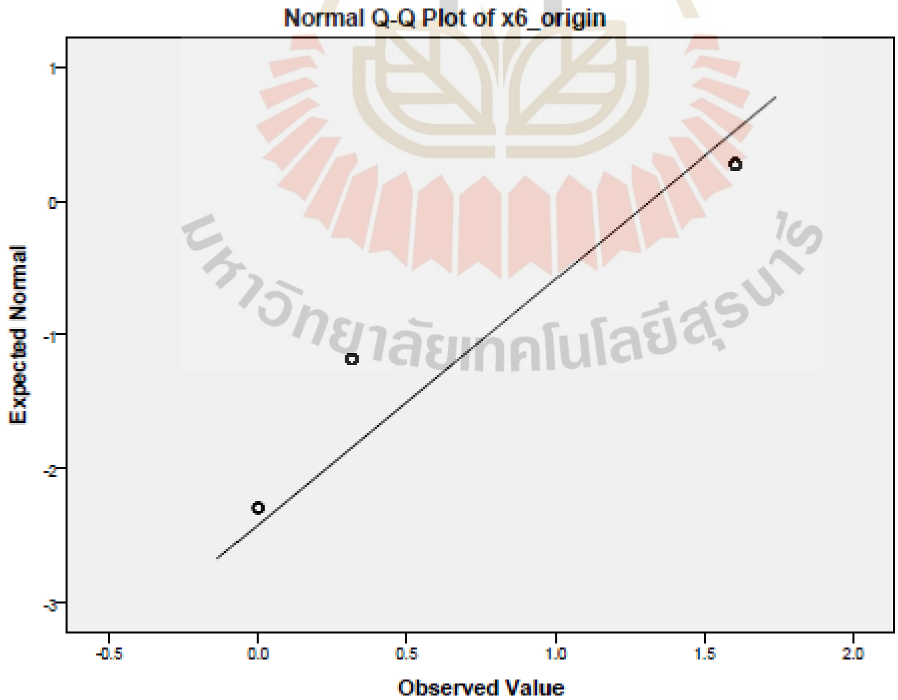
Normal Q-Q Plot of x6_origin
Expected Normal
1
0
-1
-2
-3
-0.5
0.0
0.5
1.0
1.5
2.0
Observed Value

Log 10

Case Processing Summary

	Cases					
	Valid		Missing		Total	
	N	Percent	N	Percent	N	Percent
Log_X6_origin	403	98.1%	8	1.9%	411	100.0%

Descriptives

			Statistic	Std. Error
Log_X6_origin	Mean		.0632	.01412
	95% Confidence Interval for Mean	Lower Bound	.0354	
		Upper Bound	.0909	
	5% Trimmed Mean		.0866	
	Median		.2051	
	Variance		.080	
	Std. Deviation		.28337	
	Minimum		-.50	
	Maximum		.21	
	Range		.71	
	Interquartile Range		.00	
	Skewness		-1.498	.122
	Kurtosis		.245	.243

Tests of Normality

	Kolmogorov-Smirnov[a]			Shapiro-Wilk		
	Statistic	df	Sig.	Statistic	df	Sig.
Log_X6_origin	.491	403	.000	.491	403	.000

a. Lilliefors Significance Correction

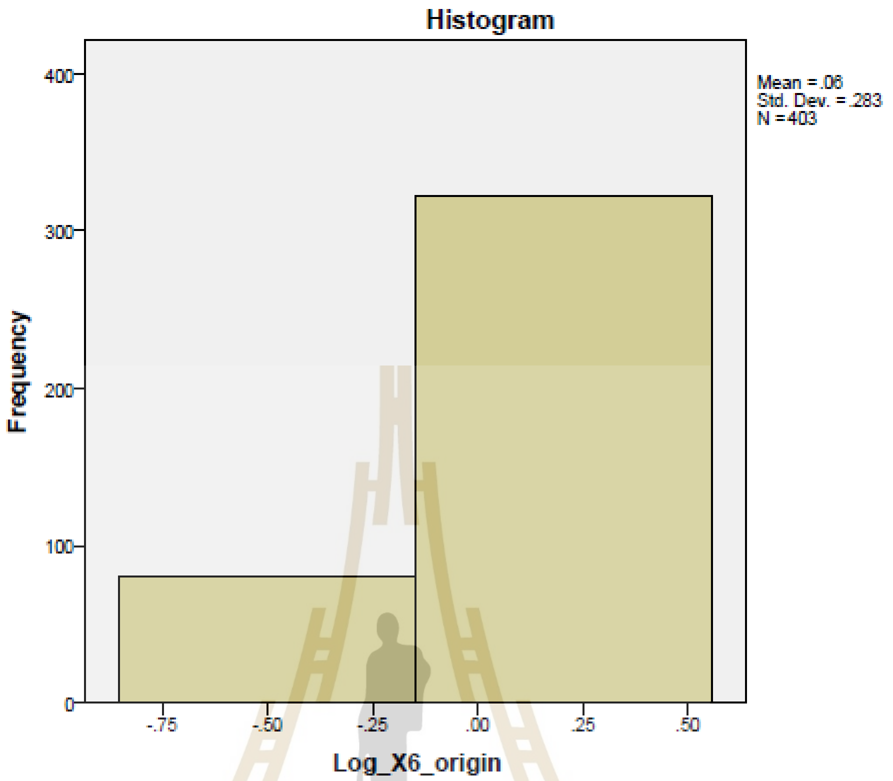
Histogram
Mean =.06
Std. Dev. =.283
N =403
Frequency
400
300
200
100
0
-.75
-.50
-.25
.00
.25
.50
Log_X6_origin

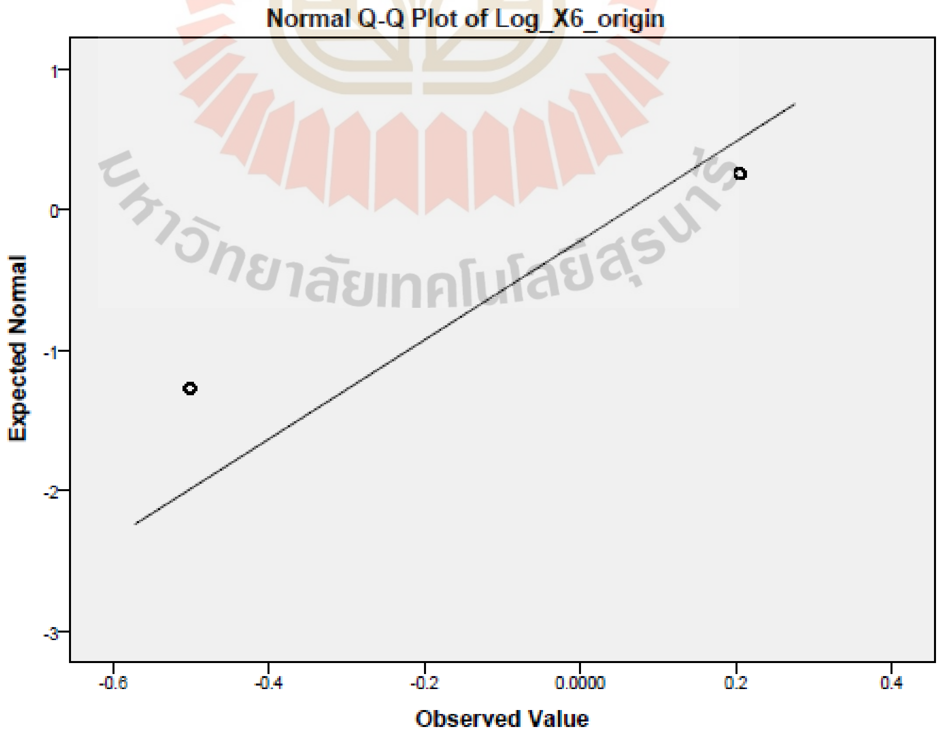
Normal Q-Q Plot of Log_X6_origin
Expected Normal
1
0
-1
-2
-3
-0.6
-0.4
-0.2
0.0000
0.2
0.4
Observed Value

SQRT

Case Processing Summary

	Cases					
	Valid		Missing		Total	
	N	Percent	N	Percent	N	Percent
SQRT_X6_origin	411	100.0%	0	0.0%	411	100.0%

Descriptives

			Statistic	Std. Error
SQRT_X6_origin	Mean		1.1028	.01580
	95% Confidence Interval for Mean	Lower Bound	1.0718	
		Upper Bound	1.1339	
	5% Trimmed Mean		1.1359	
	Median		1.2663	
	Variance		.103	
	Std. Deviation		.32031	
	Minimum		.00	
	Maximum		1.27	
	Range		1.27	
	Interquartile Range		.00	
	Skewness		-1.653	.120
	Kurtosis		1.448	.240

Tests of Normality

	Kolmogorov-Smirnov[a]			Shapiro-Wilk		
	Statistic	df	Sig.	Statistic	df	Sig.
SQRT_X6_origin	.479	411	.000	.532	411	.000

a. Lilliefors Significance Correction

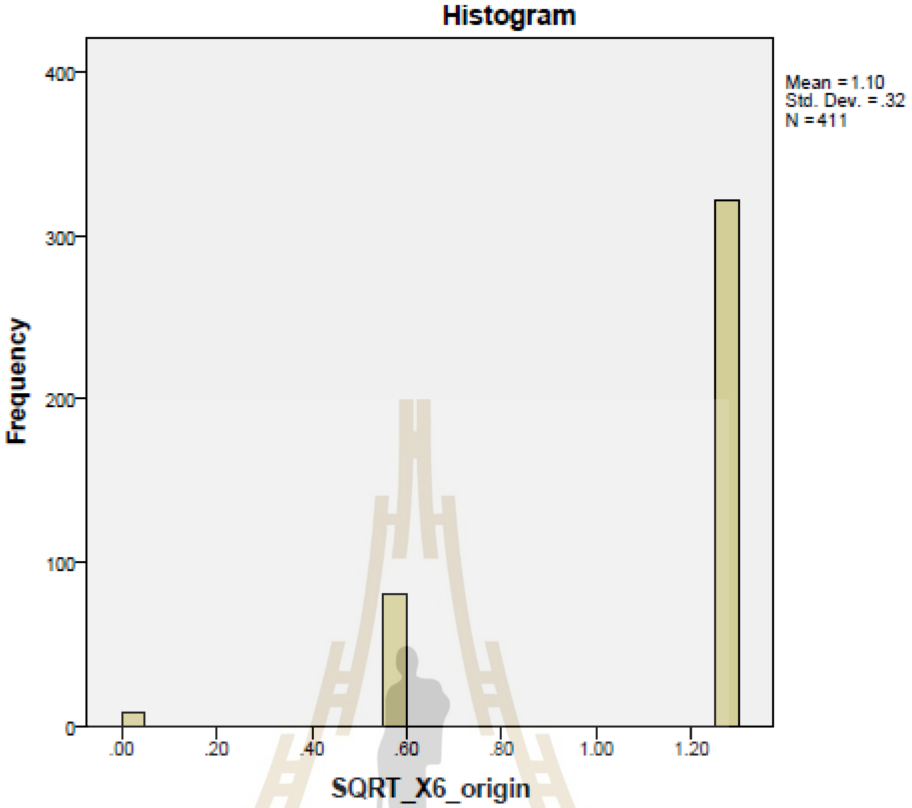
Histogram
Mean = 1.10
Std. Dev. = .32
N = 411
Frequency
400
300
200
100
0
.00
.20
.40
.60
.80
1.00
1.20
SQRT_X6_origin

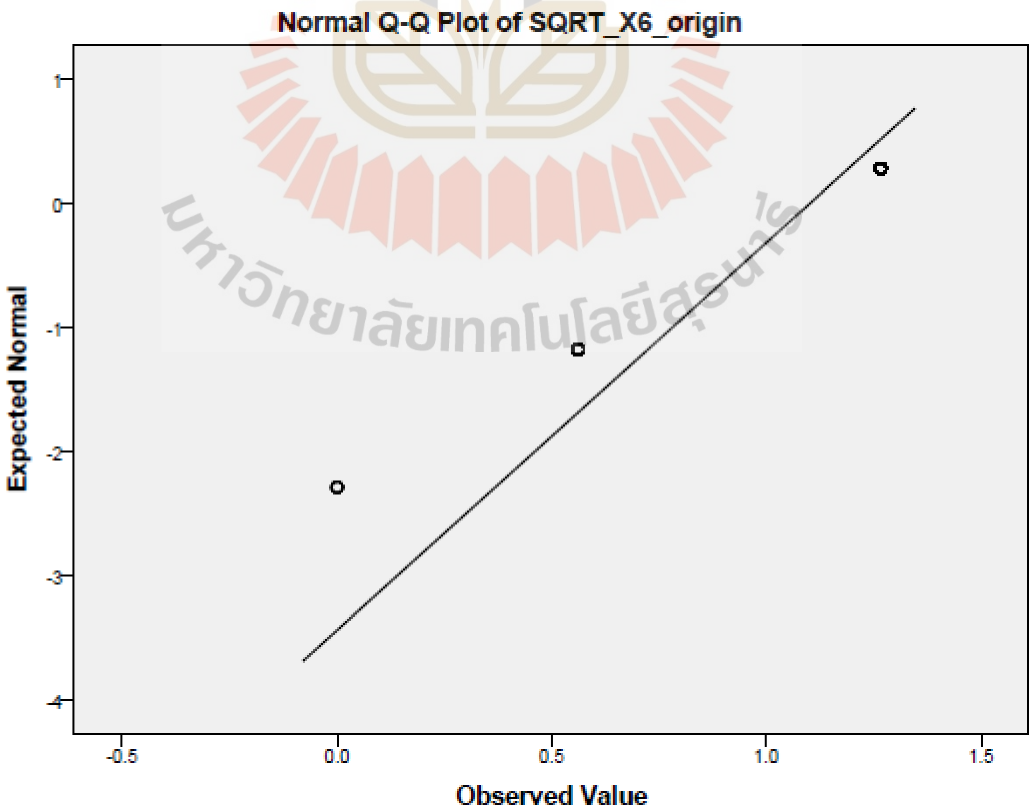
Normal Q-Q Plot of SQRT_X6_origin
Expected Normal
1
0
-1
-2
-3
-4
-0.5
0.0
0.5
1.0
1.5
Observed Value

APPENDIX B

SPATIAL AUTOCORRELATION (GLOBAL MORAN'S I)

REPORT

1) Distance to geological structures (X1)

Moran's Index: 0.887426
z-score: 10396.823864
p-value: 0.000000

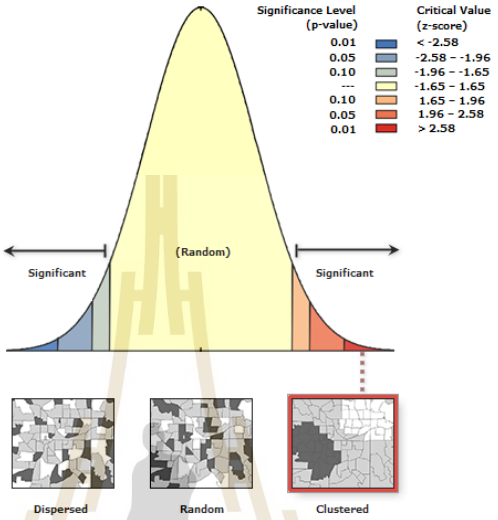

Given the z-score of 10396.82, there is a less than 1% likelihood that this clustered pattern could be the result of random chance.

Global Moran's I Summary

Moran's Index:	0.887426
Expected Index:	-0.000000
Variance:	0.000000
z-score:	10396.823864
p-value:	0.000000

Dataset Information

Input Feature Class:	LR\Spatial Autocorrelation\Convert to polygon\lox1gsne1000
Input Field:	GRIDCODE
Conceptualization:	INVERSE_DISTANCE
Distance Method:	EUCLIDEAN
Row Standardization:	False
Distance Threshold:	450.045000 Meters
Weights Matrix File:	None
Selection Set:	False

2) Locating on salt crust area and saline wet belt (X2)

Moran's Index: 0.349221

z-score: 7.989713

p-value: 0.000000

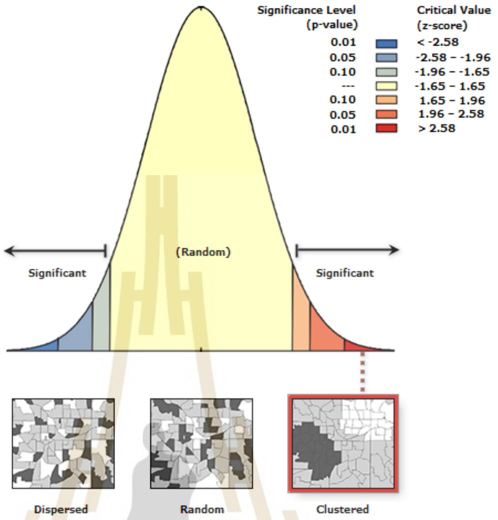

Given the z-score of 7.99, there is a less than 1% likelihood that this clustered pattern could be the result of random chance.

Global Moran's I Summary

Moran's Index:	0.349221
Expected Index:	-0.002222
Variance:	0.001935
z-score:	7.989713
p-value:	0.000000

Dataset Information

Input Feature Class:	LR\Spatial Autocorrelation\Convert to polygon\logx2scfr1000
Input Field:	GRIDCODE
Conceptualization:	INVERSE_DISTANCE
Distance Method:	EUCLIDEAN
Row Standardization:	False
Distance Threshold:	10334.866349 Unknown Units
Weights Matrix File:	None
Selection Set:	False

3) NDSI (X3)

Moran's Index: 0.546390
z-score: 3150.909762
p-value: 0.000000

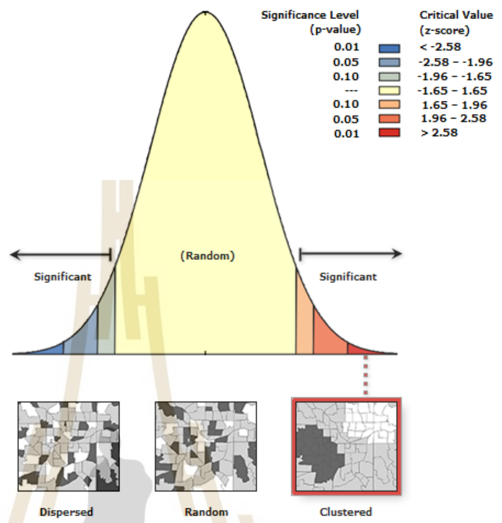

Given the z-score of 3150.91, there is a less than 1% likelihood that this clustered pattern could be the result of random chance.

Global Moran's I Summary

Moran's Index:	0.546390
Expected Index:	-0.000000
Variance:	0.000000
z-score:	3150.909762
p-value:	0.000000

Dataset Information

Input Feature Class:	LR\Spatial Autocorrelation\Convert to polygon\origix3nd1000
Input Field:	GRIDCODE
Conceptualization:	INVERSE_DISTANCE
Distance Method:	EUCLIDEAN
Row Standardization:	False
Distance Threshold:	189.755633 Meters
Weights Matrix File:	None
Selection Set:	False

4) Distance to ancient settlements (X4)

Moran's Index: 0.980689

z-score: 7986.846111

p-value: 0.000000

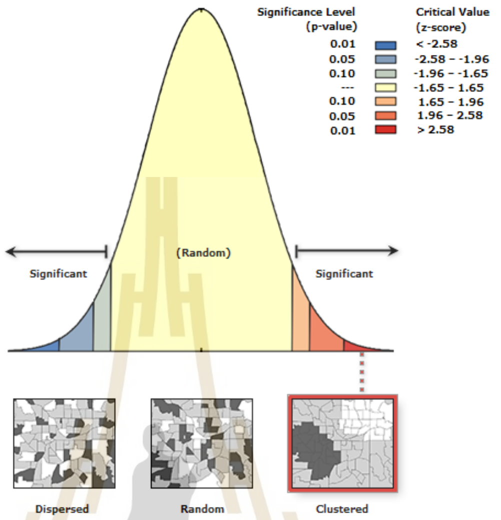

Given the z-score of 7986.85, there is a less than 1% likelihood that this clustered pattern could be the result of random chance.

Global Moran's I Summary

Moran's Index:	0.980689
Expected Index:	-0.000000
Variance:	0.000000
z-score:	7986.846111
p-value:	0.000000

Dataset Information

Input Feature Class:	LR\Spatial Autocorrelation\Convert to polygon\logx4arc1000
Input Field:	GRIDCODE
Conceptualization:	INVERSE_DISTANCE
Distance Method:	EUCLIDEAN
Row Standardization:	False
Distance Threshold:	300.030000 Meters
Weights Matrix File:	None
Selection Set:	False

5) Distance to water bodies and streams (X5)

Moran's Index: 0.895463
z-score: 13768.508732
p-value: 0.000000

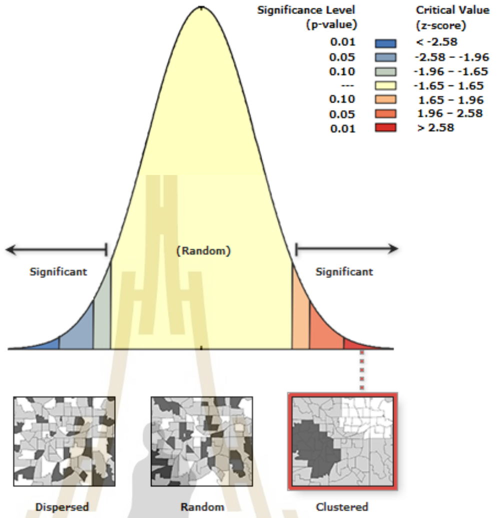

Given the z-score of 13768.51, there is a less than 1% likelihood that this clustered pattern could be the result of random chance.

Global Moran's I Summary

Moran's Index: 0.895463
Expected Index: -0.000000
Variance: 0.000000
z-score: 13768.508732
p-value: 0.000000

Dataset Information

Input Feature Class: LR\Spatial Autocorrelation\Convert to polygon\sqrtx5wa1000
Input Field: GRIDCODE
Conceptualization: INVERSE_DISTANCE
Distance Method: EUCLIDEAN
Row Standardization: False
Distance Threshold: 609.424377 Meters
Weights Matrix File: None
Selection Set: False

6) Geology (X6)

Moran's Index: 1.155346
z-score: 3.384915
p-value: 0.000712

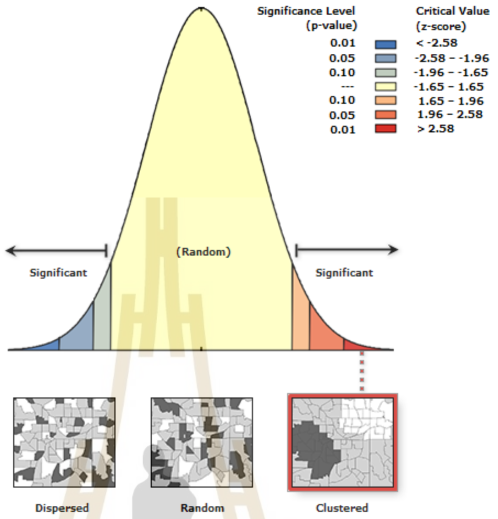

Given the z-score of 3.38, there is a less than 1% likelihood that this clustered pattern could be the result of random chance.

Global Moran's I Summary

Moran's Index:	1.155346
Expected Index:	-0.015625
Variance:	0.119673
z-score:	3.384915
p-value:	0.000712

Dataset Information

Input Feature Class:	LR\Spatial Autocorrelation\ Convert to polygon\origx6gff1000
Input Field:	GRIDCODE
Conceptualization:	INVERSE_DISTANCE
Distance Method:	EUCLIDEAN
Row Standardization:	False
Distance Threshold:	16614.588885 Meters
Weights Matrix File:	None
Selection Set:	False

7) Locations of salt mines (Y)

Moran's Index: 0.519581
z-score: 20.018213
p-value: 0.000000

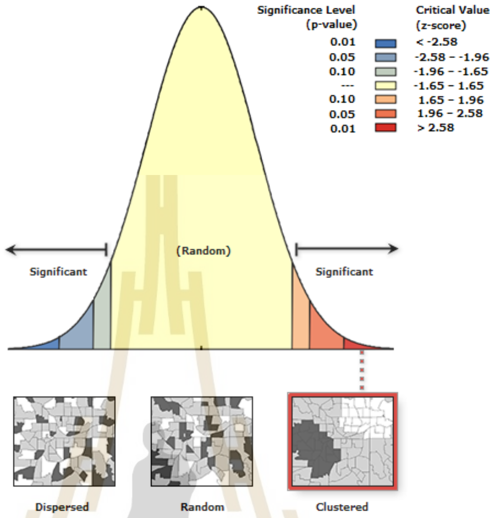

Given the z-score of 20.02, there is a less than 1% likelihood that this clustered pattern could be the result of random chance.

Global Moran's I Summary

Moran's Index:	0.519581
Expected Index:	-0.002915
Variance:	0.000681
z-score:	20.018213
p-value:	0.000000

Dataset Information

Input Feature Class:	LR\Spatial Autocorrelation\Convert to polygon\Y1000
Input Field:	GRID_CODE
Conceptualization:	INVERSE_DISTANCE
Distance Method:	EUCLIDEAN
Row Standardization:	False
Distance Threshold:	15963.153881 Meters
Weights Matrix File:	None
Selection Set:	False

CURRICULUM VITAE

Name Montri Thanaphattarapornchai

Date of Birth 26 February 1974

Place of Birth Bangkok, Thailand

Education

1992 – 1995 Bachelor of Art, Major in Archaeology, Silpakorn University, Bangkok, Thailand

Position and Place of Work

Archaeologist, the Fine Arts Department, Ministry of Culture, Thailand.